# SOME ASPECTS OF THE ELECTRONIC, EXCITONIC AND POLARONIC PROPERTIES OF A QUANTUM DOT

# A thesis submitted for the degree of **DOCTOR OF PHILOSOPHY IN PHYSICS**

Ву

# LUHLUH JAHAN K (12PHPH06)

Under the guidance of

Prof. ASHOK CHATTERJEE



SCHOOL OF PHYSICS UNIVERSITY OF HYDERABAD HYDERABAD-500 046 INDIA

**MARCH 2021** 

my beloved parents, my strength,

Basheer and Zainaba

&

To my Love, my companion,

Hafeez

**DECLARATION** 

I hereby declare that this thesis titled Some Aspects of the

Electronic, Excitonic and Polaronic Properties of a Quantum Dot

submitted by me, under the guidance and supervision of Prof. Ashok

Chatterjee is a bonafide research work and is free from plagiarism. I also

declare that it has not been submitted previously, in part or in full to this

university or any other university or institution, for the award of any

degree or diploma. I hereby agree that my thesis can be deposited in

INFLIBNET.

A report on plagiarism statistics from the university librarian is

enclosed.

Place: Hyderabad

Date:

Luhluh Jahan K

12PHPH06

ii

# **CERTIFICATE**

This is to certify that the thesis titled **Some Aspects of the Electronic, Excitonic, Polaronic Properties of a Quantum Dot** submitted by Luhluh Jahan. K. (Reg. No. 12PHPH06), in partial fulfilment of the requirements for the award of Doctor of Philosophy in Physics, is a bonafide work carried out by him under my supervision and guidance.

This thesis is free from plagiarism and has not been submitted previously, in part or in full to this or any other university or institution, for an award of any degree or diploma.

Further, the student has passed the following courses towards fulfilment of coursework requirement for PhD:

Course Code	Name of the Course	Credit	Pass/Fail
PY801	Advance Quantum Mechanics	4	Pass
PY803	Advance Statistical Mechanics	4	Pass
PY804	Advanced Electromagnetic Theory	4	Pass
PY821	Research Methodology	4	Pass

	Prof. Ashok Chatterjee
Dean	Thesis Supervisor
School of Physics	School of Physics
University of Hyderabad	University of Hyderabad

Date:

### **ACKNOWLEDGEMENT**

First and foremost, I would like to thank my advisor *Prof. Ashok Chatterjee* for providing a vibrant and academically stimulating milieu for research. I would also like to put on record my gratitude for his constant guidance and encouragement.

I am very much thankful to the doctoral committee members, *Prof. S. Srinath* and *Prof. S. V. S Nageswara Rao* for their critical reviews and useful advice. I am grateful to *Prof. Ashok Chatterjee*, *Prof. S. Chaturvedi*, *Prof. M. Sivakumar*, *Prof. V. Seshubai and Prof. Vipin Srivastava*, with whom I could get the opportunity to do teaching assistantship as part of my PhD Course. They enhanced my knowledge in physics and raised my confidence level.

I also express my sincere thanks to the former Deans of School of Physics, *Prof. R. Singh, Prof. S. Chaturvedi, Prof. Vipin Srivasthava, Prof. Bindu. A. Bambah, Prof. C. Bansal and Prof. Seshubai* for providing the necessary facilities.

I would also like to gratefully acknowledge the help I received from my collaborators *Prof. Bahadir Boyacioglu*, Ugur Erkaslan, Vocational School of Health, Ankara University, Turkey.

I thank *Mr. T. Abraham, Mrs. Deepika* and other *non-teaching staff* of School of Physics for their cooperation and assistance. I also acknowledge the financial support provided by MANF of UGC and non-NET fellowship of University of Hyderabad.

This thesis would not have been possible in the present form but for the help of my colleagues in the AC group. I am thankful to my colleague *Ch. Uma Lavanya*, for her friendship and support, and for being like a sister to me. I cannot forget the help, love and care that she extended to me. I must express my deep sense of gratitude to my seniors *Dr. Monisha PJ, Dr. I V Sankar, Dr. Sanjeev Kumar, Dr. Alu Boda*, *Dr.Ch. Narasimharaju and Dr.Atahar Parveen* for their love and care. I am very much thankful to them for the fruitful discussions and valuable suggestions. I am really thankful to my juniors, *Manasa Kalla, Hemanth Kumar Sharma, Zahid Malik, Pooja Saini, Kuntal Bhattacharyya, Debika Debnath* and *Swathi Subramanian* for their timely help. I also express my sincere thanks to *Mr. Rajendra Kumar Bhuyan*, who, though no longer with us, continues to inspire by his dedication to the world of Physics.

My special regards are due to all my *teachers* from childhood to PhD, whose teaching at different stages of my educational career has made it possible for me to see this day. Because of their kindness and support I have been able to reach a stage where I could write this thesis.

I wish to convey my gratitude to my family for their constant and unparalleled love and support. I am grateful to my brothers, *Jouhar* and *Juman*, for always being there for me. I greatly value their selfless encouragement they gave me to explore new directions in my life and to decide to shape my own career. I record my heartfelt thanks to their family also for their support and love.

I shall remain indebted forever to my parents, *Zainaba M P* and *Muhammed Basheer K*, for giving me everything that made me the person I am. They have always been an inspiration to me. I am grateful to them for having confidence in my strength and faith in my ability and giving me all the freedom to fulfill my ambition. I salute you all for the selfless love, care, pain and sacrifice you did to shape my life. I believe that all the blessings in my life are from their prayers only.

I would like to express my gratitude to my in-laws for their prayers and unfailing emotional support they have extended to me throughout these years.

Finally, I owe my deepest gratitude to the very special person, my husband, *Hafeez K T* for his continued and unfailing love, support and understanding during my pursuit of PhD degree that made the completion of thesis possible. His patience and sacrifice will remain an inspiration throughout my life. The last word goes for *Hilal Ramadan*, my naughty boy, who has been the light of my life for the last three years and who has given me a lot of extra strength and motivation to get things done.

Above all, I bow my head before 'Allah, the most merciful and the most beneficent' who blessed me with health and confidence to undertake and complete the work successfully.

#### Luhluh Jahan K



#### **PREFACE**

Recent years have witnessed extensive investigations on lowdimensional systems in which the electron's motion is restricted in all directions. The effective size of such a structure may range from a few nanometers to few hundred nanometers. Because of their ultra-small size, these systems are categorized as zero-dimensional materials or quantum dots. As a consequence of quantum confinement, these quantum dot (QD) systems have sharp energy levels and exhibit quite a few new and exotic features which are quite distinct from those observed in the corresponding bulk systems. One significant technological advantage with Quantum dots (QDs) is that they can be designed and developed in various shapes and sizes and interestingly the shape and the size of a QD system can also be tuned to obtain certain desired properties. Because of the huge design flexibility together with the important and exotic physical properties, the QD structures have enormous application potential in nano-devices like molecular transistors, spintronics and quantum computers.

It is necessary to have the knowledge of the form of the confininement potential to develop a meaningful theory of QDs. Some early experimental findings have advocated that the form of the confinement potential in a QD structure is by and large parabolic. Understandably, this proposition sparked off extensive research work on parabolic QDs. Lately, some experimental results have, however, revealed that the QD confininement potential is actually non-parabolic or anharmonic and

also the depth of the potential is finite. It has been suggested, in this context, that an attractive Gaussian potential serves as a more realistic model for confinement in QD. Consequently, a good number of researchers have studied QDs employing the Gaussian potential model. More reently, a more general model for the confinement potential has been proposed. This is the so called power-exponential (PE) potential model. This potential contains a parameter called the steepness parameter which can be tuned to obtain a family of potentials including the ones used earlier.

A semiconductor QD can have various quasi-particles. One important quasi-particle that can exist in a QD is an exciton. The formation of exciton takes place when an electron and a hole form a bound state. Quantum confinement plays an important role on the excitonic processes in a QD and therefore the optical properties of QDs which depend on excitonic processes can be significantly altered by controlling the confinement potential.

Since most of the QDs are made up of polar semiconductors that have sizable electron-phonon coupling strengths, it is but natural for polarons to form in these systems. The electron-phonon interaction has the same energy scale as the other important interactions in low-dimensional systems and it is therefore important to examine the role of polaronic effects in these systems. It has turned out that the manifestation of the polaronic interaction becomes more prominent as the dimensionality of the system is reduced.

Along with the confining potential of QD, the magnetic field and temperature also take a crucial part in influencing the QD properties. This thesis is an attempt to examine the magnetic field effect on the exciton energy spectra in QD, the effect of temperature on the energy levels and the self-energy of a polar QD, and the effect of the confinement potential profile on the energy, heat capacity, and the susceptibility of an electron and the persistent current in a GaAs QD at finite temperature.

# LIST OF ABBREVIATIONS

QD Quantum Dot

GQD Gaussian Quantum Dot PQD Parabolic Quantum Dot

GS Ground State

EBOM Effective Bond – Orbital Model

ES Excited State

LO Longitudinal Optical
e-p electron – phonon
2D Two Dimensional
3D Three Dimensional

ND N Dimensional

RSPT Rayleigh Shrödinger Perturbation Theory

QC Quantum Confinement

DoS Density of States
CM Centre of Mass

GSE Ground State Energy

BE Binding Energy

PE Power Exponential

PEQD Power Exponential Quantum Dot

PCS Photonization Cross Section

WF Wave function

SE Self Energy

GC Gaussian Confinement

# **CONTENTS**

Declaration	11
Certificate	iii
Acknowledgements	iv
Preface	viii
Abbreviations	xi
CHAPTERS	
1. Introduction	1 - 40
1.1 Nanomaterials/Low dimensional Systems	1
1.2 Quantum Dots	2
1.3 Confinement Potential	3
1.4 Fabrication of Quantum Dots	5
1.5 Properties of Quantum Dots	7
1.5.1 Density of States	7
1.5.2 Optical Properties	10
1.6 Applications of Quantum Dots	11
1.7 Review of Literature on Quantum Dots	13
1.7.1 Experimental Background	14
1.7.2 Theoretical Background	15
1.8 Excitons in Quantum Dots	17
1.9 Electron – Phonon interaction (polaron) effects in Qua	ntum
Dots	21
1.10 Organization of the Thesis	26
References	29
2. Effect of Magnetic field on the Exciton energy le	
GaAs Quantum Dots: Application to Excitonic lase	ers 41-72
	41-/2
2.1 Introduction	41
2.2 Model	43

2.3 Formulation	44		
2.4 Variational Methods	47		
2.4.1 The Exciton Ground state Energy	47		
2.4.2 The Exciton Binding Energy	48		
2.4.3 The Size of Exciton	48		
2.4.4 The Oscillator Strength	48		
2.5 1/N Expansion Method	50		
2.6 Ground state Results and Discussions	55		
2.7 Excited states	66		
2.6 Conclusions	69		
References	71		
3. Effect of Temperature on the Single Particle Ground state			
and Self -Energy of a Polar Quantum Dot wit			
Confinement	73 - 99		
3.1 Introduction	73		
3.2 Model	74		
3.3 Formulation	76		
3.4 Results and Discussions	87		
3.5 Conclusions	96		
References	98		
4. Effect of Confinement potential shape on the	,		
Thermodynamic, Magnetic and Transport Pro	-		
GaAs Quantum Dot at finite temperature	100 - 126		
4.1 Introduction	101		
4.2 Model	102		
4.3 Formulation	103		
4.4 Results and Discussions	107		
4.4 Conclusions	119		
References	121		
5. Summary	127		
List of Publications	131		

"I would like to describe a field, in which little has been done, but in which an enormous amount can be done in principle. This field is not quite the same as the others in that it will not tell us much of fundamental physics (in the sense of, What are the strange particles?) but it is more like solid-state physics in the sense that it might tell us much of great interest about the strange phenomena that occur in complex situations. Furthermore, a point that is most important is that it would have an enormous number of technical applications".

# **RICHARD FEYNMAN, CALTECH, 1959**

"There is plenty of rooms at the bottom"

1

**INTRODUCTION** 

#### 1.1 NANOMATERIALS / LOW DIMENSIONAL SYSTEMS

The area of nanoscience has occupied the limelight in research for the last four decades and has acquired even greater momentum in recent years for its role in technology. It appears that Nanotechnology serves as the key driver for the economic development in the foreseeable future. The term *nano* has come from the Greek word dwarf [1] which means small and one nanometer (nm) is equal to  $10^{-9}$  meters. The materials whose dimensions are of the order of 100 nm (or less) are usually termed as nanomaterials and they provide the foundations on which the magnificent edifice of Nanotechnology is built. Nanomaterials, in general, display very many important and interesting properties that are extremely different from the bulk materials. These properties depend on various parameters such as the structure of the atoms forming the nanomaterial, the size and shape of the nanosystem, the so called confinement potential which confines the charge particles, composition defects and so on.

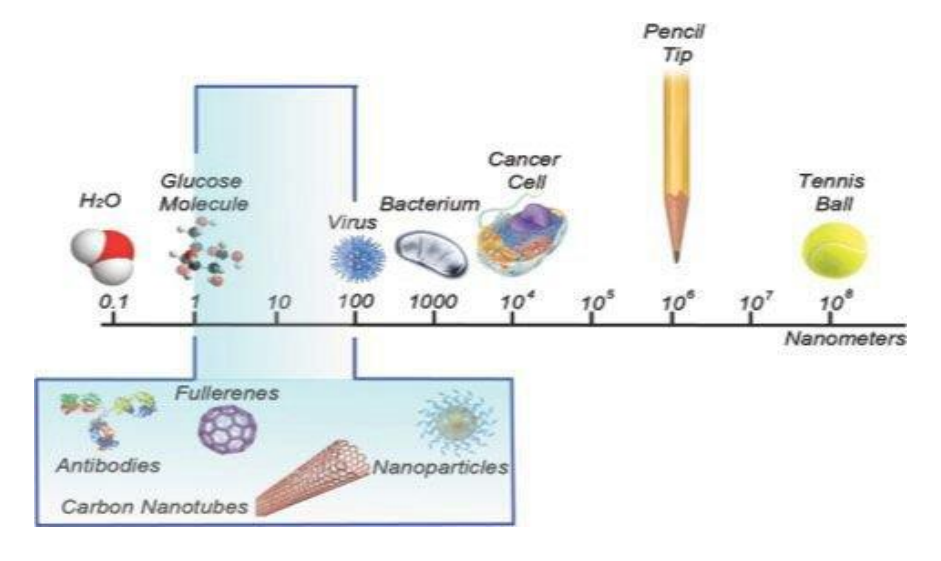


Fig. 1.1 Material having different length scales.

Research on low-dimensional systems has received an unprecedented impetus with the tremendous growth and advances in modern nanofabrication techniques such as etching techniques, molecular beam epitaxy, and nano-lithography. Indeed, it has now become viable to develop nano-scale systems where electron's motion can be restricted in all the three dimensions. This is referred to as quantum confinement (QC). The size of these structures may vary, in general, from a few nanometers to a few hundreds of nanometers. Because of the ultrasmall size of these materials, they are also called zero-dimensional objects. More technically they are referred to as quantum dots (QDs).

## 1.2 QUANTUM DOTS

A quantum dot (QD) is often composed of semiconductors of groups of II-VI, III-V, or IV-VI materials. A QD is also referred to a giant artificial atom because it may contain a number of atoms. However, it has an advantage over an atom because in a QD, the number of charge carriers can be varied at will. A QD possesses discrete number of energy levels like naturally occurring atoms or molecules [2-4]. Because of the small size of the QD, the surface to volume ratio is high in a QD and consequently, surface effects are much more important in a QD.

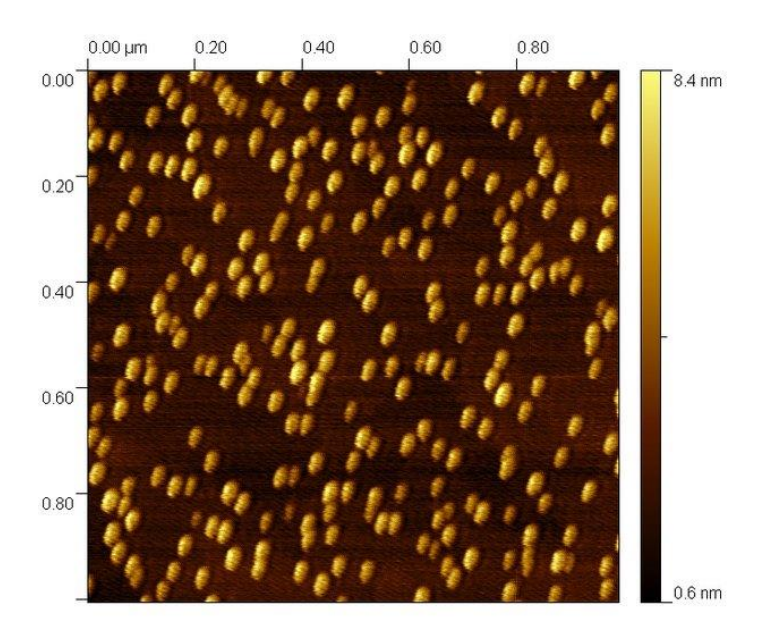


Fig. 1.2 An AFM image of QD.

When a thin sheet of lower band-gap semiconductor such as *GaAs* is placed between two thick layers of a wider band-gap semiconductor such as *AlGaAs*, electrons are forced to move in a quasi-two dimensional (quasi-2D) planar region and the structure thus produced is referred to as a Quantum well [5] or we can say that, when the electrons are allowed to move freely in two spatial dimensions and are completely confined in the third direction in a nanostructure, then such systems are called quantum wells. In a similar way, if in a system, the electrons have free motion only in one direction and their motions are confined in the other two directions, the system is known as a quantum wire. Because of the confinement in all the spatial dimensions, the QD systems show highly quantum effects. If the confinement lengths of QD are of the same

order in all the three directions it is called three dimensional (3D) QD, and, if the confinement length is much smaller in one direction compared to that in the other two directions, the corresponding system is called a 2D QD.

The subject of QDs has generated unwavering interest for the last forty years or so especially for two reasons. First, because of the small length scale, QDs are ideal objects for testing the results of quantum mechanics [6]. Secondly, the QD systems exhibit enormously novel and important physical features that are both fascinating and also fairly distinct as compared to those of their bulk counter-parts. Besides, it is possible to design QD systems in several different shapes/sizes and in both two and three dimensions. Because of the huge flexibility in design and the very many new and interesting properties, the QD structures are considered highly promising for application in nano-devices like QD lasers [7], single- or multi-molecular transistors [8], spintronics and quantum computers.

#### 1.3 CONFINEMENT POTENTIAL

In order to perform theoretical investigations on QD properties, it is necessary to first prescribe the form of the confinement potential. One simple choice would be to work with an infinite potential well. However, initial experimental results [9, 10] in conjunction with the generalized Kohn theorem [11, 12], indicated a parabolic nature for the confinement potential in a QD. As a consequence, extensive theoretical research studies on various electronic and other aspects of QDs were carried out following straight-forward quantum mechanics with parabolic or

harmonic potential as the confinement potential [13-20]. A QD with a parabolic or harmonic confinement potential is described as a parabolic QD (PQD).

Lately, a few experimental studies have revealed that the QD confinement potential is in reality anharmonic and it is not an infinite well, rather it possesses a finite depth. Adamowski et al. [21] have demonstrated that an attractive Gaussian potential serves as a much more suitable confinement potential for a QD. The generalized Kohn theorem is also approximately satisfied by the Gaussian potential. Furthermore, around the dot centre, its behaviour is harmonic. The Gaussian QD (GQD) possesses an advantage over PQD as it can describe both excitation and ionization processes. The results of Masumoto and Takagahara [22] suggest that the quantum confinement in small QDs is undeniably well approximated by a Gaussian potential. The Gaussian potential has been extensively used to probe the electronic properties of QDs [23-35].

#### 1.4 FABRICATION OF QUANTUM DOTS

There are several methods to fabricate QDs. Our ultimate aim is to confine the electrons or any charge carriers in a small region. One way to achieve this is by surrounding a metal particle with insulators [2]. We can also confine the motion of electron within the semiconductor by applying an electric field [2]. Another way to fabricate QD is by sandwiching a thin sheet of a narrow band-gap semiconducting material such as GaAs in between two thick layers of a wider band-gap semiconductor such as [36] *AlGaAs*. Since, AlGaAs has similar crystal

structure and identical lattice constant, it can be used as the sandwiching material for making a GaAs QD. We can tune the confinement and number of electrons by using metallic gates. Lateral confinement can be attained by switching on an external electric field. This method was essentially introduced by Cibert *etal*. [37] in 1986.

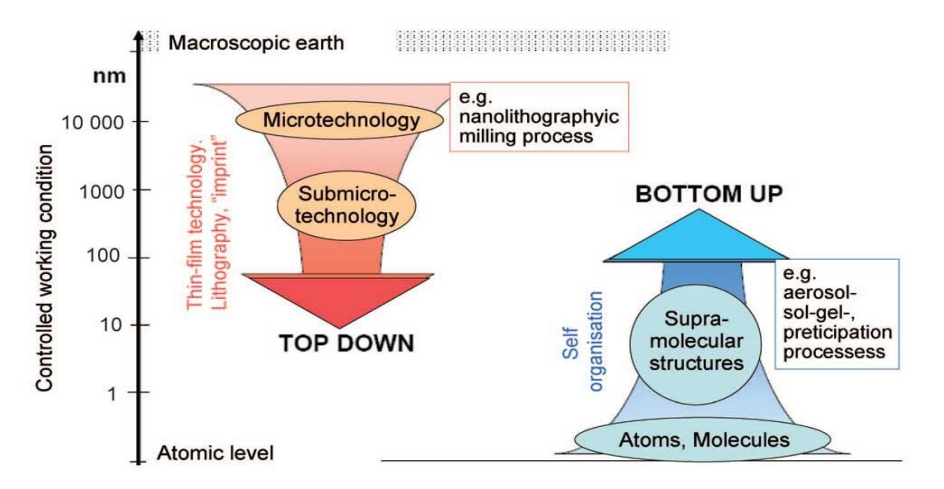


Fig 1.3. Nanoparticle production: top-down method and bottom-up method. (Image: Laboratory for Micro and Nanotechnology, Paul Scherrer Institute)

Basically, there are two main ways for the production of nanomaterials. One is called the top-down approach and the other is bottom-up method (Fig 1.3). In the Top-down approach, nanoscale particles are produced from the macroscale particles. This process uses the physical attributes for the nanoparticle production. Ion implantation, laser ablation, sputtering, high-energy milling, lithography, vapor condensation, etc. are few Top-down methods. But, in the case of a bottom-up method, one starts from atoms or molecules to process nanoparticles. Some of the

Bottom-up methods include Sol-gel technique, cluster consolidation, electrical deposition, chemical vapor deposition, self-alignment etc..

One of the early methods was the chemical etching method, first proposed by Allen et al. [38] in 1983 in a single quantum-well system and by Reed *et al.* [39] in 1986 in a multiple quantum-well super-lattice. However the name 'Quantum dot' was first introduced by Reed. Earlier, a *quasi* – 0*D* structure would be addressed as a *quantumbox* [40], *quantumbubble* [41], *quantumpoint* [42], *semiconductor crystallite* [43] etc. We can also obtain 3*D* quantum confinement by using strained layer super-lattices. Here the lattice incompatibility in the layers of a super-lattice makes the 2*D* layered structure to organize into small islands and so they are called 'self assembled QDs'. This was first achieved by Goldstein in 1984 [44] and further confirmed by Leonardo [45] in 1993.

## 1.5 PROPERTIES OF QUANTUM DOTS

Nanomaterials are being explored by the scientists in a wide range of disciplines from materials science to nanotechnology, from condensed matter to biology, from chemistry to drug delivery. The properties of QDs have turned out to be highly size-dependent with a lot of fascinating features.

#### 1.5.1 DENSITY OF STATES FUNCTION

The Density of States (DoS) function gives the number of states per energy interval and determines the distribution of carrier density in a physical system. The DoS is defined as:; g(E) = dN/dE, where dN = dN

g(E)dE is the number of electrons with an energy E lying within a narrow range of energy dE. The DoS of QD is a delta function. The DoS of different quantum strusctures are shown in the Fig. 1.4. The figure shows that DoS behaves as  $E^{1/2}$  in the bulk system (3D) and as a Heaviside function for 2D systems. In 1D systems, it is proportional to  $E^{-1/2}$  and for the 0D materials or QDs, it is given by the Dirac delta function. The formation of discrete energy levels is one of the main properties of the low dimensional systems. If the confinement potential is taken as an infinitely deep potential well, the energy levels are of the form of  $E_n = \hbar^2 \pi^2 n^2 / 2m^* L^2$ , where  $m^*$  is the Bloch mass of the particle and L is the effective length scale the QD well. Fig 1.5 presents the energy levels of a realistic quantum structure.

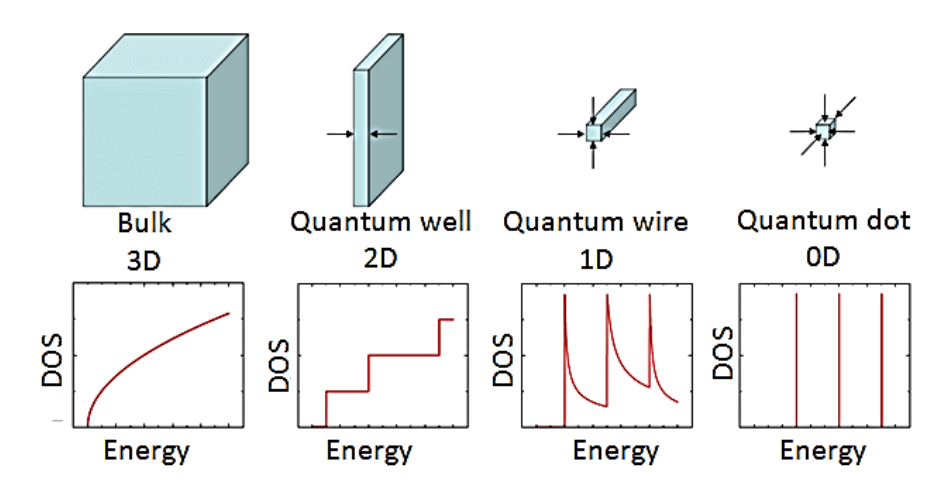


Fig. 1.4 Density of states versus energy profile in semiconducting materials.

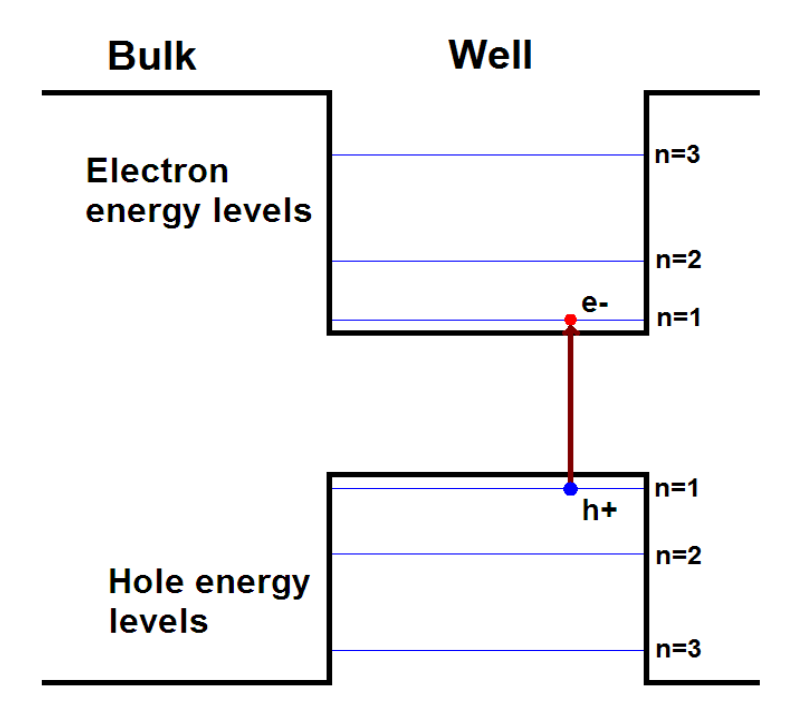


Fig. 1.5 Energy levels in a realistic quantum structure: quantum wells.

At low temperature, a significant contribution to electronic specific heat comes from the conduction electrons which are in the vicinity of the Fermi level. On the other hand, the number of electrons around a certain level is a function of the electronic DoS at that level. Since the electronic DoS at the Fermi level varies with the dimensionality of the system, the electronic specific heat of QD is naturally strongly dependent on the system's dimensionality. Also, the component of the susceptibility emerging from the conduction electrons, called the Pauli susceptibility is directly proportional to the DoS and thus depends on the dimensionality of the system.

#### 1.5.2 OPTICAL PROPERTIES

Besides the nature of the material used for the construction of a QD structure, the most important factor that affects the optical properties of a QD system is the QD size. Since the energy level spacing depends on the QD size (L), the color emitted or absorbed by a QD crystal undergoes a blue-shift as the size of the QD decreases. This is the quantum size effect. The band gap of a QD is found to be proportional to  $L^n$ , where n is between 1 and 2.

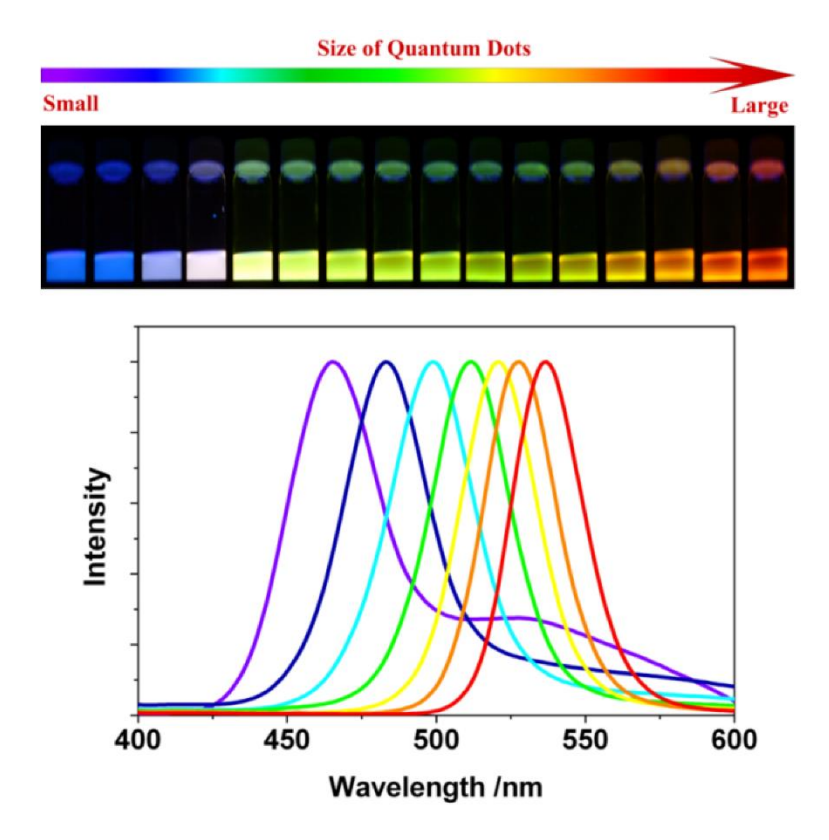


Fig. 1.6 The band gap energy and the size of a QD are approximately inversely proportional to each other. So, the smaller dots produce lights

in high frequency region while larger dots produce in the lower frequency region.

## 1.6 APPLICATIONS OF QUANTUM DOTS

Research on QDs has generated interest in different fields of study. Since the nanoparticles of metals or semiconductors of size 2-6 nm have dimensional similarities with some of the biological macromolecules such as nucleic acid, proteins etc. [46], the subject of QDs has also captured the imagination of biologists. Due to quantum confinement effect, QDs show good optical and electronic properties and so they have more advantages than the currently available flourophores like organic dyes and fluorescent proteins [47]. Since the QDs have thin emission spectral band and large absorption band, they are more useful for the multiplexed imaging in some biological studies. Photostability is an important parameter in major fluorescence applications. Since QDs are more stable and can have multiple excitation and fluorescence for a long time with high degree of luminosity, they are also more advantageous in this area. QDs are also used in gene technology. Some of the studies show that QD-conjugated oligonucleotide sequences may get bonded with DNA or mRNA [48]. Studies have also shown that red, green and blue QDs can be used in different combinations to label and identify target sequences of DNA [50]. QDs are also useful in fluorescent labeling of cellular proteins [51]. They can also have application in cell tracking and animal imaging. They are used in tumour detection and targeted drug delivery also.

QDs have potential applications in quantum information processing. They have paved the way for supercomputers called quantum computers. They can store information as qubits which are the elementary units of the quantum information processes and can be created using the two spin states of the electron.

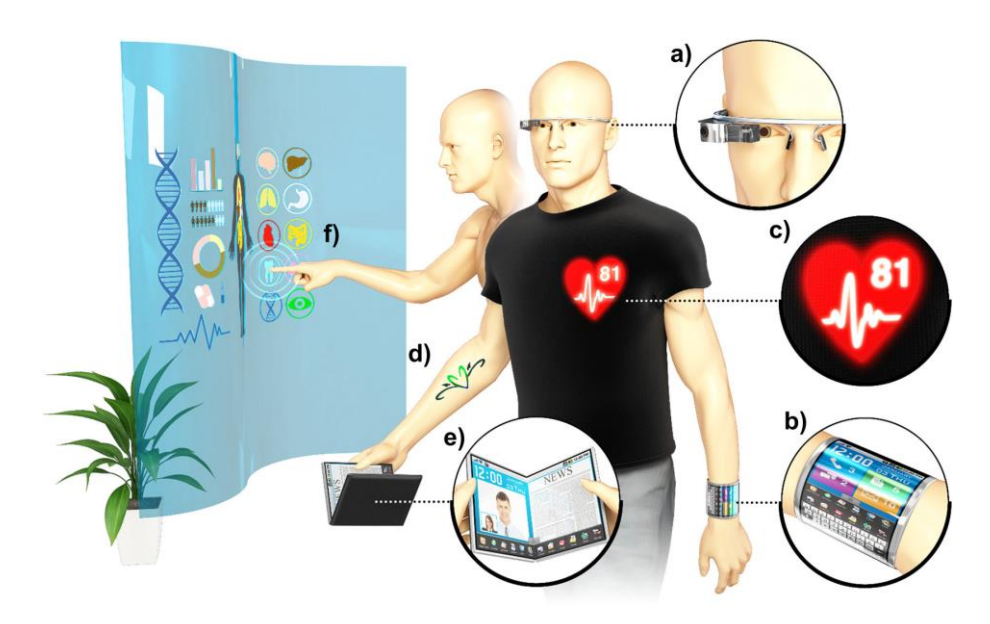


**Fig. 1.7** Some of the displays in future. (a) Glasses; (b) Watch with built-in biosensors; (c) Fabric; (d) Ultrathin electronic tattoo; (e) Flexible display; (f) Transparent windows [52].

Light absorption and exposure of the photon-sensitive material to light are the two main factors that govern the efficiency of a Solar cell. Employing QD-adsorbed materials, one can achieve light absorption to a very high degree. Using the advantage of tunability of the band gap of QDs, absorption of various wavelengths of the visible spectrum of light can be achieved. The incorporation of nanomaterials improves photoenergy absorption as the surface to volume ratio increases as we

go to lower dimensions. Most of the solar energy received by the earth is mainly in the IR and near IR region. One important advantage with a QD solar cell is that it can work in the IR region, which is not the case with the conventional solar cells. The QD solar cells are less expensive to fabricate than conventional solar cells and have better efficiencies. So, QD solar cells are a highly desirable alternative.

Recently, Quantum Dot Light Emitting Diode (QLED) is being used in display technology. Because of the outstanding color purity, high brightness, low operation voltage and easy processability, QLED displays are getting much attention in the scientific world. The inorganic QDs enable increased life of the system because of the high thermal and air stability they have. Furthermore, recent developments in patterning techniques have enabled the accomplishment of ultrahigh-resolution QLED array in full colour range. Conventional display processing technologies could not implement these techniques [52].

#### 1.7 REVIEW OF LITERATURE ON QUANTUM DOTS

In the last four decades, research investigations using both theory and experiment have been conducted quite extensively on low-dimensional systems in general and quantum dots in particular. These studies have uncovered quite a few interesting physical properties of matter at the fundamental level.

#### 1.7.1 EXPERIMENTAL BACKGROUND

In the last four decades, a vast number of experimental investigations have gone into studying the physical behavior of the confined charge carriers in zero dimension. Ashoori *et al.* [53] have explained a spectroscopic tool for the study of discrete quantum energy levels in a quantum dot. A few-electron QD energy spectrum was studied by Meurer *et al.* using far infrared spectroscopy on GaAs QD [54]. Su *et al.* have considered a few-electron QD created in a laterally confined double-barrier heterostructure and investigated resonant tunneling through it [55]. They have found that if the electron number in QD is larger than or equal to 3, then the energy needed to add another electron to QD is independent of the number of electrons present in QD. Norris et al. have studied the excited states of QD using luminescence excitation spectroscopy [56]. Medeiros-Ribeiro et al. have made a capaciatance spectroscopic study of InAs self-assembled QD grown on GaAs [58]. They have shown the effect of inter- and intra-dot Coulomb interactions on the capacitance spectra. Some researchers have observed the charge fluctuations in QD using semiconductor electrometer [59].

Kulakovskii *et al.* [61] have used magneto-photoluminescence to investigate the influence of QD asymmetry and electron-hole exchange interaction on the emission properties of a confined biexciton in single 3D CdSe/ZnSe QD. The role a magnetic field plays on the recombination spectrum of strongly correlated electrons and holes in a self-assembled InGaAs/GaAs QD has been demonstrated by Raymond *et al.* [62]. The effect of magnetic field on the Zeeman splitting and the diamagnetic shift in the magneto-luminescence lines have been studied by Rinaldi *et al.* [63]. They have used  $In_xGa_{1-x}As$  with parabolic confinement in their studies. A third harmonic generation associated with the intraband transition in a self-assembled InAs /GaAs QDs has

been observed by Sauvage *et al.* [64]. Lee *et al.* have reported a reflection high-energy electron diffraction study of InAs self-organized QDs grown on GaAs (001). Dekel *et al.* [66] have carried out a spectroscopical study on a single self-assembled QD and have given a successful explanation for its power-dependent PL spectra. An experimental study of multimode spectral emission in a QD laser has been studied by Patane *et al.* [67]. They have investigated the electroluminescence spectra of edge-emitting lasers with active medium being self-assembled quantum dots. Zhao *et al.* [68] have reported a work on single-emitter that studies the emission characteristics of graphene QDs. They have shown that these QDs are stable and efficient emitters of single photons at room temperature. Also the emission wavelength of these emitters is adjustable via the functionalization of their edges.

#### 1.7.2 THEORETICAL BACKGROUND

Several theoretical works have been carried out in the field of QDs in the last four decades. A variational study of an electron-hole system in a finite barrier QD using effective mass theory was first reported by Efros and Efros [69] and then by Brus [70]. Marzin and Bastard [71] have performed an effective mass calculation for the energy levels in InAs QD embedded in GaAs. Yip [72] has studied the absorption lines for a system of electrons in a PQD placed in a magnetic field. The calculation for nonlinear optical rectification of the electric field- biased parabolic QDs have been done by Gu and Guo [73]. They have shown

that that the rectification becomes more pronounced as we reduce the dimensionality of QD.

Using the Chandrasheskhar-type wave function, variational solutions of the ground state (GS) of negative donor centres in QDs have been obatined by Zhu et al. [74]. They have also found the exact solutions of the GS of neutral donor centres in different QDs. It has been shown that the electron correlation effects depend strongly on the QD dimensionality and weakly on the QD geometry. Bryant [75] has considered a system of two electrons in an infinite rectangular well. They could see that the ratio  $l_x/l_y$ , where  $l_x$  and  $l_y$  are the dimensions of the box, has a strong effect on the energy spectrum. A many body calculation has been carried out for a realistic QD geometry using the Hatree approximation by Kumar *et al.* [76]. Later, Pfannkuche *et al.* [77] have compared the results for the QD electron system obtained by using the Hatree and the Harttree-Fock approximations. They have pointed out that the results obtained by the Hartree mehod are inaccurate and those obtained by the Hatree-Fock method cannot be trusted either, particularly for small number of electrons, for they do not include the correlation effect. Johnson and Payne [78] have made a breakthrough in the field of theoretical studies by considering a model problem which is simple enough to admit an exact solution but contains the essential features of the actual problem. In this model problem, they have considered a PQD with many spinless electrons interacting through a repulsive parabolic interaction in a magnetic field. They have obtained the exact solution for the electronic energy levels in terms of the number

of electrons and the strength of the applied magnetic field. Taut [79] has considered a 2D PQD with two electrons interacting through Coulomb interaction and obtained an exact analytical solution for certain magnetic field strengths. The impact of electron-electron interaction on compressibility, capacitance and inverse compressibility of electrons in a QD has been studied by Berkovits and Altshuller [80] using the random phase approximation. The existence of the GS persistent current in coherent 2D QD arrays in an external magnetic field has been predicted by Kotlyar and Das Sarma [81]. Brouwer and Aleiner [82] have studied the electron-electron interaction effect on the conductance of open QDs. The size dependence of impurity levels in QD has been studied by Bellesa and Combescot [83]. Ferreyra and Proetto [84] have studied the properties of an exciton in an inhomogeneous QD in the strong confinement regime. Andreev and Lipvoskii [85] have experimentally and theoretically investigated the optical spectra of spherical PbSe and PbS QDs.

# 1.8 EXCITONS IN QUANTUM DOTS

Quantum confinement of charge carriers in semiconductor QDs makes them the objects of intense studies as they lead to numerous effects of fundamental character. A semiconductor QD can have several excitations. "Exciton" is one of them. A valence-band electron, after acquiring some external energy, can get energized to be elevated to the conduction band in a semiconductor. In this process a hole is created in the valence band. The conduction band electron can however still interact with the hole left behind by it in the valence band and constitute

a bound pair. This bound state of the electron and the hole is known as an Exciton. By illuminating a semiconductor with light, one can accomplish the creation of an exciton. It goes without saying that excitonic processes would have a crucial effect on several optical properties of QD. Quantum confinement can strongly alter these properties. The explanation for this is simple. It is easy to show that confinement increases a particle's energy. In the case of an exciton, there is another effect. This is the Coulomb interaction between the electron and the hole. The confinement would decrease the exciton size and would consequently increase the attractive interaction or reduce the energy. Thus there are two contrasting effects whose interplay may lead to some interesting excitonic phenomena. Also, with increasing confinement, the electron and hole would come close to each other increasing the possibility of radiative recombination. Thus there are several excitonic processes that are crucially dependent on confinement and other QD parameters. It is therefore important to study the effects of all these processes and examine how they can be tuned by controlling different parameters of QD in order to obtain desired optical properties.

The studies on excitons have started long ago. Last few decades have witnessed a number of exciting investigations on an exciton confined in a low-dimensional system. Henry and Nassau [86] could calculate the lifetime of a weakly-bound exciton in CdS which has a giant oscillator strength that leads to extremely fast radiative lifetime. They have found that  $\tau_{I_1} = 1.03 \pm 0.1$  nsec and  $\tau_{I_2} = 0.5 \pm 0.1$  nsec, where  $I_1$  refers to an exciton bound to a neutral acceptor and  $I_2$  that to a neutral donor. The

binding energy (BE) of an exciton in a quantum well has been calculated by Bastard et al. [87]. They have determined the GS BE for a GaAs-GaAlAs quantum well using variational approach and have found that, as we increase the thickness of the quantum well, GS BE decreases monotonically. Degani and Hipolito [88] have also used a variational calculation to get the exciton BE in a GaAs quantum wire (surrounded by  $Ga_{1-x}Al_xAs$ ). They have found that the energy has a strong sizedependence and also the magnitude is greater than that in a corresponding quasi-two dimensional quantum well structure. The effect on an exciton trapped in a quantum box has been studied by Bryant [89]. He has employed a variational calculation to study the GS energy and the optical properties. Confinement has been shown to enhance the exciton kinetic energy, the Coulomb energies and the oscillator strength and to reduce the electron-hole separation. Both the theoretical and experimental confirmation for the states of the biexciton in a semiconductor QD has been first provided by Hu [90]. He could see that as we reduce the QD size there is an increase in the biexciton BE. Einevoll [91] has studied theoretically the confinement of exciton in small CdS and ZnS QDs. Using a combined effective bond-orbital model (EBOM) and effective-mass approach, he could calculate the energies of a single-hole in ZnS crystallites and the exciton energies in CdS and ZnS crystallites. EBOM and the effective mass approximation are expected to overestimate the confinement energies whereas the tightbinding approximation is likely to underestimate them. The effect of confinement on an exciton in QDs of indirect band-gap materials has been studied by Takagahara and Takeda [92]. They have proposed a

mechanism for the conversion of the band-gap character. With the help of two - photon absorption and magneto-luminescence experiments, Rinaldi et al. [93] have determined the exciton Bohr radius and BE of an exciton in a V-shaped GaAs quantum wire. Lamouche and Lepine [94] have used a two-band variational method for the study of the GS of an exciton in a 2D QD superlattice which has been grown on a terraced substrate. Heller et al. [95] have investigated the role of an electric field on the excitons in QDs. With the help of micro-photoluminescence spectroscopy, they could uncover the role of an electric field on excitons that are confined by monolayer width fluctuations in narrow QWs. They have been able to observe a redshift of GS and several excited states (ESs) by switching on an electric field. It has been noticed that this stark shift decreases with increasing number of exitons in QD due to the screening of the electric filed. Oshiro et al. [96] have considered a spherical QD and employed a variational approach to find the sizedependence of a few polaronic properties. Song and Ulloa [97] have investigated the role of magnetic field and confinement on an exciton in a quantum ring and obtained the energy by numerically diagonalizing the relevant effective-mass Hamiltonian. Using the density matrix method, Karabulut et al. [98] have explored the part excitons play in influencing the nonlinear optical features of semi-parabolic QDs. Sakiroglu *et al.* [99] have considered a parabolic confinement potential and used the Ritz variational method with a Hylleraas-like trial wave function to examine the role of confinement on the exciton GS energy in a spherical and in a disc-like QD. Florez and Camacho [100] have

studied the role of excitons on second-order nonlinear optical features of QDs with semi-pherical geometry.

Effects of excitonic processes have been observed in experiments on photoluminescence [101]. It has also been realized that excitonic processes have a major part to play in semiconductor-QD-based optoelectronic devices [92,102-106].

Guo and Yu [107] have explored the excitonic effect on the third harmonic generation in  $Si/Si\ O_2$  PQD. They have demonstrated that incorporation of the excitonic effect increases the third harmonic generation by about a factor of 2. Using an exact diagonalization method, Yuan *et al.* [108] have examined the effect of excitons on the optical absorptions in PQD. Their results show that quantum confinement significantly enhances the optical absorption coefficients and the excitonic effects increase it by about hundred percent.

## 1.9 ELECTRON - PHONON INTERACTION (POLARON) EFFECTS IN QUANTUMDOTS.

The idea of Polaron was first predicted by Landau [109] more than 80 years ago. He suggested that an electronic charge carrier moving slowly through an ionic medium can shift the equilibrium position of the ions as shown in the Fig. 1.8. The term Polaron was coined by Pekar [110]. Shift in the equilibrium positions of the ions can lead to the formation of a potential well for the charge carrier. If the potential well is sufficiently deep, the electron gets trapped inside the potential well. This phenomenon is known as self-trapping, as the potential trapping the

electron has been created by the electron itself. The self-trapped charge carrier together with the lattice distortions is defined as the strong polaron [111].

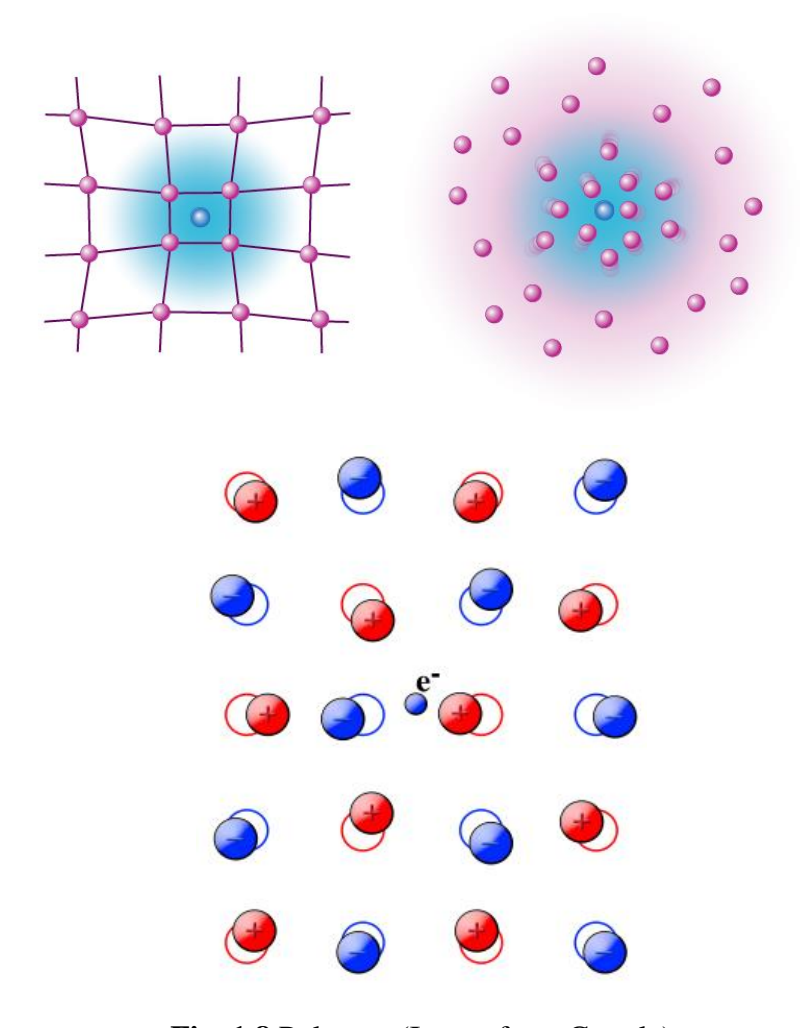


**Fig. 1.8** Polarons (Image from Google)

The quantum mechanical description of the polaron was given by Fröhlich. In this description, an extra electron in a polar solid would distort the lattice around it. The electron together with the lattice distortion forms a quasi-particle called the polaron which can also be viewed as an electron dressed with virtual longitudinal optical (LO) phonons. This is precisely the effect of electron-phonon (e-p) interaction. When the distortion of the lattice ranges over a few lattice units, we have a large polaron. A large polaron possesses small velocity and can thus move inside the solid medium essentially as a free electron with a renormalized mass which is higher than the Bloch mass. If the lattice deformation is confined within one lattice unit, the resulting polaron is known as a small polaron. The motion of such a polaron is generally described as taking place through a succession of occasional phonon-assisted jumps between adjacent sites.

Two electrons experience a repulsive force from each other because of the coulomb interaction. But when they are in a phonon bath, there will be an additional phonon-mediated attractive interaction. If this attractive force happens to be stronger than the Coulomb repulsion, then the two electrons can form a bound pair called bipolaron [112]. Thus, a bipolaron consists of two electrons together with a phonon cloud.

During the last three decades, many investigations have been made to examine the effect of polaronic interaction on the electronic properties of low-dimensional systems like QDs. Scmit-Rink, Miller and Chemla [114] have studied theoretically the optical properties of InSb and GaAs QDs. They have observed that if the QD size is much smaller than the

bulk exciton size, the spectrum is linear with a sequence of lines and they have studied the phonon broadening of these lines. Bockelmann and Bastard [115] have investigated both theoretically and experimentally the optical phonon broadening in QDs and have shown that the strength of electron-phonon (e-p) coupling for polar semiconductors is independent of the size. The static and dynamic electronic properties of nanometer-size CdSe clusters have been studied by Bawendi *et al.* [117] using optical experiments. They have also been able to obtain the value of the strength of the e-p interaction.

The polaronic properties in a 2D QD with harmonic potential have been studied by Zhu and Gu [118] by means of the second-order Rayleigh-Schrödinger perturbation theory (RSPT). They have observed that the corrections in the GS and ES energies and the transition energies increase with decreasing QD size. In a subsequent paper [119], they have concluded that the phonon-confinement effect on polaron self-energy is significantly large in small QDs. They have also examined the role of polaronic interaction on the electron cyclotron mass in a GaAs PQD using RSPT [120]. They have established that if the cyclotron frequency  $\omega_c$  is much larger than phonon frequency, the cyclotron mass splits into two cyclotron masses  $(m_+^* \text{ and } m_-^*), m_+^* (m^*)$  being smaller (greater) than the Bloch mass. By increasing the size of the QD,  $m_+^*$  can be enhanced and made to approach the 2D value while  $m^*$  may have a significant value in small QDs. The cyclotron resonance of a bound magnetoplaron in a 3D QD with strong parabolic confinement has been studied by Yeung et al. [121]. They have shown that there exists a pinning effect in the presence of Coulomb impurity and the parabolic potential. Chen *et al.* [122] have analyzed the impurity levels in a QD and calculated the impurity BE in the presence and absence of e-p interaction using second-order perturbation theory. Their investigation reveals that BE depends crucially on the effective confinement length of the QD, if it is reduced to the same length scale as the polaron size.

Mukhopadhyay and Chatterjee have obtained a closed-form analytical result for the GS polaron self-energy in a polar semiconductor QD in both 2D and 3D using RSPT. They have been able to provide a dimensional scaling relation for the polaron GS energy [123]. They have also studied the Zeeman effect for the first excited energy levels of a 2D PQD of GaAs perturbatively in the presence of polaronic interaction [124]. Polaronic effects have been investigated by Yanar *et al.* [125] in a symmetric N-dimensional (ND) Gaussian QD using RSPT, a modified Lee–Low–Pines method, and the path-integral formalism due to Haken. They have provided numerical results for the polaronic corrections to the energy for N = 2 and N = 3.

Ribeiro *et al.* [126] have explored the polaron dynamics in armchair graphene nanoribbons (GNRs) in an electric field. They have noticed that polaron transport is dependent on the appropriate balance between the e-p coupling strength and the GNR width. They have also examined the role of spin-orbit coupling on the polaron properties in GNR [127].

#### 1.10 ORGANIZATION OF THE THESIS

In **CHAPTER 2**, we have considered the exciton problem in 2D and 3D Gaussian QDs (GQDs) of GaAs placed in a magnetic field by means of (a) the Rayleigh-Ritz variational approach, (b) the 1/N expansion technique and (c) the shifted 1/N expansion scheme. We have obtained the GS energy and BE of the exciton in terms of the (i) QD size, (ii) strength of the confinement potential and (iii) the applied magnetic field and made a comparison of our results with the available reported results. The Rayleigh-Ritz variational approach provides a higher limit to the GS energy while the  $\frac{1}{N}$  -expansion technique provides a lower bound. It is shown that the results obtained by shifted 1/N expansion technique match remarkably well with the exact numerical results. We have studied the behaviour of the size of the exciton and its oscillator strength with respect to QD size. Use of the shifted 1/N expansion technique has also enabled us to compute the excited states. We have shown that by controlling QD parameters we can realize the desired number of bound excitonic states in GQD. This can pave the way for realizing excitonic lasers using semiconductor QDs.

In **CHAPTER 3**, we have analyzed the impact of temperature on polaron effects in GQD by means of Lee-Low-Pines-Huybrechts (LLPH) unitary transformation, the Rayleigh-Ritz variational method and statistical mechanics. Our calculations reveal that the electron GS energy should increase with increase in temperature while the polaron self-energy should reduce. We have also analyzed how the confinement strength affects the polaron GS energy and BE. It has been shown that the GS energy is higher for a 3D QD as compared to a 2D QD. Finally,

the polaronic effects have been shown to increase as the dimensionality of GQD is reduced.

In **CHAPTER 4**, we have studied the role of the nature of confinement on different aspects of a GaAs QD considering a power-exponential potential model. This potential contains a steepness parameter p which determines the shape of the QD potential. A small value of p gives a soft potential while a large p leads to a hard potential. We have determined the average thermodynamic energy, magnetic susceptibility, specific heat, and persistent current. It has been observed that for a soft potential, the average thermodynamic energy has a strong dependence on p, while in the case of hard confinement, it hardly depends on p. We have observed that at low temperature, for the chosen magnetic field strength, the potential profile has no bearing on the heat capacity. It has also been observed that there can be a magnetic field-driven paramagneticdiamagnetic transition in the system. It has been further observed that beyond a certain critical value of the magnetic field, the system exhibits a diamagnetic behaviour for a shallow potential and then the shape of the potential becomes unimportant. We have also found that if the magnetic field belongs to a certain range and p lies in a certain window, a diamagnetic phase can show a re-entrant behaviour. Finally, we have demonstrated that the nature of the persistent current in the QD considered here is diamagnetic and its magnitude shows an increasing behaviour with increasing potential depth. However it does not show any dependence on the steepness parameter p.

Finally, in **CHAPTER 5**, we have summarized the important results of this thesis and presented our conclusions.

#### 1.11 REFERENCES

- [1] Michael F. Ashby, Paulo J.Ferraira, Daniel L.Schodek, *Nanomaterials, Nanotechnologies and Design*, Elsevier.
- [2] M. A. Kastner, *Artificial Atoms*, *Phys.* Today **46**, 24 (1993).
- [3] N. F. Johnson, J. Phys. Condens. Matter **7**, 965 (1995)
- [4] R.C. Ashoori, *Electrons In Artificial Atoms*, Nature **379**, 413 (1996).
- [5] S.M. Sze and K.K. Ng, *Physics of Semiconductor Devices*, John Wiley & Sons, Inc., (2006)
- [6] K. D. Zhu & S. W. Gu, Temperature dependence of polarons in harmonic quantum dots. Phys. Lett. A 171, 113–118 (1992).
- [7] P.Bhattacharya, et al. In(Ga)As self-organized quantum dotLasers: DC and small-signal modulation properties. IEEE Trans. Electr. Devices 46, 871–883 (1999).
- [8] M. A. Kastner, *The single –electron transistor*. Rev. Mod. Phys. **64**, 849–858 (1992).
- [9] C. Sikorski & U. Merkt, *Spectroscopy of electronic states in InSb quantum dot*. Phys. Rev. Lett. **62**, 2164–2167 (1989).
- [10] B. Meurer, D. Heitmann, &K. Ploog, *Single electron charging of Quantum dot atoms*. Phys. Rev. Lett. **68**, 1371–1374 (1992).
- [11] F. M. Peeters. *Magneto-optics in parabolic quantum dots*. Phys. Rev. B **42**, 1486–1487 (1990).
- [12] S. K. Yip, Magneto-optical absorption by electrons in the presence of parabolic confinement potentials. Phys. Rev. B 43, 1707–1718 (1991).
- [13] S. Mukhopadhyay & A. Chatterjee, *Rayleigh-Schrodinger* perturbation theory for electron-phonon interaction effects in polar semiconductor quantum dots with parabolic confinement. Phys. Lett. A **204**, 411–417 (1995).

- [14] S. Mukhopadhyay & A.Chatterjee, *Polaronic enhancement in the ground-state energy of an electron bound to a Coulomb impurity in a parabolic quantum dot.* Phys. Rev. B **55**, 9279 (1997).
- [15] S. Mukhopadhyay & A. Chatterjee, *Relaxed and effective-mass excited states of a quantum- dot polaron*. Phys. Rev. *B* **58**, 2088–2093(1998).
- [16] S. Mukhopadhyay & A. Chatterjee, *Polaronic correction to the first excited electronic energy level in semiconductor quantum dots with parabolic confinement*. Phys. Lett. A **240**, 100 (1998).
- [17] S. Mukhopadhyay & A. Chatterjee, *Polaronic correction to the first excited electronic energy level in semiconductor quantum dots with parabolic confinement*. Phys. Lett. A **242**, 355 (1998).
- [18] S. Mukhopadhyay & A. Chatterjee, Suppression of Zeeman splitting in a GaAs quantum dot. Phys. Rev. B **59**, R7833 (1999).
- [19] S. Mukhopadhyay & A. Chatterjee, *The ground and the first excited states of an electron in a multidimensional polar semiconductor quantum dot: an all coupling variational approach.* J. Phys.: Condens. Matter **11**, 2071 (1999).
- [20] S. Mukhopadhyay & A. Chatterjee, *Polaronic effects in quantum dots*. Acta Phys. Pol. B **32**, 473 (2001).
- [21] J. Adamowski, M. Sobkowicz, B. Szafran, & S. Bednarek, *Electron pair in a Gaussian confining potential*. Phys. Rev. B **62**, 4234 (2000).
- [22] Y. Masumoto & T. Takagahara, *Semiconductor Quantum Dots: Physics*. Spectroscopy and Applications. (Springer, Berlin, 2002).
- [23] J. Gu & J. Liang, Energy spectra of D-centres quantum dots in a Gaussian potential. Phys. Lett. A **335**, 451 (2005).
- [24] W. Xie, Exciton states in spherical Gaussian potential wells. Commun. Theor. Phys **42**, 923 (2004).

- [25] B. Boyacioglu, M. Saglam & A. Chatterjee, Two-electron singlet states in semiconductor quantum dots with Gaussian confinement: a single-parameter variational calculation. J. Phys.: Condens. Matter 19, 456217 (2007).
- [26] W. Xie, Binding energy of an off-center hydrogenic donor in a spherical Gaussian quantum dot. Physica B **403**, 2828 (2008).
- [27] Y. P. Bao, & W. F. Xie, Binding Energy of D and D0 Centers Confined by Spherical Quantum Dots. Commun. Theor. Phys. **50**,1449–1452 (2008).
- [28] S. Yanar, et al. Polaronic effects in Gaussian quantum dots. Superlatt. Microstruct. 43, 208 (2008).
- [29] S. S Gomez & R. H. Romero, Binding energy of an off-center shallow donor D— in a spherical quantum dot. Physica E 42, 1563 (2010).
- [30] R. Khordad, & H. Bahramiyan, *The second and third-harmonic generation of modified Gaussian quantum dots under influence of polaron effects*. Superlattices and Microstruct. **76**, 163 (2014).
- [31] A. Boda, A. & A. Chatterjee, Ground state and binding energies of (D0), (D-) centres and resultant dipole moment of a (D-) centre in a GaAs quantum dot with Gaussian confinement. Physica E **45**, 36 (2012).
- [32] B. Boyacioglu & A. Chatterjee, *Persistent current through a semiconductor quantum dot with Gaussian confinement*. Physica B **407**, 3535 (2012).
- [33] B. Boyacioglu & A. Chatterjee, *Heat capacity and entropy of a GaAs quantum dot with Gaussian confinement*. J. Appl. Phys. **112**, 083514 (2012).
- [34] A. Boda, B. Boyacioglu, & A. Chatterjee, *Ground state properties of a two-electron system in a three-dimensional GaAs quantum dot with Gaussian confinement in a magnetic field.* J.Appl. Phys. **114**, 044311–7 (2013).

- [35] A. Boda & A. Chatterjee, *Effect of external magnetic field on the ground state properties of D- centres in a Gaussian quantum dot.* Superlattices and Microstruct. **71**, 261 (2014).
- [36] L. J challis, *Physics in less than three dimensions*. Contemporary physics 33, 111 (1992)
- [37] J. Cibert, P.M. Petroff, G.J. Dolan, S.J. Pearton, &A.C. Gossard, J.H. English, *Optically detected carrier confinement to one and zero dimension in GaAs quantum well wires and boxes*, Appl. Phys. Lett. **49**, 1275, (1986).
- [38] S.J. Allen, H.L. Störmer & J.C.M. Hwang, Dimensional resonance of the two-dimensional electron gas in selectively doped GaAs/AlGaAs heterostructures, Phys. Rev. B. 28, 4875, (1983).
- [39] M.A. Reed, R.T. Bate, K. Bradshaw, W.M. Duncan, W.R. Frensley, J.W. Lee, & H.D. Shih, *Spatial quantization in GaAs–AlGaAs multiple quantum dots*, J. Vac. Sci. Technol. B. **4**, 358, (1986).
- [40] J. Allen, H.L. Störmer & J.C.M. Hwang, Dimensional resonance of the two-dimensional electron gas in selectively doped GaAs/AlGaAs heterostructures, Phys. Rev. B. 28, 4875, (1983).
- [41] W.T. Tsang, Quantum confinement heterostructure semiconductor lasers, Semiconductors and Semimetals **24**, 397 (1987)
- [42] A.O. Govorov & A. V. Chaplik, *Magnetoabsorption at quantum points*, J. Exp. Theor. Phys. Lett. **52**, 681, (1990).
- [43] A.D. Yoffe, Low-dimensional systems: quantum size effects and electronic properties of semiconductor microcrystallites (zero-dimensional systems) and some quasi-two-dimensional systems, Adv. Phys. **42**, 173, (1993).
- [44] L. Goldstein, F. Glas, J. Y.Marzin, M. N. Charasse & G.Le Roux, *Growth by molecular beam epitaxy and characterization*

- of InAs/GaAs strained-layer superlattices, Appl. Phys. Lett. 47, 1099 (1984)
- [45] D. Leonard, M. Krishnamurty, C. M. Reaves, S.P. Denbaar & P.M.Petroff, *Direct formation of quantum-sized dots from uniform coherent islands of InGaAs on GaAs surfaces*, Appl. Phys.Lett. **63**, 3202 (1993)
- [46] W C W Chan, D. J Maxwell, X. H Gao, R. E Bailey, M. Y. Han & S. M. Nie, Luminescent quantum dots for multiplexed biological detection and imaging. Curr Opin Biotechnol 13 40 (2002).
- [47] F. Wang, W. B. Tan, Y. Zhang, X. P. Fan & M. Q. Wang. Luminescent nanomaterials for biological labelling. Nanotechnology 17, R1 (2006);17: R1–R13
- [48] S. athak, S. K. Choi, N. Arnheim & M. E. Thompson. *Hydroxylated quantum dots as luminescent probes for in situ hybridization*. J Am Chem Soc **123** 4103(2001).
- [49] D. Gerion, W. J. Parak, S. C. Williams, D. Zanchet, C. M. Micheel & A. P. Alivisatos, *Sorting fluorescent nanocrystals with DNA*. J Am Chem Soc **124** 7070 (2002),
- [50] M. Y.Han,X. H. Gao, J. Z. Su & S. Nie S. *Quantum-dot-tagged microbeads for multiplexed optical coding of biomolecules*. Nat Biotechnol **19**, 631 (2001).
- [51] T. Jamieson, R. Bakhshi, D. Petrova, R. Pocock, M. Imani& A.M. Seifalian, *Biological applications of Quantum Dots*. Biomaterials., **28** 4717 (2007).
- [52] Moon Kee Choi, Jiwoong Yang, Taeghwan Hyeon and Dae-Hyeong Kim., *Flexible quantum dot light-emitting diodes for next-generation displays*, npj Flexible Electronics **2**, Article No:10 (2018)
- [53] R. C. Ashoori, H.L. Stormer, J. H. Weiner, L. N. Pfeiffer, S. J. Peatron, K. Baldwin and K. W. West, *Single-electron*

- *capacitance spectroscopy of discrete quantum levels* Phys. Rev. Lett. **68**, 3088(1992)
- [54] B. Meurer, D. Heitmann and K. Ploog, *Single-electron charging of quantum-dot atoms*, Phys. Rev. Lett. **68**, 1371(1992).
- [55] B. Su, V. J. Goldman and J.E. Cuningham, *Single-electron tunneling in nanometer-scale double-barrier heterostructure devices.*, Phys. Rev. B **46**,7644 (1992).
- [56] D.J Norris, A. Sacra, C. B Murray and M. G Bawendi, *Measurement of the size dependent Hole spectrum in CdSe quantum dots*, Phys. Rev. Lett. **72** 2612 (1994).
- [57] D. J Norris And M. G Bawendi, *Measurement and assignment of the size-dependent optical spectrum in CdSe quantum dots*, Phys Rev. B **53** 16338 (1996).
- [58] G. Medeiros- Ribeiro, F. G. Pikus, P. M. Petroff and A. L. Efros, Single-electron charging and Coulomb interaction in InAs selfassembled quantum dot arrays, Phys. Rev. B **55** 1568 (1997)
- [59] L. W. Molenkap, K. F lensberg and M. Kemernik, *Scaling of the Coulomb Energy Due to Quantum Fluctuations in the Charge on a Quantum Dot*, Phys. Rev. B **75**, 4282 (1995).
- [60] K. Flensberg, Capacitance and conductance of mesoscopic systems connected by quantum point contacts, Phys. Rev. Let. **48** 11156 (1993).
- [61] V. D Kulakovski et al. Fine Structure of Biexciton Emission in Symmetric and Asymmetric CdSe/ZnSe Single Quantum Dots, Phys. Rev. Lett. **82** 1780 (1999)]
- [62] S. Raymond et al, Exciton droplets in zero dimensional systems in a magnetic field, Solid State Commun. **101** 883 (1997)
- [63] R Rinaldi et al., Magneto-optical properties of strain-induced  $In_xGa_{1-x}As$  parabolic quantum dots, Phys. Rev. B **57** 9763 (1998)

- [64] S. Sauvage et al., *Third-harmonic generation in InAs/GaAs self-assembled quantum dots*, Phys.Rev.B **59**, 9830 (1999)
- [65] H. Lee, R. Low-Webb, W. Yang and P.C. Sercel, *Determination* of the shape of self-organized InAs/GaAs quantum dots by reflection high energy electron diffraction, Appl. Phys. Lett. **72** 812 (1998)
- [66] E. Dekel, D. Gershoni, E. Ehrenfreund, D. Spektor, J. M. Garcia, and P. M. Petroff, *Multiexciton Spectroscopy of a Single Self-Assembled Quantum Dot.*, Phys. Rev. Lett. **80** 4991 (1998).
- [67] A. Patane et al., Experimental studies of the multimode spectral emission in quantum dot lasers J. Appl. Phys. 87 1943 (2000).
- [68] S. Zhao et al, Single photon emission from graphene quantum dots at room temperature., Nature. Commun, **9** 3470 (2018).
- [69] Al. L.Efros and A.L. Efros, *Interband Absorption of Light in a Semiconductor Sphere*'.,Sov. Phys. Semicond. **16**, 772 (1982).
- [70] L. E. Brus, Electron–electron and electron-hole interactions in small semiconductor crystallites: The size dependence of the lowest excited electronic state., J. Chem. Phys. **80**, 4403 (1984).
- [71] J. Y. Marzin and G. Bastard, *Calculation of the energy levels in InAsGaAs quantum dots*, Solid State Commun. **92** 437 (1994).
- [72] S. K. Yip, Magneto-optical absorption by electrons in the presence of parabolic confinement Potentials., Phys. Rev. B 43 1707 (1991).
- [73] S. W. Gu and K. X. Guo, *Nonlinear optical rectification in the electric-field-biased parabolic quantum dots.* Soid state Commun. **89** 1023 (1993).
- [74] J. L Zhu, J. H. Zhao and J. J Xiong, *Neutral and negative donors in quantum dots*, J. Phys. Condens. Matt. **6**, 5097(1994).
- [75] G. W. Bryant, *Electronic structure of ultrasmall quantum-well boxes*, Phys. Rev. Lett. **59**, 1140 (1987).

- [76] A. Kumar, S. E Laux and F. Stern, *Electron states in a GaAs quantum dot in a magnetic field*, Phys. Rev. B **42** 5166 (1990).
- [77] D. Pfannkuche, V. Gudmundsson P. A. Maksym, *Comparison of a Hartree, a Hartree-Fock, and an exact treatment of quantum-dot helium,* Phys. Rev. B **47**, 2244 (1993).
- [78] N. F. Johnson and M. C. Pyne, *Exactly solvable model of interacting particles in a quantum dot.*, Phys. Rev. Lett. **67** 1157 (1991).
- [79] S. Taut, Two electrons in a homogeneous magnetic field: particular analytical solutions., J. Phys. A, Math. Gen. 27, 1045(1994).
- [80] R. Berkovits and B. L. Altshuler, Compressibility, capacitance, and ground-state energy fluctuations in a weakly interacting quantum dot., Phys. Rev. B 55 5297 (1997).
- [81] R. Kotlyar and S. Das Sarma, *Persistent current in an artificial quantum-dot molecule.*, Phys. Rev. B **55** R10205 (1997)
- [82] P. W.Brouwer and I. L. Aleiner, *Effects of Electron-Electron Interaction on the Conductance of Open Quantum Dots.*, Phys. Rev. Lett. **82** 390 (1999)
- [83] J. Bellessa and M. Combescot, Size dependance of impurity levels in quantum dots: exact versus variational results., Solid State Commun. 111, 275 (1999).
- [84] J. M. Ferreyra and C. R. Proetto, *Excitons in inhomogeneous quantum dots*, Phys. Rev. B **57** 9061 (1998).
- [85] A. D.Andreev and A.A. Lipovskii, *Anisotropy-induced optical transitions in PbSe and PbS spherical quantum dots.*, Phys. Rev. B **59** 15402 (1999).
- [86] C.H Henry and K. Nassau., *Lifetimes of Bound Excitons in CdS*. Phys. Rev. B **1** 1628 (1970).
- [87] G. Bastard, E.E. Mendez, L.L. Chang and L. Esaki, *Exciton binding energy in quantum wells.*, Phys. Rev.B. **26** 1947 (1982).

- [88] Marcos H. Degani and Oscar Hipolito., *Exciton binding energy in quantum wells.*, Phys. Rev. B **35** 9345 (1987).
- [89] Garnett W. Bryant, Excitons in quantum boxes: Correlation effects and quantum confinement, Phys. Rev. B **37** 8763 (1988).
- [90] Y. Z. Hu, et al., *Biexcitons in semiconductor quantum dots.*, Phys. Rev. Lett **64** 1805 (1990)
- [91] G.T. Einevoll, *Confinement of excitons in quantum dots.*, Phys. Rev. B **45** 3410 (1992).
- [92] T. Takagahara and K. Takeda, *Theory of the quantum confinement effect on excitons in quantum dots of indirect-gap materials.*, *Phys Rev B* **46** 15578 (1992)
- [93] R. Rinaldi et al., Exciton Binding Energy in GaAs V-Shaped Quantum Wires., Phys. Rev. Lett 73 2899 (1994).
- [94] Guy Lamouche and Yves Lepine, Ground-state energy of an exciton in a quantum-dot superlattice grown on a terraced substrate., Phys. Rev. B **54** 4811(1996)
- [95] W. Heller, U. Bockelmann, G. Abstreiter, *Electric-field effects on excitons in quantum dots.*, *Phys. Rev. B* **57** 6270 (1998)
- [96] K. Oshiro, K. Akai and M. Matsuura, Size dependence of polaronic effects on an exciton in a spherical quantum dot., *Phys. Rev. B* **59** (1999) 10850.
- [97] Jakyoung Song and Sergio E. Ulloa, *Magnetic field effects on quantum ring excitons.*, *Phys. Rev. B* **63** (2001) 125302];
- [98] I. Karabulut, H. Safak and M. Tomak, Excitonic effects on the nonlinear optical properties of small quantum dots., J. Phys. D: Appl. Phys. 41 (2008) 155104
- [99] S. Sakiroglu et al., Ground state energy of excitons in quantum dot treated variationally via Hylleraas-like wavefunction., Chin. Phy. B 18 (2009) 1578

- [100] Jefferson Florez and Angela Camacho, Excitonic effects on the second-order nonlinear optical properties of semi-spherical quantum dots., Nanoscale Research Lett. 6 (2011) 268
- [101] P. Nandakumar, Y. Murti & C. Vijayana, *Optical absorption and photoluminescence studies on CdS quantum dots in Nafion*. J. App. Phys. **91**, 1509 (2002).
- [102] D. Gammon, E. S.Snow, B.V. Shanabrook, D. S. Katzer & D. Park., *Fine structure splitting in the optical spectra of single GaAs quantum dots*. Phy. Rev. Lett **76**, 3005 (1996).
- [103] J. Gu, & J. Liang, Energy spectra of an exciton in a Gaussian potential and magnetic field. Phy. Lett. A **323**, 132 (2004).
- [104] R. D. Schaller & V. I. Klimov, *High efficiency carrier multiplication in PbSe nanocrystals: Implications for solar energy conversion.* Phys. Rev.Lett **92** 186601 (2004).
- [105] A. Khan, K. Balakrishnan & T. Katona, *Ultraviolet light-emitting diodes based on group three nitrides*. Nat. Photonics **2**, 77 (2008).
- [106]. G. T. Einevoll, Confinement of excitons in quantum dots. Phy. Rev. B **45**, 3410 (1992).
- [107] K. X. Guo, Y. B. Yu, Nonlinear Optical Susceptibilities in Si/SiO2 Parabolic Quantum Dots. Chinese. J. Phys. 43, 932 (2005).
- [108] J. H. Yuan, Y. Zhang, D. Huang, J. Zhang, & X. Zhang, Exciton effects on dipole-allowed optical absorptions in a two-dimensional parabolic quantum dot. Journal of Luminescence. 143, 558 (2013).
- [109] L. D. Landau, *Electron motion in crystal lattices*. Phys Z. Sowjetunion **3**, 664 (1993).
- [110] Pekar., S. I., ZhETF **16** 341 (1946).
- [111] D. Emin, *Polarons*, Cambridge University Press, 2013

- [112] A.S. Alexandrov & N.F. Mott, *Bipolarons*, Rep. Prog. Phys. B **57**, 1197(1994).]
- [113] J.T. Devreese & A.S. Alexandrov, *Fröhlich polaron and bipolaron: recent developments*, Rep. Prog. Phys. **72**, 066501 (2009)
- [114] S. Scmit-Rink, D.A.B. Miller and D. S. Chemla, *Theory of the linear and nonlinear optical properties of semiconductor microcrystallites*. Phys. Rev. B 35, 8113 (1987)
- [115] U. Bockelmann and G. Bastar., *Phonon scattering and energy relaxation in two-, one-, and zero- dimensional electron gases.* Phys. Rev. B **42** 8947(1990)
- [116] M. C. Klein, F. Hache, D. Ricard and C. Flytzanis., *Size dependence of electron-phonon coupling in semiconductor nanospheres: The case of CdSe.* Phys. Rev. B **42** 11123(1990)
- [117] M. G. Bawendi, W.L.Wilson, L. Rothberg, P.J Carrol, T. M. Jedju, M. L. Steigerwald and L. E Brus. *Electronic structure and photoexcited-carrier dynamics in nanometer-size CdSe clusters*. Phys. Rev. Lett. 65 1623 (1990)
- [118] K.D. Zhu and S. W. Gu, *Polaronic states in a harmonic quantum dot*. Phys. Lett. A **163** 435(1992).
- [119] K. D Zhu and S. W. Gu *The polaron self-energy due to phonon confinement in quantum boxes and wires.* J. Phys. Condens. Matter **4**, 1291 (1992).
- [120] K. D. Zhu and S. W. Gu. Cyclotron resonance of magnetopolarons in a parabolic quantum dot in strong magnetic fields. Phys. Rev. B 47, 12941 (1993).
- [121] T. C Au-Yeung, S. L Kho, S. W.Gu, L. H. Hong and E. Mc.Wong, *The cyclotron resonance of a three-dimensional impurity magnetopolaron in the presence of a strong parabolic potential* J. Phys. Condens. Matter **6**, 6761 (1994).

- [122] C Y Chen, P. W. Jin, W.S Li and D. I. Lin, *Thickness effect on impurity-bound polaronic energy levels in a parabolic quantum dot in magnetic fields* Phys. Rev. B 56, 14913 (1997).
- [123] S. Mukhopadhyay and A. Chatterjee, Rayleigh-Schrödinger perturbation theory for electron-phonon interaction effects in polar semiconductor quantum dots with parabolic confinement. Phys. Lett. A., **204**, 411(1995)]
- [124] S. Mukhopadhyay and A. Chatterjee, *Suppression of Zeeman splitting in a GaAs quantum dot*. Phys. Rev B., **59** R7833(1999)
- [125] S. Yanar, A. Sevim, B. Boyacioglu, M. Saglam, S. Mukhopadhyaya and A.Chatterjee., *Polaronic effects in a Gaussian quantum dot.* Superlattices and Microstructures **43** 208 (2008).
- [126] Luiz Antonio Ribeiro, Jr., Wiliam Ferreira da Cunha, Antonio Luciano de Almeida Fonseca, Geraldo Magela E Silva and Sven Stafström, *Transport of Polarons in Graphene Nanoribbons* J. Phys. Chem. Lett. **6**, 510(2015).
- [127] Luiz Antonio Ribeiro, Jr, Gesiel Gomes da Silva, Rafael Timóteo de Sousa Jr., Antonio Luciano de Almeida Fonseca, Wiliam Ferreira da Cunha and Geraldo Magela e Silva, Spin-Orbit Effects on the Dynamical Properties of Polarons in Graphene Nanoribbons. Scientific Reports, 8:1914 1 (2018).

2

# Effects of Magnetic field on the Exciton Energy levels of a GaAs Quantum Dot: Applications to Excitonic Lasers

#### Abstract

We have studied the energetics of an exciton confined in two and threedimensional Gaussian GaAs quantum dots in a magnetic field employing a variational approach, the 1/N expansion technique and the shifted 1/N expansion scheme. We have calculated the ground state energy of the exciton and its binding energy in terms of the effective confinement length, the strength of confinement and the magnetic field strength and made a comparison of our results with the ones that have been reported. The Ritz variational approach leads to an upper limit to the energy while the 1/N expansion technique is known to yield a lower bound. We have demonstrated that the energies calculated employing the shifted 1/N expansion scheme match remarkably well with the exact results obtained numerically. The behaviour of the size of the exciton as well as its oscillator strength has also been investigated with respect to the effective confinement length of the quantum dot. Finally, the energies of the exciton excited states have been calculated with the help of the shifted 1/N expansion technique and it has been predicted that by controlling the parameters of the quantum dot one can generate a desired number of bound excitonic states in a quantum dot. This observation is important in view of achieving excitonic lasers using quantum dots.

#### 2.1 INTRODUCTION

Excitons are one kind of excitations in QDs that are fundamentally important in determining several key optical properties semiconductors [1-3]. Besides depending on the electrostatic interaction between the electron and the hole, the exciton energy spectra depend crucially on the confinement potential of the quantum dot (QD) [4-7]. During the last two decades, there have been several studies in the field of excitonic physics in the context of QDs. Einevoll has considered small CdS and ZnS QDs and studied the exciton problem in these systems theoretically [8]. He has calculated and compared the exciton energies for dots having diameter in the range of 10-80 Å. Que has studied the excitonic properties in a parabolic OD (POD) [9]. Jaziri et al. [10] have examined the role of electric and magnetic fields on excitons in PQD using a combination of the perturbation and variational theories. Xiao [11] has considered a spherical GaAs QD in a magnetic field and determined the exciton binding energy (BE) in this system with the help of a variational technique. The exciton binding energies in finite potential quantum discs of GaAs have been calculated by Safwan et al. [12].

As mentioned earlier, QD with Gaussian confinement will be called a Gaussian QD (GQD). Though much attention has been directed to the study of exciton ground-state (GS) problem in GQD, only a very few studies are available on the exciton excited states [13, 14]. Undoubtedly, the role of the excited states of an exciton is very crucial from in the context of infrared and two-photon spectroscopic studies [15]. Xie [16]

has determined the GS and excited state (ES) excitonic energies in GQD using the method of matrix diagonalization.

A magnetic field is known to produce an added localizing potential which may be utilized to control the electron's motion in a more regulated way. Gu and Liang [14] have examined the role of a magnetic field on the exciton energy levels in GQD employing the technique of matrix diagonalization. As the exciton problem in GQD is not exactly soluble, an exact numerical diagonalization certainly serves a useful purpose. But, quite a few times, the numerical solutions may not offer some of the most intriguing and important aspects of the physical system under consideration. Also, the wave function chosen in course of matrix diagonalization procedure hardly offers any understanding or insight about the physics of the system unlike in the case of analytical methods. It is therefore only appropriate to devise approximate analytical methods that would incorporate all the salient aspects of the system and provide results that would agree well with the numerical data.

In this chapter we present our calculation of the GS exciton energy and the corresponding BE in a spherically symmetric GQD placed in a magnetic field. We show how the GS energy and BE of the exciton vary with the QD size, magnetic field strength and the potential depth with the help of the conventional variational approach, the  $\frac{1}{N}$  - expansion technique and the shifted  $\frac{1}{N}$  - expansion scheme. We also study how the exciton size and oscillator depend on QD size. Finally, we calculate the ES excitonic energies for some sets of parameter values.

#### 2.2 MODEL

An exciton in GQD in a magnetic field  $\mathbf{B}$  (0, 0, B) may be described by the Hamiltonian

$$H = \sum_{i=e}^{\infty} \left[ \frac{1}{2m_i^*} \left( \boldsymbol{p}_i + \frac{q_i}{c} \boldsymbol{A}_i \right)^2 - V_0 e^{-r_i^2/2R^2} \right] - \frac{e^2}{\varepsilon |\boldsymbol{r}_e - \boldsymbol{r}_h|}, \quad (2.1)$$

where i=e (h) denotes an electron (a hole),  $q_e$  ( $q_h$ ) denotes the electron (hole) charge,  $\mathbf{r}_i=\mathbf{r}_e$  ( $\mathbf{r}_h$ ) refers to the electron (hole) coordinates and  $\mathbf{p}_i=\mathbf{p}_e$  ( $\mathbf{p}_h$ ) the corresponding momentum operator,  $m_i^*=m_e^*$  ( $m_h^*$ ) stands for the band mass of the electron (hole),  $\mathbf{A}_i=\mathbf{A}_e(\mathbf{A}_h)$  describes the vector potential for the electron (hole) corresponding to  $\mathbf{B}$ , R and  $V_0$  give the range and depth of GQD respectively and  $\varepsilon$  represents the permittivity of the QD material. Writing the  $\mathbf{A}=\left(-\frac{By}{2},\frac{Bx}{2},0\right)$  (symmetric gauge), we have, for the Hamiltonian,

$$H = \sum_{i=e,h} \left[ -\frac{\hbar^2}{2m_i^*} \nabla_i^2 - V_0 e^{-r_i^2/2R^2} + \frac{1}{8} m_i^* \omega_{ci}^2 r_i^2 \right] + \frac{1}{2} (\omega_{ce} L_{ze} - \omega_{ch} L_{zh}) - \frac{e^2}{\varepsilon |\mathbf{r}_e - \mathbf{r}_h|}.$$
(2.2)

The spin of the charge carriers is not considered here.  $\omega_c$  represents the cyclotron frequency and  $L_{ze(h)}$  is the orbital angular momentum of the electron (hole) in the z direction.

#### 2.3 FORMULATION

Now let us rewrite the Hamiltonian by adding and subtracting the terms  $\sum_{i=e,h}\frac{1}{2}m_i\omega_i^2r_i^2+V_{0i}.$  The total Hamiltonian H is then written as :  $H=H_0+H_1$ , with

$$H_{0} = \sum_{i=e,h} \left[ -\frac{\hbar^{2}}{2m_{i}^{*}} \nabla_{i}^{2} + \frac{1}{2} m_{i}^{*} \tilde{\omega}_{i}^{2} r_{i}^{2} \right] - V_{0} + \frac{1}{2} (\omega_{ce} L_{ze} - \omega_{ch} L_{ze}) - \frac{e^{2}}{\varepsilon |\mathbf{r}_{e} - \mathbf{r}_{h}|},$$
(2.3)

$$H_1 = -\lambda \sum_{i=e,h} \left[ \frac{1}{2} m_i^* \omega_{i0}^2 r_i^2 + V_0 \left( e^{-\frac{r_i^2}{2R^2}} - 1 \right) \right]$$
 (2.4)

where

$$\tilde{\omega}_i^2 = \omega_{i0}^2 + \frac{\omega_{ci}^2}{4} \; ; \qquad \omega_{i0}^2 = \frac{V_0}{m_i^* R^2},$$
 (2.5)

For parabolic confinement,  $\lambda$  is equal to zero and in the case of Gaussian confinement,  $\lambda$  is equal to 1. For GS, the angular momentum terms can be ignored. Furthermore, we make an assumption that  $H_1$  essentially renormalizes the frequency  $\tilde{\omega}_i$ . Thus we replace  $H_1$  by

$$H_{1} = \lambda \sum_{i=e,h} \left[ \frac{V_{0}}{\langle r_{i}^{2} \rangle} - \frac{1}{2} m_{i}^{*} \omega_{0i}^{2} - \frac{V_{0} \langle e^{-r_{i}^{2}/2R^{2}} \rangle}{\langle r_{i}^{2} \rangle} \right] r_{i}^{2} = \lambda \sum_{i=e,h} \omega_{i}^{2} r_{i}^{2}, \quad (2.6)$$

where the averaging state is GS of the Hamiltonian:  $\left[-\frac{\hbar^2}{2m_i^*}\nabla_i^2 + \frac{1}{2}m_i^*\tilde{\omega}_i^2r_i^2\right]$  [11]. Thus the wave functions we have used to find the expectation values are:

For a three-dimensional (3D) QD,

$$\phi_0 = \left(\frac{m\widetilde{\omega}_i}{\pi\hbar}\right)^{3/4} e^{-m\widetilde{\omega}_i r^2/2\hbar} \quad , \tag{2.7}$$

and a for two-dimensional (2D) QD,

$$\phi_0 = \left(\frac{m\widetilde{\omega}_i}{\pi\hbar}\right)^{1/2} e^{-m\widetilde{\omega}_i r^2/2\hbar} \ . \tag{2.8}$$

Since for three dimensions,

$$\langle r_e^2 \rangle = \langle r_h^2 \rangle = \frac{3}{2} \left( \frac{\hbar}{m\widetilde{\omega}} \right)$$
 (2.9)

and

$$\langle e^{-r_e^2/2R^2} \rangle = \langle e^{-r_h^2/2R^2} \rangle = m\widetilde{\omega}^{3/2} \left( \frac{2R^2}{2m\widetilde{\omega}R^2 + \hbar} \right)^{3/2}$$
 (2.10)

and for two dimensions,

$$\langle r_e^2 \rangle = \langle r_h^2 \rangle = \frac{\hbar}{m\widetilde{\omega}},$$
 (2.11)

and

$$\langle e^{-r_e^2/2R^2} \rangle = \langle e^{-r_h^2/2R^2} \rangle = \frac{2m\widetilde{\omega}R^2}{2m\widetilde{\omega}R^2 + \hbar}, \qquad (2.12)$$

we can write  $\widetilde{\omega}_e^2 + 2(\lambda/m_e^*)\omega_e^2 = \widetilde{\omega}_h^2 + 2(\lambda/m_h^*)\omega_h^2 \equiv \omega^2$ . Now our problem with Gaussian potential reduces to a problem having an effective parabolic potential and the Hamiltonian becomes

$$H = \frac{p_e^2}{2m_e^*} + \frac{1}{2}m_e^*\omega^2 r_e^2 + \frac{p_h^2}{2m_h^*} + \frac{1}{2}m_h^*\omega^2 r_h^2 - 2V_0 - \frac{2}{\varepsilon|\mathbf{r}_e - \mathbf{r}_h|}.$$
 (2.13)

Now we introduce two new coordinates  $\boldsymbol{r}$  and  $\boldsymbol{R}$  to solve this problem. We define:  $\boldsymbol{r}=(\boldsymbol{r}_e-\boldsymbol{r}_h)$  and  $\boldsymbol{R}=(m_e^*\boldsymbol{r}_e+m_h^*\boldsymbol{r}_h)/M$ , where  $M=m_e+m_h$ . Using the corresponding momenta:  $\boldsymbol{p}=-i\hbar\nabla_r$  and  $\boldsymbol{P}=-i\hbar\nabla_R$ , the electron and hole momenta  $\boldsymbol{p}_e$  and  $\boldsymbol{p}_h$  are then written as:  $\boldsymbol{p}_e=\boldsymbol{p}+(m_e^*/M)\boldsymbol{P}$ ;  $\boldsymbol{p}_h=-\boldsymbol{p}+(m_h^*/M)\boldsymbol{P}$ . The Hamiltonian H now reads

$$H = H_R + H_r \tag{2.14}$$

with

$$H_r = -\nabla_r^2 + \frac{1}{4}\omega^2 r^2 - \frac{2}{r} - 2V_0$$
,  $H_R = -\nabla_R^2 + \frac{1}{4}\omega^2 R^2$ , (2.15)

where for a 3D QD,

$$\omega = \left[ (1 - \lambda) \frac{\omega_0^2}{2} + \frac{\omega_c^2}{8} + \frac{2\tilde{\omega}\lambda V_0}{3} - \frac{2\tilde{\omega}\lambda V_0}{3} \left( \frac{\tilde{\omega}R^2}{1 + \tilde{\omega}R^2} \right)^{\frac{3}{2}} \right]^{1/2}, \quad (2.16)$$

and for a 2D QD,

$$\omega = \left[ (1 - \lambda) \frac{\omega_0^2}{2} + \frac{\omega_c^2}{8} + 2\lambda V_0 \left( \frac{\tilde{\omega}}{1 + \tilde{\omega}R^2} \right) \right]^{\frac{1}{2}}$$
 (2.17)

Here all the energies are measured in Rydberg units  $R_y^* = (\mu e^4/2\hbar^2 \epsilon^2)$  and the lengths in Bohr radius  $a_0^* = (\hbar^2 \epsilon/\mu e^2)$ ,  $\mu(=[m_e^* m_h^*]/M)$  being the reduced mass of the electron-hole system.

#### 2.4 VARIATIONAL METHOD

#### 2.4.1 THE EXCITON GROUND STATE ENERGY

To calculate the energies of an exciton in QD, we have used the Ritz variational method. If  $\Psi(r_e, r_h)$  is the eigenfunction of H, then we can write:

$$\Psi(\mathbf{r}_{e}, \mathbf{r}_{h}) = \phi(\mathbf{r})\chi(\mathbf{R}) \tag{2.18}$$

where  $\phi(r)$  and  $\chi(R)$  are the eigenfunctions of  $H_r$  and  $H_R$  with the eigenvalues  $E_r$  and  $E_R$  respectively. The variational energy is given by,

$$E = \frac{\langle \psi | H | \psi \rangle}{\langle \psi | \psi \rangle} \tag{2.19}$$

Since we have:  $H = H_R + H_r$ , the exciton energy E is given by:

$$E = E_R + E_r = \frac{\langle \psi | H_R | \psi \rangle}{\langle \psi | \psi \rangle} + \frac{\langle \psi | H_r | \psi \rangle}{\langle \psi | \psi \rangle}$$
(2.20)

The eigen values of the  $H_R$  is well known (Harmonic oscillator). Therefore, the GS energy for the centre of mass (CM) motion is  $E_R$  (=  $3\omega/2$ ) in 3D. In general, it is not possible to do the exact analytical evaluation of  $E_r$  and hence we employ the conventional variational approach with the trial wave function:

$$\phi(\mathbf{r}) \sim e^{-\alpha r^2 - \beta r} \tag{2.21}$$

where  $\alpha$  and  $\beta$  are variational parameters.

#### 2.4.2 THE EXCITON BINDING ENERGY.

The exciton BE,  $E_b$  is defined as:

$$E_b = (E_e + E_h - E) (2.22)$$

where  $E_e$  ( $E_h$ ) denotes the electron (hole) GS energy in the QD.

#### 2.4.3 THE SIZE OF EXCITON.

The size of the exciton is given by:

$$\langle r \rangle = \langle \Psi | r | \Psi \rangle \tag{2.23}$$

#### 2.4.4 THE OSCILLATOR STRENGTH.

Another important quantity we are interested in is the exciton oscillator strength. We can derive the f – sum rule for a multi-electron system as [17]

$$\sum_{s} f_{s,t} = N_e \tag{2.24}$$

where the summation is to be performed over all states,  $N_e$  denotes the electron number and

$$f_{s,t} = \frac{2|\langle s|\sum_{i} P_{x_i}|t\rangle|^2}{m_e^*(E_s - E_t)}$$
 (2.25)

is the oscillator strength,  $m_e^*$  being the Bloch electron mass and i running from 1 to  $N_e$ . The GS exciton oscillator strength is calculated as,

$$f_{ex} = \frac{2|\langle ex | \sum_{i} P_{x_i} | 0 \rangle|^2}{m(E_{ex} - E_0)} . \tag{2.26}$$

We can re-write this expression for the exciton oscillator strength [18] in the envelop-function approximation as,

$$f_{ex} = \frac{2P^2}{m_0(E_{ex} - E_0)} \left| \int \Psi(\mathbf{r}_e, \mathbf{r}_e) d\mathbf{r}_e \right|^2,$$
 (2.27)

where P describes the intracell matrix-element effects,  $m_0$  is the bare electron mass, and  $E_{ex} - E_0 = E + E_g$ , with  $E_g$  as the optical band gap. Making use of Eq. (2.18), we can write

$$\Psi(\mathbf{r}_e, \mathbf{r}_e) = \chi(\mathbf{r}_e)\phi(0) \tag{2.28}$$

so that Eq. (2.27) becomes

$$f_{ex} = \frac{2P^2}{m_0(E_{ex} - E_0)} |\phi(0)|^2 \left| \int \chi(r_e) dr_e \right|^2$$
 (2.29)

### 2.5 $\frac{1}{N}$ – EXPANSION TECHNIQUE

The  $\frac{1}{N}$  - expansion technique, where N is the dimensionality of the system, is a powerful approach to obtain the energies of rotationally invariant systems in quantum mechanics [19-22]. The  $\frac{1}{N}$  -expansion technique hinges on expanding the wave function and energy in powers of the parameter 1/k = 1/(N+2l), where l is the angular momentum quantum number. Since it is a non-perturbative method, it is suitable for all values of the interaction coefficients. The  $\frac{1}{N}$  -expansion technique often suffers from slow convergence problem. This particularly happens for higher energy levels. To circumvent this problem, Sukhatme and Imbo [20] have suggested a modified  $\frac{1}{N}$  -expansion scheme which is known as the shifted  $-\frac{1}{N}$  -expansion method. In this modified method, an additional parameter 'a' is introduced in the expansion parameter. The new expansion parameter is written as: 1/k = 1/(N+2l-a).

In N-dimensional (ND) space, the Schrödinger equation for the radial part R(r) is given by,

$$\left[ -\frac{\hbar^2}{2\mu} \left( \frac{d^2}{dr^2} + \frac{N-1}{r} \frac{d}{dr} \right) + \frac{l(l+N-2)}{2r^2} + V(r) \right] R = ER \quad (2.30)$$

where V(r) is a spherically symmetric potential. Making the substitution:  $R(r) = r^{-(N-1)/2}u(r)$  in Eq. (2.30), we get

$$-\frac{\hbar^2}{2\mu}\frac{d^2u}{dr^2} + \left(\frac{(k-1)(k-3)}{8\mu r^2} + k^2\tilde{V}(r)\right)u = Eu$$
 (2.31)

which is an effective 1D equation and where k=(N+2l) and  $\tilde{V}(r)=V(r)/k^2$ . For  $\frac{1}{N}$  —expansion, one starts from Eq. (2.31). In the shifted  $\frac{1}{N}$  —expansion, one brings in an extra parameter 'a' and the expansion parameter becomes:  $1/\bar{k}=1/(N+2l-a)$ . On using this new parameter, Eq. (2.31) reads

$$-\frac{d^2u}{dr^2} + \left(\frac{\left[\bar{k} - (1-a)\right]\left[\bar{k} - (3-a)\right]}{4r^2} + \bar{k}^2\tilde{V}(r)\right)u = Eu \quad (2.32)$$

where  $\tilde{V}(r) = V(r)/\bar{k}^2$  and we have chosen to work in units in which  $\hbar = 2\mu = 1$ . In the limit:  $N \to \infty$ ,  $\bar{k} \to \infty$ , and in this limit, leading term in E can be written as:

$$E_{\infty} = \bar{k}^2 (1/4r_0^2 + \tilde{V}(r_0)) = \bar{k}^2 V_{eff}(r_0)$$
 (2.33)

where at  $r=r_0$ , the effective potential  $V_{eff}(r)$  has the minimum. We now define:  $x=-\bar{k}^{1/2}(1-r/r_0)$  and perform a Taylor-series expansion of (2.33) around x=0. This gives

$$\left(-\frac{d^2}{dx^2} + \frac{\Omega^2}{4}x^2 + \varepsilon_0 + \hat{V}(x)\right)u(x) = \lambda u(x), \qquad (2.34)$$

where

$$\Omega = \left(3 + \frac{r_0 V''(r_0)}{V'(r_0)}\right)^{1/2},\tag{2.35}$$

$$\varepsilon_0 = \frac{\bar{k}}{4} - \frac{(2-a)}{2} + \frac{(1-a)(3-a)}{4\bar{k}} + r_0^2 \bar{k} \tilde{V}(r_0), \qquad (2.36)$$

$$\lambda = \frac{Er_0^2}{\bar{k}} \tag{2.37}$$

and

$$\hat{V}(x) = \frac{1}{\bar{k}^{1/2}} (\varepsilon_1 x + \varepsilon_3 x^3) + \frac{1}{\bar{k}} (\varepsilon_2 x^2 + \varepsilon_4 x^4) + \frac{1}{\bar{k}^{3/2}} \left( \delta_1 x + \delta_3 x^3 + \delta_5 x^5 + \frac{1}{\bar{k}^2} (\delta_2 x^2 + \delta_4 x^4 + \delta_6 x^6) + \cdots \right)$$
(2.38)

with

$$\varepsilon_1 = (2 - a) \tag{2.39}$$

$$\varepsilon_2 = -\frac{3(2-a)}{2} \tag{2.40}$$

$$\varepsilon_3 = \left[ -1 + \frac{r_0^5 V'''^{(r_0)}}{6\bar{k}^2} \right] \tag{2.41}$$

$$\varepsilon_4 = \left[ \frac{5}{4} + r_0^6 V^{\prime\prime\prime\prime}(r_0) / 24 \bar{k}^2 \right] \tag{2.42}$$

$$\delta_1 = -\frac{(1-a)(3-a)}{2} \tag{2.43}$$

$$\delta_2 = \frac{3(1-a)(3-a)}{4} \tag{2.44}$$

$$\delta_3 = 2(2 - a),\tag{2.45}$$

$$\delta_4 = -\frac{5(2-a)}{2},\tag{2.46}$$

$$\delta_5 = -\frac{3}{2} + \frac{r_0^7 V'''''(r_0)}{120\bar{k}^2},\tag{2.47}$$

$$\delta_6 = \frac{7}{4} + \frac{r_0^8 V'''''(r_0)}{720\bar{k}^2} \tag{2.48}$$

Incorporating the effect of  $\hat{V}(x)$  in (2.34) to fourth-order in perturbation theory, we get

$$\lambda_n = \lambda_n^{(0)} + \lambda_n^{(1)} + \lambda_n^{(2)} + \lambda_n^{(3)} + \lambda_n^{(4)} + \cdots$$
 (2.49)

$$\lambda_n^{(0)} = \varepsilon_0 + \left(n + \frac{1}{2}\right)\Omega \tag{2.50}$$

$$\lambda_n^{(0)} = \varepsilon_0 + \left(n + \frac{1}{2}\right) \tag{2.51}$$

$$\lambda_n^{(1)} = g[(1+2n)\tilde{\varepsilon}_2 + 3(1+2n+2n^2)\tilde{\varepsilon}_4]$$

$$+ g^2[(1+2n)\tilde{\delta}_2 + 3(1+2n+2n^2)\tilde{\delta}_4$$

$$+ 5(3+8n+6n^2+4n^3)\tilde{\delta}_6]$$
(2.52)

$$\lambda_n^{(2)} = -\frac{g}{\Omega} \left[ \tilde{\varepsilon}_1^2 + 6(1+2n)\tilde{\varepsilon}_1 \tilde{\varepsilon}_3 + (11+30n+30n^2)\tilde{\varepsilon}_3^2 \right] - \frac{g^2}{\Omega} \left[ (1+2n)\tilde{\varepsilon}_2^2 + 12(1+2n+2n^2)\tilde{\varepsilon}_2 \tilde{\varepsilon}_4 + 2(21+59n+51n^2+34n^3)\tilde{\varepsilon}_4^2 + 2\tilde{\varepsilon}_1 \tilde{\delta}_1 \right] + O(g^3)$$
(2.53)

$$\begin{split} &\lambda_{n}^{(3)} \\ &= \frac{g^{2}}{\Omega^{2}} [4\tilde{\varepsilon}_{1}^{2}\tilde{\varepsilon}_{2} + 36(1+2n)\tilde{\varepsilon}_{1}\tilde{\varepsilon}_{2}\tilde{\varepsilon}_{3} + 24(1+2n)\tilde{\varepsilon}_{1}^{2}\tilde{\varepsilon}_{4} \\ &+ 8(11+30n+30n^{2})\tilde{\varepsilon}_{2}\tilde{\varepsilon}_{3}^{2} + 8(31+78n+78n^{2})\tilde{\varepsilon}_{1}\tilde{\varepsilon}_{3}\tilde{\varepsilon}_{4} \\ &+ 12(57+189n+225n^{2}+150n^{3})\tilde{\varepsilon}_{3}^{2}\tilde{\varepsilon}_{4}] \\ &+ O(g^{3}) \end{split} \tag{2.54}$$

$$\lambda_n^{(4)} = -\frac{g^2}{\Omega^3} [8\tilde{\varepsilon}_1^3 \tilde{\varepsilon}_3 + 108(1+2n)\tilde{\varepsilon}_1^2 \tilde{\varepsilon}_3^2 + 48(11+30n+30n^2)\tilde{\varepsilon}_1 \tilde{\varepsilon}_3^3 + 30(31+109n+141n^2+94n^3)\tilde{\varepsilon}_3^4] + O(g^3)$$
(2.55)

where  $g = 1/\bar{k}$ ,  $\tilde{\varepsilon}_j = \varepsilon_j/(2\mu\Omega/\hbar)^{j/2}$ ,  $\tilde{\delta}_j = \delta_j/(2\mu\Omega/\hbar)^{j/2}$ . In the conventional  $\frac{1}{N}$  – expansion approach, 'a' is equal to zero whereas in the shifted scheme, 'a' is obtained from the prescription:  $E^{(-1)} = 0$ .

This yields:  $a = 2 - (2n + 1)\Omega$ . From Eq. (15), we can see that in the present case,  $V(r) = \omega^2 r^2 / 4 - 2/r - 2V_0$ . Results for the energies have been obtained by employing both the unshifted and the shifted versions of the  $\frac{1}{N}$  – expansion technique.

### 2.6 GROUND STATE RESULTS AND DISCUSSIONS

The theories delineated in Section 2.5 are fairly general and we can apply them to any QD. As an example, we consider a GaAs QD and choose:  $\varepsilon=12.8$ ,  $m_e^*=0.067m_e$  and  $m_h^*=0.099m_e$  (light-hole mass). Consequently, we obtain:  $a_0^*=17.7~nm$ ,  $R_y^*=3.1~meV$ ,  $E_g=1.51~eV$ ,  $P^2/m_0=1~eV$ . We furthermore introduce a quantity  $\gamma$  which is linear in B. More specifically,  $=e\hbar B/2\mu cR_y^*$ . It is easy to see that  $1\gamma=0.47226B$  (T) [9,11].

In Fig.2.1, we show the exciton electron/hole distributions in a GaAs QD. We find that the distribution decreases with increasing potential depth. Also, the hole distribution is little higher than the electron distribution. We see from Fig. 2.2 that the distribution decreases with increasing magnetic field.

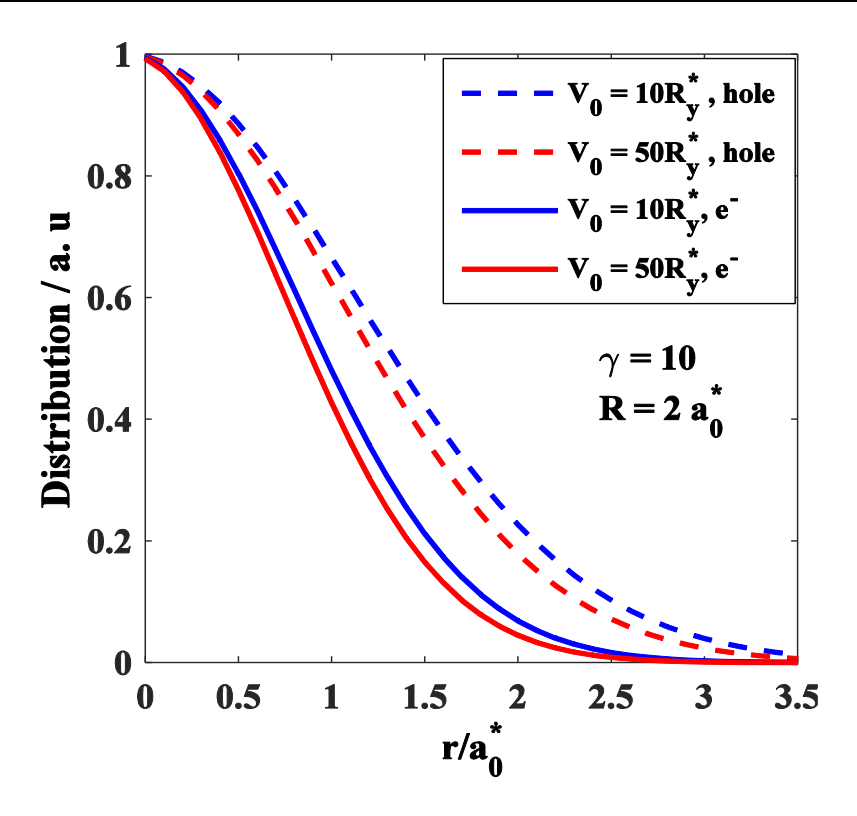


**Fig. 2.1** Exciton electron/hole distribution in a GaAs QD for two values of  $V_0$ .

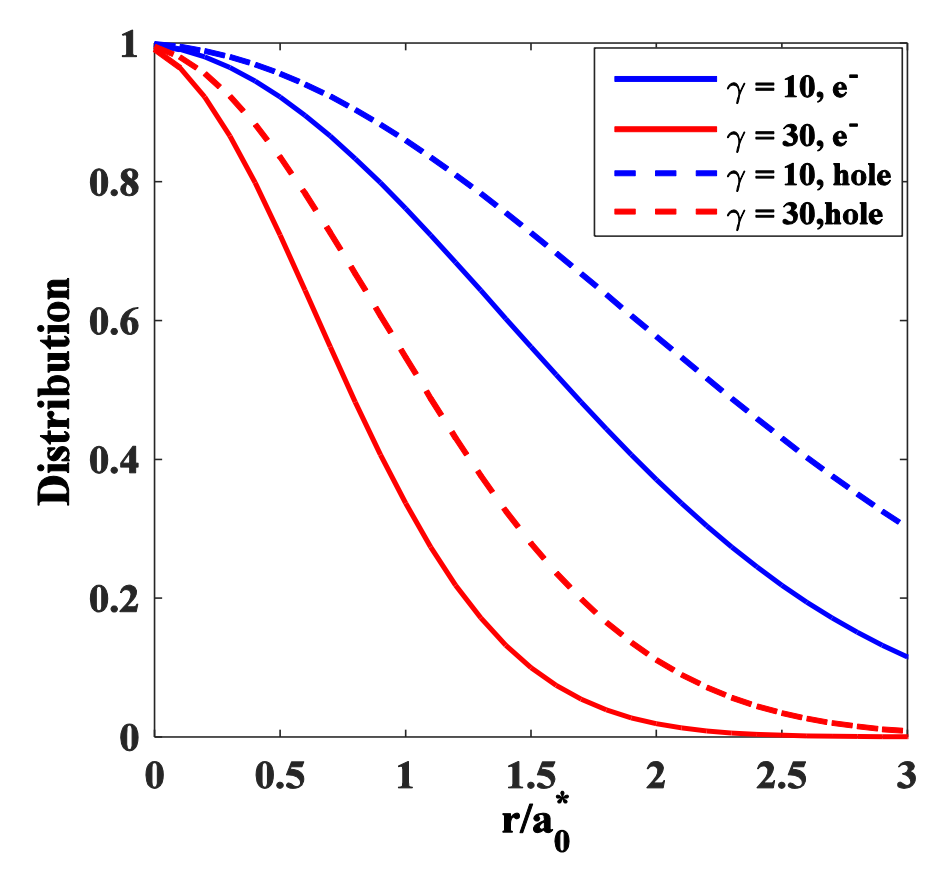


**Fig. 2.2** Exciton electron/hole distribution in a GaAs QD for two values of  $\gamma$ .

We calculate the light-hole exciton GS energies in 2D and 3D GaAs QDs with the help of the conventional variational approach,  $\frac{1}{N}$  – expansion technique and the shifted  $\frac{1}{N}$  – expansion scheme and plot them in Fig. 2.3 with respect to R for  $V_0 = 6meV$  and B = 10 T. All the methods used here suggest that the exciton energy rises monotonically as R is reduced and the rise in energy turns significantly rapid if the QD size is made smaller than a certain

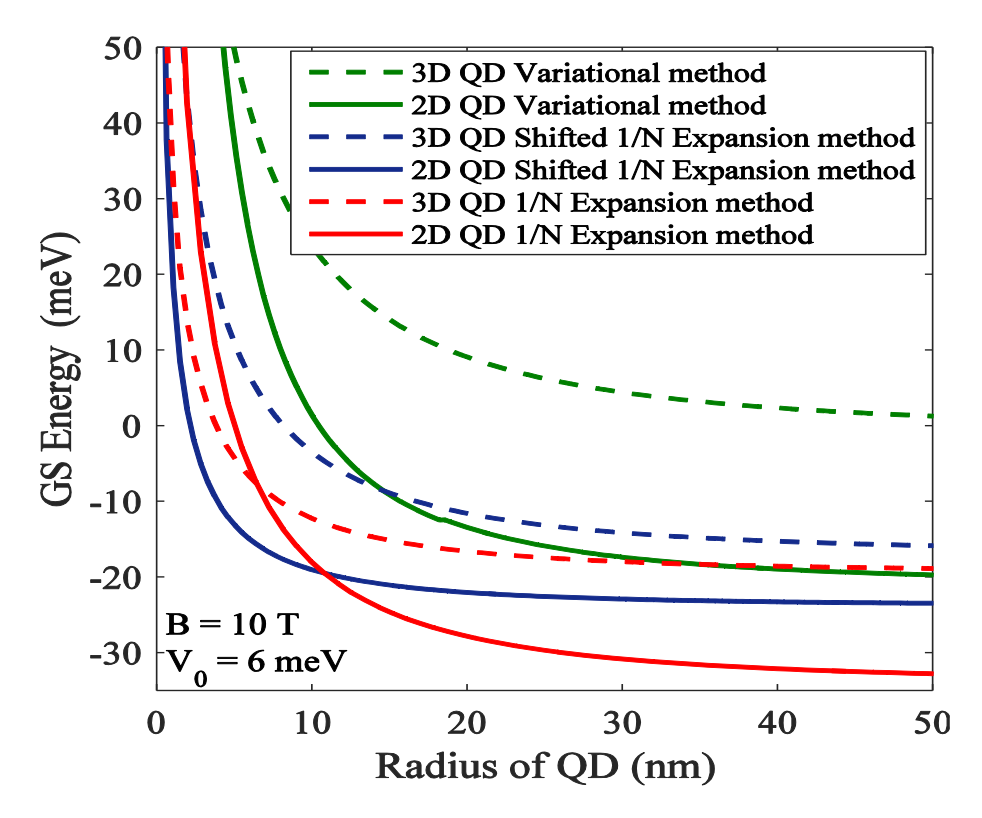


**Fig. 2.3** Exciton GS energy vs. QD size in 3D and 2D GQDs of GaAs for B = 10 T.

value. The explanation of this effect is simple. A decrease in R increases the uncertainty in the exciton momentum. Consequently, the exciton momentum itself is increased and hence the exciton kinetic energy also increases. Thus, the GS energy undergoes an enhancement as R is reduced. Also, it can be observed that the exciton GS has a lower energy value in 2D than in 3D, as the QD confinement effect is stronger in the former. The Ritz variational approach is known to provide an upper limit

to the energy while the  $\frac{1}{N}$  – expansion technique provides a lower limit. It is interesting that the GS energy obtained from the shifted  $\frac{1}{N}$  –expansion scheme lies somewhere in between the energies obtained from the other two methods.

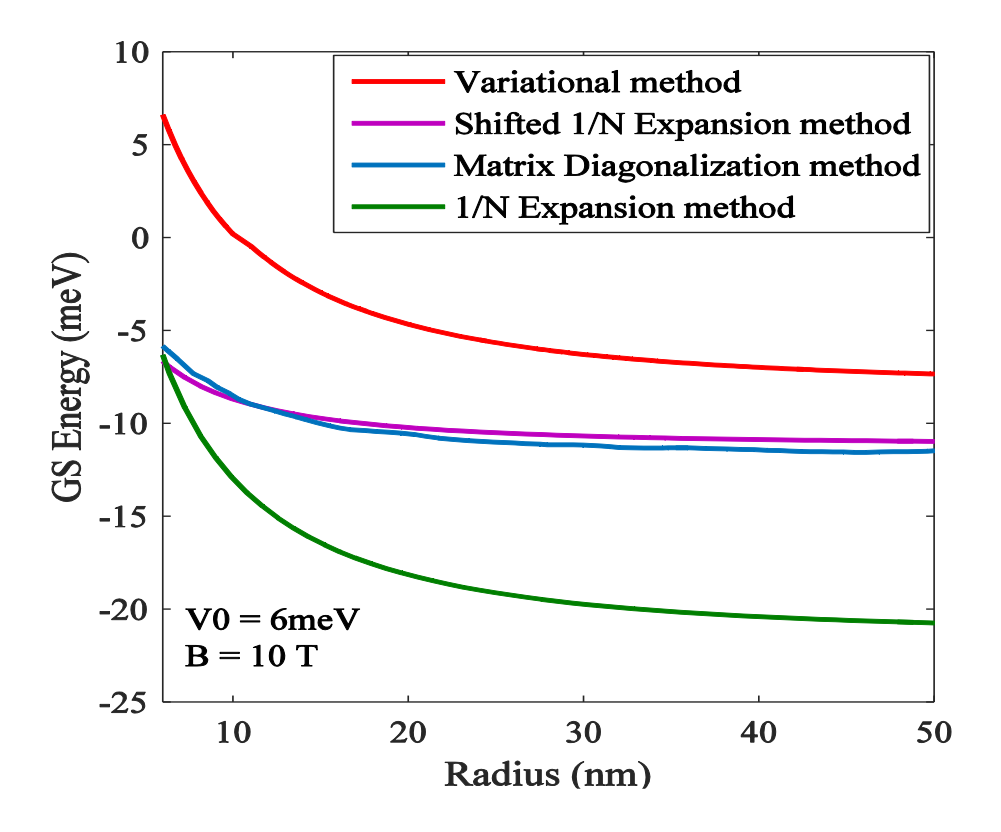


**Fig. 2.4** Exciton GS energies calculated by our methods and their comparison with those determined by Matrix diagonalization by Gu and Liang.

In Fig. 2.4, we have plotted the GS energy values calculated using the methods mentioned above. We have also plotted for comparison the results of Gu and Liang [14] obtained by the matrix diagonalization method. The comparison reveals that the energy values calculated by the shifted  $\frac{1}{N}$  —expansion scheme agree excellently with the exact results computed numerically.

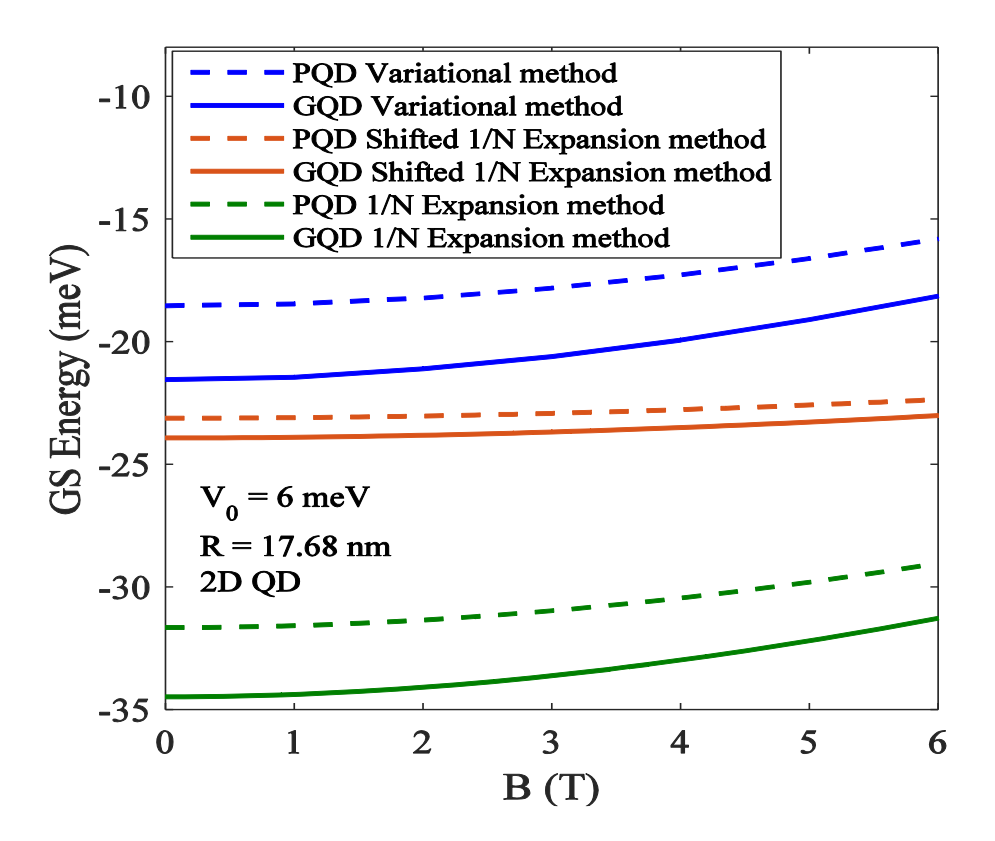


**Fig. 2.5** Exciton GS energy vs *B* in 2D PQD and GQD of GaAs.

We depict in Fig. 2.5, how the exciton GS energy for a 2D QD with  $V_0 = 6$  meV and R = 17.68 nm, varies with B. As B is increased, the GS energy is found to increase. This is again a behaviour one would normally expect. Though the parabolic and Gaussian potentials qualitatively provide a similar trend for the variation for the GS energy with B, the parabolic potential model apparently yields a higher value for the exciton GS energy.

We find that the potential profile becomes essentially irrelevant when the QD size is made sufficiently large (not shown here). Also it may be mentioned that the shifted  $\frac{1}{N}$ —expansion technique has quite a few palpable advantages as compared to the numerical method. First, as mentioned earlier, it gives the energy in the analytical form. Secondly, it can also provide analytical expression for the wave functions and thus offers more insight about the system. Thirdly, once the wave functions are determined, expectation values of different observables can be calculated. Finally, as we obtain the whole set of energy eigenvalues from this method, it becomes possible to obtain the thermodynamic averages of the quantities relevant to the system.

In Fig. 2.6, we present the behaviour of the exciton BE in GQD with respect to QD size. As the confinement potential is always negative, the necessary condition for the formation of an exciton bound state is that it should have a negative energy. However, this is not the sufficient condition for a stable bound state. For a stable bound state, BE must have a positive value. One may notice that as the QD confinement length is reduced, the exciton binding becomes stronger and the enhancement

in the strength of binding becomes more rapid at smaller confinement lengths. This may be understood as follows. As the QD size is reduced, the electron and hole have the higher probability of coming closer and consequently the attractive Coulomb interaction between them will rise. Our results also reveal that exciton binding is stronger in a 2D QD than in a QD system. As indicated by Fig. 2.3, the shifted  $\frac{1}{N}$  – expansion results are most trustworthy.

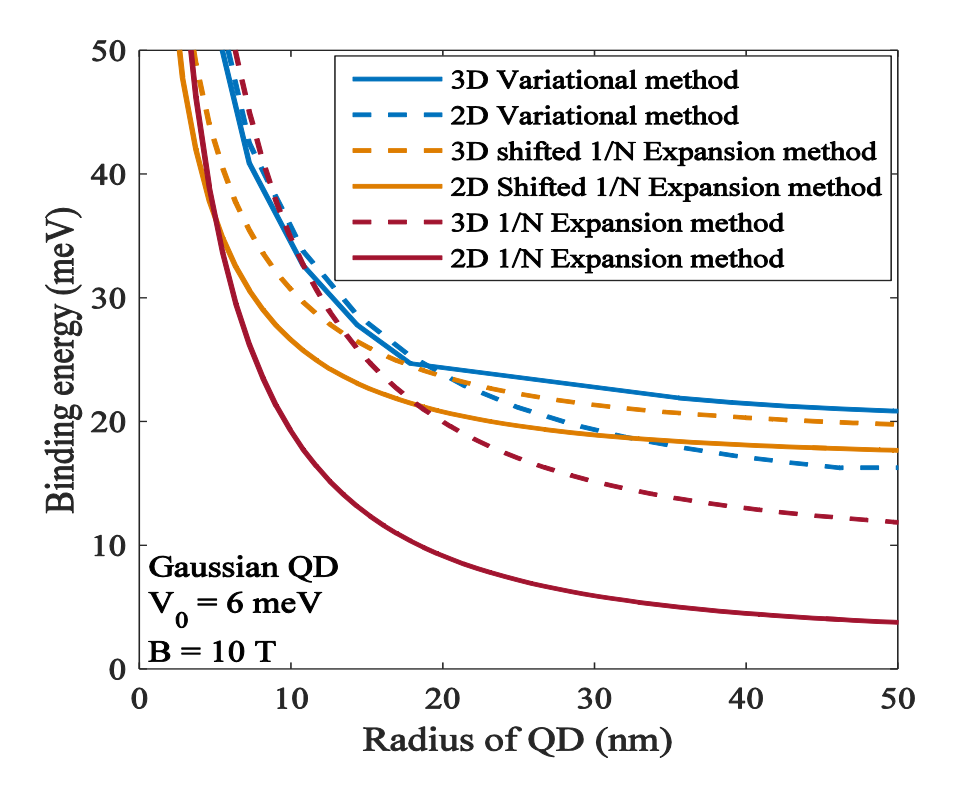


**Fig. 2.6** BE vs R for 2D and 3D GQDs of GaAs for B = 10 T.

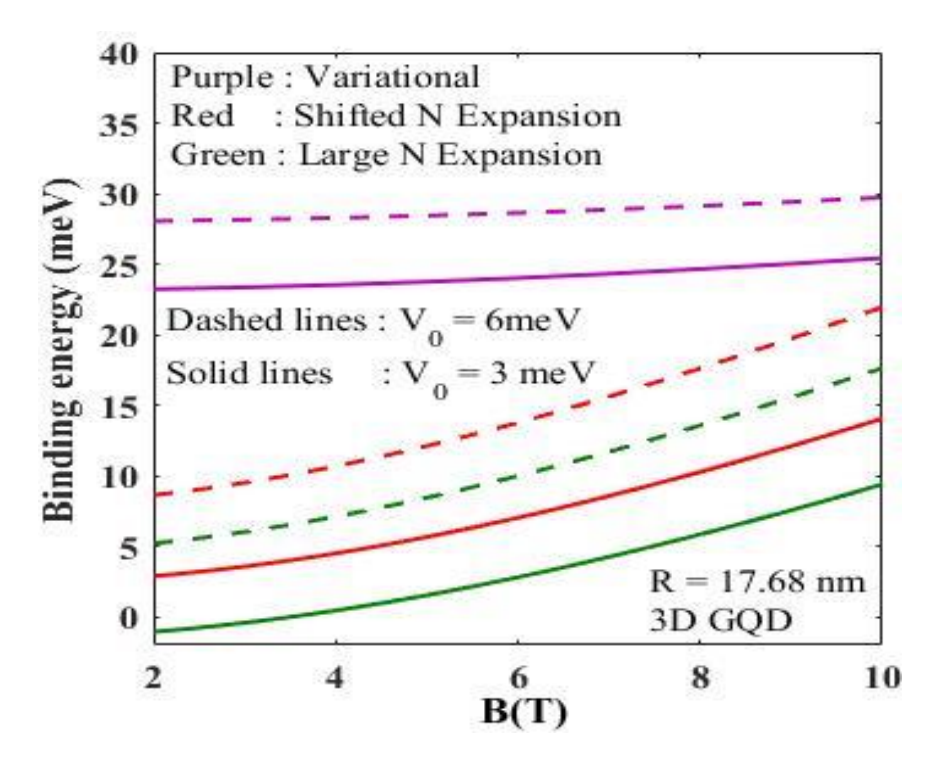


**Fig. 2.7** Exciton BE vs. B in GQD for two values of  $V_0$ .

In Fig. 2.7, we plot the exciton BE with respect to B for  $V_0 = 3$  meV and  $V_0 = 6$  meV. As one would normally expect, BE shows a monotonically increasing behaviour with B. We observe that Gaussian confinement provides stronger binding than the parabolic confinement for the excitonic bound state.

In Fig. 2.8, we plot the exciton size versus R for three values of B. One can see that the exciton size initially grows with R, but as R is made to exceed a certain length, the exciton size reaches a saturation value. This is of course the exciton size for the corresponding bulk system. From the figure, the exciton size is also found to decrease with increasing B. The genesis of this phenomenon can be attributed to the confining effect of

the magnetic field. One can draw another conclusion from Figs. 2.6 and 2.8. Fig. 2.8 shows that the exciton size grows with R, while one observes from Fig. 2.6 that as R increases, BE decreases. Thus, from these two observations, we infer that BE reduces with the increase in the exciton size. Fig. 2.9 describes the behaviour of the exciton size with respect to B. As can be expected, the exciton size decreases as B increases. Also, the exciton size decreases with increasing value of  $V_0$ .

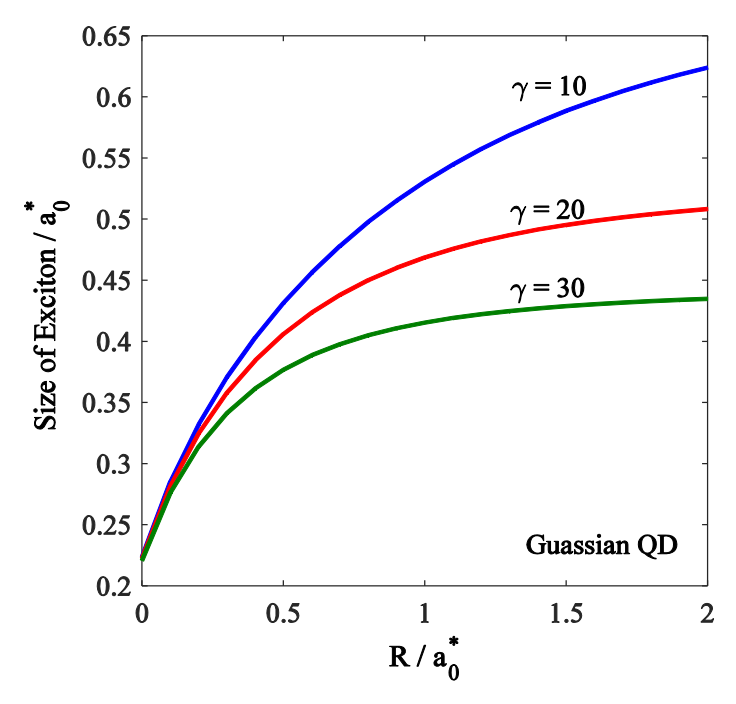
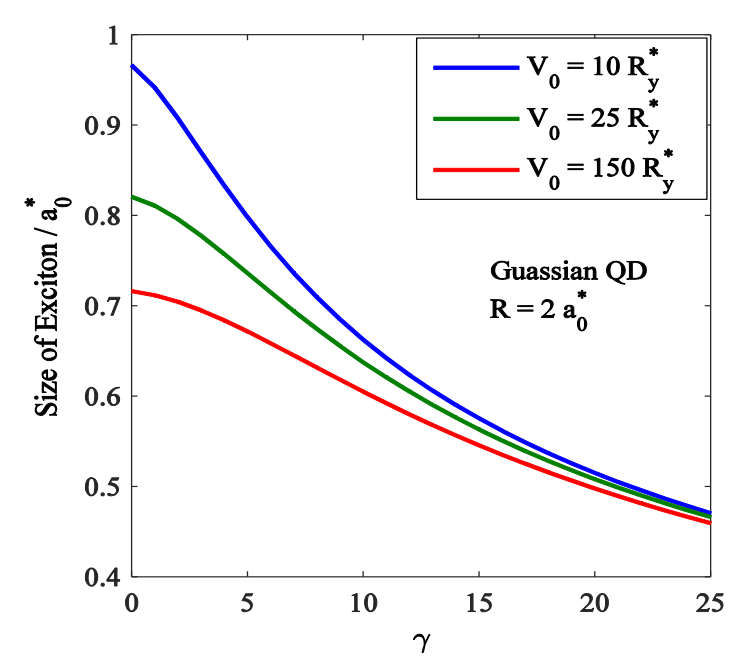
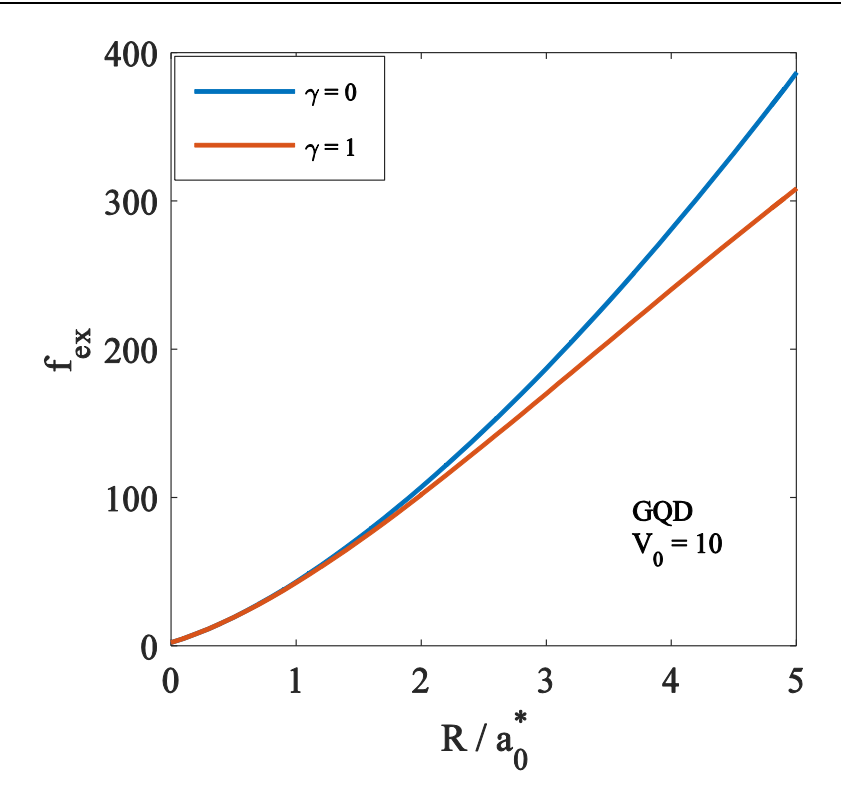


Fig. 2.8 Light-hole exciton size vs. QD size R in a 3D GQD.



**Fig. 2.9** Light-hole exciton size vs. *B* in a 3D GQD.

Fig. 2.10 gives the behaviour of the exciton oscillator strength  $f_{ex}$  with respect to R. One may note that  $f_{ex}$  decreases with decreasing R. The explanation is simple. The decrease in R increases the exciton energy and hence in turn reduces  $f_{ex}$ . One can also see from Fig. 2.10 that  $f_{ex}$  decreases as B is strengthened. The explanation is again straightforward. The magnetic field provides an added confining effect which causes an enhancement in the exciton energy and therefore one can conclude that the oscillator strength should decrease with increasing B.



**Fig. 2.10** GS Exciton oscillator strength vs *R* in GQD for two values of *B*.

# 2.7 EXCITED STATES

From Eqs. (2.49) - (2.55), we can obtain the exciton energy spectrum. Table 2.1 gives the ground and the excited state energy values of a Gaussian GaAs QD with R=88.5 nm,  $V_0=12$  meV, situated in a magnetic field of strength B=1T. One would immediately notice that 18 bound states can be accommodated in this QD, though the calculation of BE will only ensure the stability of these states. However, here we shall loosely refer to all these states as bound states. If an exciton state

has a positive energy, then, of course, it cannot be a bound state. It is clear that we can have as many bound states as we wish by controlling the QD parameters. For example, as displayed in Table 2.2, a GQD of GaAs with R=53 nm,  $V_0=3.98$  meV and placed in magnetic field of strength B=4 T, will have at the most four exciton states. Table 2.3 gives the BE values for a set of QD parameters.

**Table. 2.1** Exciton energy values (in meV) in a 2D GQD of GaAs obtained by shifted 1/N - expansion technique with  $R = 88.5 \, nm$ ,  $V_0 = 12 \, meV$  and B = 1T.

n	0	1	2	3	4	5	6	7	8	9	10
0	-27.46	-15.88	-15.36	-15.08	-14.85	-14.63	-14.43	-14.24	-14.05	-13.86	9.698
1	-16.25	-15.23	-13.09	-8.57							
2	-14.19	-9.59	-1.47	11.38							
3	-5.86	5.97									
4	14.17										

**Table 2.2.** Exciton energy values in GQD of GaAs with R = 53 nm,  $V_0 = 3.98 \text{ meV}$  and B = 4T.

n	0	1	2	3
0	-17.39	-5.088	-3.732	15.18
1	-1.603	28.43		
2	60.274			

**Table 2.3.** BE of an exciton in a GQD with  $R = 17.7 \, nm$ ,  $V_0 = 3.98 \, meV$  and  $B = 1 \, T$ .

l											
n	0	1	2	3	4	5	6	7	8	9	10
0	12.68	10.46	9.52	8.23	6.53	4.42	3.25	2.15	1.28	0.32	0.032
1	9.23	6.79	5.42	3.67	1.51	0.73					
2	8.11	5.43	4.67	2.77	0.76						
3	3.78	2.63	1.97	1.28	0.52						
4	1.52										

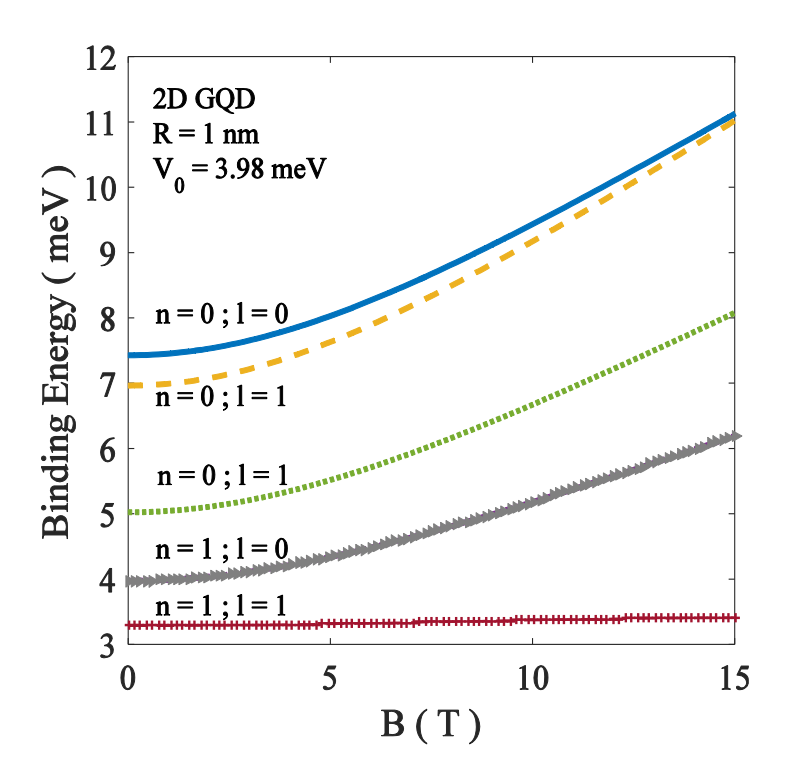


**Fig. 2.11** Exciton BE vs B for a few states in GQD with R = 1 nm,  $V_0 = 3.98 \, meV$ .

The BE behaviour of a few excitonic states in GQD with R = 1 nm,  $V_0 = 3.98 \, meV$  is examined with respect to B in Fig. 2.11. The binding is evidently weaker for an excited state that is higher in energy. The binding, however, becomes stronger with the increase in B. This can be explained again in the light of the extra confining effect introduced by the magnetic field.

# 2.8 CONCLUSION

In this chapter, the GS energy, BE and the size of an exciton in a GQD of GaAs placed in a magnetic field have been obtained in both 2D and 3D by employing three approximate methods namely, the conventional variational approach,  $\frac{1}{N}$  — expansion technique and the shifted  $\frac{1}{N}$  — expansion scheme. The variational approach provides an energy higher than the exact GS energy while the 1/N-expansion technique provides a lower limit to the GS energy. Comparative analysis of the results obtained from our work with those from exact numerical diagonalization shows that the shifted  $\frac{1}{N}$  — expansion technique provides highly accurate values. We find that the electron/hole distribution reduces as the QD confinement and the magnetic field are enhanced. Our results also show that the exciton GS energy rises with reduction in QD size and acquires considerably large values as QD size is made very small.

Our calculation reveals that the GS exciton binding becomes stronger as *R* decreases. Our results also reveal that the GS binding becomes

stronger as the confinement is increased. BE also increases with increasing field B, we furthermore observe that the exciton reduces in size as the confinement length is reduced. The exciton size also shrinks as the potential is made deeper or the strength of the magnetic field is enhanced.

Next, we have demonstrated that the GS oscillator strength of an exciton in GQD becomes weaker with decreasing QD size or increasing magnetic field.

Finally we have obtained the energies of a few excitonic ESs in a 2D GQD placed in a magnetic field. We have shown that it is possible to generate a specified number of exciton states in GQD by controlling certain characteristic system parameters. To be more specific, we have demonstrated a case in which four bound states can at most occur in GQD of GaAs. This interesting property of tunability may be usefully utilized in fabricating excitonic lasers with QDs. It may however be noted that in the work discussed in this chapter, we have ignored the spin-Zeeman term which may have important effect on exciton energetics.

# 2.9 REFERENCES

- [1] S. Jaziri and R. Bennaceur, *Excitonic Properties in GaAs Parabolic Quantum Dots*, J. Phys. III France **5** 1565(1995).
- [2] D. Gammon, E. S. Snow, B. V. Shanabrook, D. S. Katzer and D. Park, *Fine Structure Splitting in the Optical Spectra of Single GaAs Quantum Dots*, Phys. Rev. Lett. **76** 3005 (1996).
- [3] W. Xie, Exciton states trapped by a parabolic quantum dot, Physica B **358** 109 (2005).
- [4] L. E. Brus, A simple model for the ionization potential, electron affinity, and aqueous redox potentials of small semiconductor crystallites, J. Chem. Phys. **79** 5566 (1983).
- [5] A.I Ekimov, Al. L. Efros, and A.A. Onushchenko. *Quantum size effect in semiconductor microcrystals*, Solid state Commun. **56** 921 (1985).
- [6] Y. Kayanuma, Quantum-size effects of interacting electrons and holes in semiconductor microcrystals with spherical shape, Phys. Rev. B **38** 9797(1988).
- [7] P.E. Lippens and M. Lannoo, Comparison between calculated and experimental values of the lowest excited electronic state of small CdSe crystallites, Phys. Rev. B **41** 6079 (1990).
- [8] G.T. Einevoll. *Confinement of excitons in quantum dots*, Phys. Rev. B **45** 3410 (1992).
- [9] W. Que. Excitons in quantum dots with parabolic confinement, Phys. Rev. B **45** 11036 (1992).
- [10] S. Jaziri and R. Bennaceur. *Excitons in parabolic quantum dots in electric and magnetic Fields*. Sci. Technol. **9** 1775 (1994).
- [11] Z. Xiao. Exciton binding energy in spherical quantum dots in a magnetic field. J. Appl. Phys. **86**, 4509 (1999).
- [12] S. A. Safwan, M. H. Hekmat and N. A. El-Meshad., Exciton states in a quantum dot., Fizika A (Zagreb) **16,** 1 (2007).

- [13] W. Xie and J. GU. Exciton states trapped by a parabolic quantum dot, Commun. Theor. Phys. **40**, 619 (2003).
- [14] J. GU and J. Liang. Energy spectra of an exciton in a Gaussian potential and magnetic field, Phys. Lett. A. **323**, 132 (2004).
- [15] K. Miyajima, Edamatsu K, and Itoh T. *Infrared transient absorption and excited-states of excitons and biexcitons confined in CuCl quantum dots.*, J. Luminescence 108 371(2004).
- [16] W. Xie, Exciton states in spherical Gaussian potential wells. Commun. Theor. Phys. **42**, 923 (2004).
- [17] G. W. Bryant., Excitons in quantum boxes: Correlation effects and quantum confinement., Phys. Rev. B **37**, 8763 (1988).
- [18] W. Que, Excitons in quantum dots with parabolic confinement. Phys. Rev. B **45**, 11036 (1992).
- [19] A. Chatterjee, Large-N expansions in quantum mechanics, atomic physics and some O(N) invariant systems., Phys. Reports **186** 249 (1990).
- [20] U. Sukhatme, & T.Imbo, Shifted 1/N expansions for energy eigenvalues of the Schrödinger equation, Phys. Rev. D 28 418 (1983).
- [21] T. Imbo, A. Pagnamenta & U. Sukhatme, Energy eigenstates of spherically symmetric potentials using the shifted 1/N expansion., Phys. Rev. D 29 1669 (1984).
- [22] A. Chatterjee., 1/N expansion for Gaussian potential, J.Phys.A: Math. Gen. 18 2403 (1985).

3

# Effect of Temperature on The Single-Particle Ground-State and Self Energy of a Polar Quantum Dot with Gaussian Confinement

# Abstract

The effect of temperature on polarons in a Gaussian quantum dot has been studied by employing the Lee-Low-Pines-Huybrechts unitary transformation, Ritz variational method and statistical mechanics. The calculations reveal that with increasing temperature, the ground-state energy increases while the ground state polaron self-energy corrections. The results also uncover the role of quantum confinement on the polaron ground-state and binding energies. It is also demonstrated that the ground-state energy is higher in a three-dimensional dot than in a two-dimensional one. In general, the polaronic effects become stronger with the reduction in dimensionality.

### 3.1 INTRODUCTION

The study of temperature dependence of polarons is of foremost importance in the context of practical applications. However, the investigations carried out hitherto on this issue have not yielded any unequivocal answer. Two conflicting viewpoints have been reported in the literature. There are some investigations that claim that with increasing temperature, the phonon cloud of the polaron becomes thinner and as a result the polaron binding becomes weaker. There is another set of works that suggest that the polaron binding increases with temperature with a concomitant increase in its effective mass [1-7].

Peeters and Devreese [1] have studied the temperature dependence of polaron mass using the Feynman Polaron model. They have shown that the polaron mass increases with the temperature. They have also compared their results with those from experimental investigations. The temperature dependence of polaron correction to the electron effective mass in a  $GaAs - Al_xGa_{1-x}As$  heterostructure has been studied by Xeaoguang et al. [8] in zero magnetic field. They have found that the polaron mass increases with increasing temperature up to 100K and then starts decreasing with further increase in temperature. The effect of temperature on bipolaronic properties in a quantum dot (QD) has been investigated by Eerdunchalu and Xin [9] in the strong-coupling limit. They have shown that the polaronic effects undergo an enhancement with temperature and polaron coupling.

There have been quite a few investigations on the effect of temperature on polarons in QDs. Zhi-Xin Li has studied the temperature effect on the polaronic properties in a triangular QD [10]. Quite a few studies have been made to examine the effect of temperature in parabolic quantum dots [11-20] with symmetric and asymmetric confinement. Shan et al. [11] have considered the case of an impurity-bound strongly-coupled magneto-polaron in an asymmetric QD. In this work, the Lee-Low-Pines (LLP) transformation and an additional set of canonical transformations have been carried out to show that the binding energy (BE) and the average number of phonons in the polaron cloud increase with temperature. A similar method has been used by Cai et al. [12] to study the temperature effect on the binding energy of a strong-coupling magneto-polaron in a RbCl QD with parabolic confinement.

However, apparently no detailed research investigations have hitherto been taken up on Gaussian QD (GQD). This chapter will be devoted to the delineation of the results of our recent study on the effects of temperature and effective confinement length on the self-energy of an electron in a polar GQD.

### 3.2 MODEL

We consider the motion of an electron with band mass m in an N -dimensional (ND) GQD. The electron interacts with the longitudinal optical (LO) phonons of frequency  $\omega_0$  which is considered dispersionless. The system under study can be represented by the model Hamiltonian

$$H = \frac{p^2}{2m} + V'(r') + \hbar\omega_0 \sum_{\mathbf{q}'} b_{\mathbf{q}'}^{\dagger} b_{\mathbf{q}'} + \sum_{\mathbf{q}'} \left[ \xi_{\mathbf{q}'}' e^{-i\mathbf{q}' \cdot \mathbf{q}'} b_{\mathbf{q}'}^{\dagger} + h.c \right] (3.1)$$

where r', p', q', etc. are all ND vectors. Here r' and p' refer respectively to the position and momentum operators of the electron,  $b_{q'}^{\dagger}(b_{q'})$  represents the LO-phonon creation (destruction) operator, q' being the phonon wave vector and  $\omega_0$  the frequency,  $\xi'_{q'}$  gives the measure of the electron–phonon (e-p) interaction strength and the Gaussian confinement potential V'(r') is chosen as

$$V'(\mathbf{r}') = -V_0' e^{-\frac{{\mathbf{r}'}^2}{2R'^2}}$$
 (3.2)

where  $V'_0$  gives a measure of how deep is the potential and R' gives the length scale over which the potential goes to zero. This range R' can be considered as the effective size of QD or the confinement length.

We use, in our calculation, the Feynman units. In this system of units,  $\hbar\omega_0$  is chosen as the scale of energy,  $r_0(=(\hbar/m\omega_0)^{1/2})$  as the scale of length (which can be identified as the free polaron radius in the weak-coupling regime) and  $q_0=1/r_0$  as the scale of the wave vector. The choice of the Feynman units essentially means choosing  $\hbar=m=\omega_0=1$ . Then the Hamiltonian can be written as

$$H = \frac{p^2}{2} - V_0 e^{-(r^2/2R^2)} + \sum_{\vec{q}} b_q^{\dagger} b_q + \sum_{\vec{q}} (\xi_q e^{-iq \cdot r} b_q^{\dagger} + hc) . \quad (3.4)$$

where everything is dimensionless and  $\left|\xi_{q}\right|^{2}$  is given by

$$\left|\xi_{q}\right|^{2} = \left[\frac{\Gamma\left(\frac{N-1}{2}\right)2^{(N-3/2)}\pi^{(N-1)/2}}{v_{N}q^{N-1}}\right]\alpha$$
, (3.5)

where N is the system dimensionality,  $v_N$  the system volume and  $\alpha$  is the e-p coupling constant. For a 2D system:

$$\left|\xi_q\right|^2 = \left(\frac{\sqrt{2}\pi}{vq}\right)\alpha \quad , \tag{3.5}$$

and for a 3D system

$$\left|\xi_q\right|^2 = \left(\frac{2\sqrt{2}\pi}{vq^2}\right)\alpha \qquad . \tag{3.6}$$

# 3.3 FORMULATION

Huybrechts modified the Lee-Low-Pines method to make it valid even in the strong coupling limit. The results are satisfactory for the weak as well as the strong-coupling regime [40,41]. In the Lee-Low-Pines-Huybrechts (LLPH) approach, two unitary transformations are successively performed on the Hamiltonian using the operators,

$$U_1 = e^{S_1} = exp \left[ -ia \sum_{\boldsymbol{q}} (\boldsymbol{q} \cdot \boldsymbol{r}) b_{\boldsymbol{q}}^{\dagger} b_{\boldsymbol{q}} \right] , \qquad (3.7)$$

and

$$U_2 = e^{S_2} = exp \left[ \sum_{q} (f_q b_q^{\dagger} - f_q^* b_q) \right] , \qquad (3.8)$$

where a and  $f_q$  are variational parameters. The transformed Hamiltonian is then averaged using the phonon vacuum state and the system's ground state (GS) energy is finally calculated by averaging the effective electronic Hamiltonian using an appropriate electron wave function.

The above-mentioned procedure is same as a variational calculation with the following trial wave function

$$|\psi\rangle = e^{\left[-ia\sum_{q}(q,r)b_{q}^{\dagger}b_{q}\right]} * e^{\left[\sum_{q}\left(f_{q}b_{q}^{\dagger}-f_{q}^{*}b_{q}\right)\right]}|0\rangle|\phi(r)\rangle, \qquad (3.9)$$

where  $|0\rangle = \prod_q |0_q\rangle$  denotes the phonon vacuum or the phonon GS and  $|\phi(\mathbf{r})\rangle$  is the electron state. We wish to compute the GS energy for (3.4). Therefore we make the following prescription for  $|\phi(\mathbf{r})\rangle$ :

$$|\phi(\mathbf{r})\rangle = \left(\frac{\delta^N}{\pi^{N/2}}\right)^{1/2} e^{-(\delta^2 r^2/2)}$$
 , (3.10)

The variational energy can be written as,

$$E = \langle \psi | H | \psi \rangle = \langle \phi(r) | \langle 0 | \widetilde{H} | 0 \rangle | \phi(r) \rangle \tag{3.11}$$

where

$$\widetilde{H} = U_2^{-1} U_1^{-1} H U_1 U_2 = U_1^{-1} \widetilde{H} U_1 \tag{3.12}$$

Effect of Temperature on The Single-Particle Ground-State ....

$$\widetilde{H} = U_1^{-1} H U_1 \tag{3.13}$$

or

$$\widetilde{H} = \frac{1}{2} (U_1^{-1} \mathbf{P} U_1)^2 - V_0 e^{-r^2/2R^2} + \sum_{\mathbf{q}} U_1^{-1} b_{\mathbf{q}}^{\dagger} b_{\mathbf{q}} U_1$$

$$+ \sum_{\mathbf{q}} (\xi_{\mathbf{q}} e^{-i\mathbf{q}.\mathbf{r}} U_1^{-1} b_{\mathbf{q}}^{\dagger} U_1 + \text{hc}).$$
(3.14)

In Eq. (3.14), we use the Campbell-Baker-Hausdorff Formula:

$$U_1^{-1} \mathbf{P} U_1 = e^{-S_1} \mathbf{P} e^{S_1} = \mathbf{P} + [s_1, \mathbf{P}] + \frac{1}{2} [s_1, [s_1, \mathbf{P}]] + \cdots$$
 (3.15)

where

$$[s_1, P] = -a \sum_q \mathbf{q} b_q^{\dagger} b_q$$

and

$$[s_1, [s_1, \mathbf{P}]] = 0 (3.16)$$

Eq. (3.15) becomes

$$U_1^{-1}\mathbf{P}U_1 = \mathbf{P} - a\sum_{\mathbf{q}} \mathbf{q}b_{\mathbf{q}}^{\dagger}b_{\mathbf{q}}$$
 (3.17)

Similarly, we get

$$\tilde{b}_q = U_1^{-1} b_q U_1 = b_q + [s_1, b_q] + \frac{1}{2} [s_1, [s_1, b_q]] + \cdots$$
 (3.18)

or

$$\tilde{b}_{q} = e^{-ia\sum_{q}(q,r)}b_{q} \tag{3.19}$$

and

$$\tilde{b}_{q}^{\dagger} = e^{ia\sum_{q}(q,r)}b_{q}^{\dagger} \tag{3.20}$$

Therefore, we can write

$$\widetilde{H} = \frac{1}{2} \left( \mathbf{P} - a \sum_{\mathbf{q}} \mathbf{q} b_{\mathbf{q}}^{\dagger} b_{\mathbf{q}} \right)^{2} + \sum_{\mathbf{q}} e^{ia \sum_{\mathbf{q}} (\mathbf{q} \cdot \mathbf{r})} b_{\mathbf{q}}^{\dagger} e^{-ia \sum_{\mathbf{q}} (\mathbf{q} \cdot \mathbf{r})} b_{\mathbf{q}}$$
$$-V_{0} e^{-\mathbf{r}^{2}/2R^{2}} + \sum_{\mathbf{q}} \left( \xi_{\mathbf{q}} e^{-i\mathbf{q} \cdot \mathbf{r}} e^{ia \sum_{\mathbf{q}} (\mathbf{q} \cdot \mathbf{r})} b_{\mathbf{q}}^{\dagger} + h. c \right)$$
(3.21)

$$= \frac{\mathbf{P}^{2}}{2} - a \sum_{q} P. \mathbf{q} b_{q}^{\dagger} b_{q} + \frac{a^{2}}{2} \sum_{q,q'} \mathbf{q}. \mathbf{q}' b_{q}^{\dagger} b_{q} b_{q'}^{\dagger} b_{q'} - V_{0} e^{-r^{2}/2R^{2}}$$

$$+ \sum_{q} b_{q}^{\dagger} b_{q} + \sum_{q} (\xi_{q} e^{-i(1-a)\mathbf{q}.\mathbf{r}} b_{q}^{\dagger} + h. c), \qquad (3.22)$$

Finally, we obtain

$$\widetilde{H} = \frac{\mathbf{P}^{2}}{2} + \sum_{q} \left( 1 + \frac{a^{2}q^{2}}{2} - a \, \mathbf{P} \cdot \mathbf{q} \right) b_{q}^{\dagger} b_{q} + \frac{a^{2}}{2} \sum_{q,q'} \mathbf{q} \cdot \mathbf{q}' \, b_{q}^{\dagger} b_{q} \, b_{q'}^{\dagger} b_{q'}$$

$$- V_{0} e^{-\mathbf{r}^{2}/2R^{2}} + \sum_{q} \left( \xi_{\mathbf{q}} e^{-i(1-a)\mathbf{q} \cdot \mathbf{r}} b_{q}^{\dagger} + h \cdot c \right), \quad (3.23)$$

Now,

$$\widetilde{\widetilde{H}} = U_2^{-1} \widetilde{H} U_2 \tag{3.24}$$

$$U_2^{-1}b_qU_2 = b_q - [s_2, b_q] + \frac{1}{2}[s_2, [s_2, b_q]]... \quad (3.25)$$

$$[s_2, b_q] = \left[\sum_{\mathbf{q}} (f_{\mathbf{q}} b_{\mathbf{q}}^{\dagger} - f_{\mathbf{q}}^* b_{\mathbf{q}}), b_{\mathbf{q}}\right] = f_{\mathbf{q}}$$
 (3.26)

$$\left[ s_{2}, \left[ s_{2}, b_{q} \right] \right] = 0$$
 (3.27)

Therefore,

$$U_2^{-1}b_qU_2 = b_q + f_q (3.28)$$

Now,

$$\widetilde{\widetilde{H}} = \frac{\mathbf{p}^{2}}{2} - V_{0}e^{-r^{2}/2R^{2}} + \sum_{\mathbf{q}} \left(1 - a\mathbf{p}.\,\mathbf{q} + \frac{a^{2}q^{2}}{2}\right) \left(b_{\mathbf{q}}^{\dagger} + f_{\mathbf{q}}^{\star}\right) \left(b_{\mathbf{q}} + f_{\mathbf{q}}\right) 
+ \frac{a^{2}}{2} \sum_{\mathbf{q}} \mathbf{q}.\,\mathbf{q}' \left(b_{\mathbf{q}}^{\dagger} + f_{\mathbf{q}}^{\star}\right) \left(b_{\mathbf{q}'}^{\dagger} + f_{\mathbf{q}'}^{\star}\right) \left(b_{\mathbf{q}} + f_{\mathbf{q}}\right) \left(b_{\mathbf{q}'} + f_{\mathbf{q}'}\right) 
+ \sum_{\mathbf{q}} \left[\xi_{\mathbf{q}}e^{-i(1-a)\mathbf{q}.\mathbf{r}} \left(b_{\mathbf{q}}^{\dagger} + f_{\mathbf{q}}^{\star}\right) + h.c\right] .$$
(3.29)

Averaging (3.29) with respect to  $|0\rangle$  gives

$$\langle 0 | \widetilde{H} | 0 \rangle = \frac{\mathbf{p}^{2}}{2} - V_{0} e^{-r^{2}/2R^{2}} + \sum_{\mathbf{q}} \left( 1 - a\mathbf{p} \cdot \mathbf{q} + \frac{a^{2}q^{2}}{2} \right) |f_{q}|^{2}$$

$$+ \frac{a^{2}}{2} \left[ \sum_{\mathbf{q}} \mathbf{q} |f_{q}|^{2} \right]^{1/2} + \sum_{\mathbf{q}} \left[ \xi_{\mathbf{q}} e^{-i(1-a)\mathbf{q} \cdot \mathbf{r}} f_{\mathbf{q}}^{\star} + h \cdot c \right]. \quad (3.30)$$

The averaging over the electron state gives the LLPH variational energy,

$$E_{LLPH} = \left\langle \phi(r) \left| \left\langle 0 \right| \widetilde{H} \right| 0 \right\rangle \left| \phi(r) \right\rangle$$

$$= \left\langle \phi(r) \left| \frac{\mathbf{p}^2}{2} \right| \phi(r) \right\rangle - \left\langle \phi(r) \left| V_0 e^{-r^2/2R^2} \right| \phi(r) \right\rangle$$

$$+ \sum_{\mathbf{q}} \left( 1 - a\mathbf{p} \cdot \mathbf{q} + \frac{a^2 q^2}{2} \right) \left| f_q \right|^2 + \frac{a^2}{2} \left[ \sum_{\mathbf{q}} \mathbf{q} \left| f_q \right|^2 \right]^{\frac{1}{2}}$$

$$+ \sum_{\mathbf{q}} \left[ \xi_{\mathbf{q}} e^{-i(1-a)\mathbf{q} \cdot \mathbf{r}} f_{\mathbf{q}}^{\star} + h \cdot c \right], \qquad (3.32)$$

Minimizing  $E_{LLPH}$  with respect to  $f_q^*$  gives,

$$\frac{\partial E_{LLPH}}{\partial f_{\mathbf{q}}^{\star}} = \left(1 - a\langle \phi | \mathbf{P} | \phi \rangle. \mathbf{q} + \frac{a^2 q^2}{2}\right) f_q + \xi_{\mathbf{q}} \rho_q^* = 0$$
 (3.33)

or,

$$f_q = -\frac{\xi_{\mathbf{q}} \rho_q^*}{\left(1 - a\langle \phi | \mathbf{P} | \phi \rangle, \mathbf{q} + \frac{a^2 \mathbf{q}^2}{2}\right)}$$
(3.34)

where,

$$\rho_q^* = \langle \phi | e^{-i(1-a)\mathbf{q}\cdot\mathbf{r}} | \phi \rangle. \tag{3.35}$$

We now use the following condition which is reasonable for symmetric quantum dots,

$$\sum_{\mathbf{q}} \mathbf{q} |f_{\mathbf{q}}|^2 = 0 \text{ and } \langle \phi | \mathbf{p} | \phi \rangle = 0.$$
 (3.36)

The ground state energy can be obtained as

$$E_{LLPH} = \frac{1}{2} \langle \phi(r) | P^2 | \phi(r) \rangle - V_0 \langle \phi(r) | e^{-r^2/2R^2} | \phi(r) \rangle$$

$$+ \sum_{q} \frac{\left| \xi_q \right|^2 \left| \rho_q \right|^2}{1 + \frac{a^2 q^2}{2}} . \tag{3.37}$$

Now using Eq. (3.10) averaging over electronic states,

$$\langle \phi | P^2 | \phi \rangle = \langle \phi | \nabla^2 | \phi \rangle = -\frac{1}{2} \delta^2 ,$$
 (3.38)

$$\langle \phi(r) | e^{-r^2/2R^2} | \phi(r) \rangle = \left[ 1 + \frac{\beta^2}{\delta^2} \right]^{-1/2}$$
 (3.39)

where,

$$\beta^2 = \frac{1}{2R} \ , \tag{3.40}$$

$$\rho_q = e^{-\frac{(1-a)^2}{4\delta^2}q^2} \quad . \tag{3.41}$$

Inserting Eqs. (3.38), (3.39), and (3.41) in Eq. (3.37), the GS state energy reads as,

$$E_{LLPH} = \frac{1}{4} \sum_{i} \delta_{i}^{2} - V_{0} \left[ 1 + \frac{\beta^{2}}{\delta_{i}^{2}} \right]^{-\frac{1}{2}}$$

$$-\left[\frac{\Gamma\left(\frac{N-1}{2}\right)2^{(N-3/2)}\pi^{(N-1)/2}}{v_N}\right]\alpha\sum_{q}\frac{e^{-\sum_{l}\frac{(1-a)^2}{4\delta_{l}^2}q_{l}^2}}{q^{N-1}\left(1+\frac{a^2q^2}{2}\right)}.(3.42)$$

We can write

$$\sum_{q} \longrightarrow \frac{v_N}{(2\pi)^N} \int dq \qquad (3.43)$$

Therefore Eq. (3.42) becomes,

$$E_{LLPH} = \frac{1}{4} \sum_{i} \delta_{i}^{2} - V_{0} \left[ 1 + \frac{\beta^{2}}{\delta_{i}^{2}} \right]^{-\frac{1}{2}}$$

$$- \left[ \frac{\Gamma\left(\frac{N-1}{2}\right) 2^{(N-3/2)} \pi^{(N-1)/2}}{v_{N}} \right] \alpha \frac{v_{N}}{(2\pi)^{N}} \int dq \frac{e^{-\sum_{i} \frac{(1-a)^{2}}{4\delta_{i}^{2}} q_{i}^{2}}}{q^{N-1} \left( 1 + \frac{a^{2}q^{2}}{2} \right)}$$
(3.44)

For a symmetric QD,  $\delta_1 = \delta_2 = \delta_3 = \cdots \dots = \delta$ . So, we can write

$$E_{LLPH} = \frac{N}{4} \delta^2 - V_0 \left[ 1 + \frac{\beta^2}{\delta^2} \right]^{-\frac{N}{2}} + \frac{\Gamma\left(\frac{N-1}{2}\right)}{2\sqrt{2}\pi^{\frac{N+1}{2}}} \alpha \int dq \frac{e^{-\sum_i \frac{(1-a)^2}{4\delta_i^2} q_i^2}}{q^{N-1} \left(1 + \frac{a^2 q^2}{2}\right)}.$$
(3.45)

We can also write,

$$\int dq = \int \dots q^{N-1} dq \int d\Omega , \qquad (3.46)$$

and

$$\int d\Omega = \frac{2\pi^{N/2}}{\Gamma(N/2)} \quad . \tag{3.47}$$

Thus Eq. (3.42) reduces to

$$E_{LLPH} = \frac{N}{4} \delta^2 - V_0 \left[ 1 + \frac{\beta^2}{\delta^2} \right]^{-\frac{N}{2}}$$
$$-\frac{\sqrt{\pi}}{2} \frac{\Gamma\left(\frac{N-1}{2}\right)}{\Gamma(N/2)} \frac{\alpha}{a} e^{\left(\frac{1-a}{a\delta}\right)^2} erfc\left(\frac{1-a}{a\delta}\right). \tag{3.48}$$

Let us define a parameter t which is related to a as

$$t = \frac{1 - a}{\delta a} \quad , \tag{3.49}$$

or

$$\frac{1}{a} = 1 + t\delta \qquad . \tag{3.50}$$

The GS energy then reads

$$E_{LLPH} = \frac{N}{4} \delta^2 - V_0 \left[ 1 + \frac{\beta^2}{\delta^2} \right]^{-N/2}$$

$$-\frac{\sqrt{\pi}\alpha}{2} \frac{\Gamma\left(\frac{N-1}{2}\right)}{\Gamma\left(\frac{N}{2}\right)} (1+t\delta) e^{t^2} erfc(t)$$
 (3.51)

The average phonon number in the polaron GS is defined as

$$N_{\rm ph} = \langle \psi | \sum_{q} b_{q}^{\dagger} b_{q} | \psi \rangle \tag{3.52}$$

which gives

$$N_{\rm ph} = \sum_{q} \frac{\left|\xi_q\right|^2 \left|\rho_q\right|^2}{1 + \frac{a^2 q^2}{2}}$$
 (3.53)

$$= \left[ \frac{\Gamma\left(\frac{N-1}{2}\right) 2^{(N-3/2)} \pi^{(N-1)/2}}{v_N} \right] \alpha \sum_{q} \frac{e^{-\sum_{i} \frac{(1-a)^2}{4\delta_i^2} q_i^2}}{q^{N-1} \left(1 + \frac{a^2 q^2}{2}\right)}$$
(3.54)

or,

$$N_{ph} = \frac{\Gamma(\frac{N-1}{2})}{4 \Gamma(\frac{N}{2})} \alpha (1+t\delta) [2t + (1-2t^2)\sqrt{\pi} e^{t^2} Erfc(t)]$$
 (3.55)

or,

$$N_{ph} - \frac{\Gamma\left(\frac{N-1}{2}\right)}{4\Gamma\left(\frac{N}{2}\right)} 2\alpha t (1+t\delta)$$

$$= \frac{\alpha\sqrt{\pi}}{4} \frac{\Gamma\left(\frac{N-1}{2}\right)}{\Gamma\left(\frac{N}{2}\right)} \left[ (1-2t^2)e^{t^2} (1+t\delta)Erfc(t) \right] \quad (3.56)$$

We can rearrange Eq. (3.48) as

$$\frac{\sqrt{\pi}\alpha}{2} \frac{\Gamma\left(\frac{N-1}{2}\right)}{\Gamma\left(\frac{N}{2}\right)} (1+t\delta)e^{t^2} Erfc(t)$$

$$= \frac{N}{4}\delta^2 - V_0 \left[1 + \frac{\beta^2}{\delta^2}\right]^{-N/2} - E_{LLPH} \tag{3.57}$$

From Eqn (3.56) and (3.57) we can write,

$$N_{ph} - \frac{\Gamma\left(\frac{N-1}{2}\right)}{4\Gamma\left(\frac{N}{2}\right)} 2\alpha t (1+t\delta)$$

$$= \frac{(1-2t^2)}{2} \left[ \frac{N}{4} \delta^2 - V_0 \left[ 1 + \frac{\beta^2}{\delta^2} \right]^{-N/2} - E_{LLPH} \right], \quad (3.58)$$

Or

$$E_{LLPH} = \frac{N}{4} \delta^2 - V_0 \left[ 1 + \frac{\beta^2}{\delta^2} \right]^{-\frac{N}{2}} - \frac{2}{(1 - 2t^2)} \left[ N_{ph} - \frac{\Gamma\left(\frac{N-1}{2}\right)}{4\Gamma\left(\frac{N}{2}\right)} 2\alpha t (1 + t\delta) \right]. \quad (3.59)$$

We now replace  $N_{ph}$  by the phonon distribution function given by

$$\overline{N} = \frac{1}{e^{(\hbar\omega_0/K_BT)} - 1} \tag{3.60}$$

The GS energy at finite temperature becomes,

$$E_{LLPH} = \frac{N}{4} \delta^2 - V_0 [1 + (\beta^2/\delta^2)]^{-\frac{N}{2}} - \frac{2}{1 - 2t^2} \overline{N} + \frac{\alpha}{2(1 - 2t^2)} \frac{\Gamma(\frac{N - 1}{2})}{\Gamma(\frac{N}{2})} 2t(1 + t\delta)$$
(3.61)

The variational parameters t and  $\delta$  are determined by minimizing Eq. (3.62) numerically with respect these parameters and the GS energy and polaronic correction are obtained at finite temperatures for N=2 and N=3.

### 3.4 RESULTS AND DISCUSSIONS

The numerical computations have been carried out for small, intermediate and large  $\alpha$  values. Fig. 3.1 presents the polaron GS energy (*GSE*) behaviour in a 3D GQD with respect to temperature (*T*) for  $V_0 = 10$ , R=2 and 6 and  $\alpha = 4.8$ , 5.0 and 5.2. It

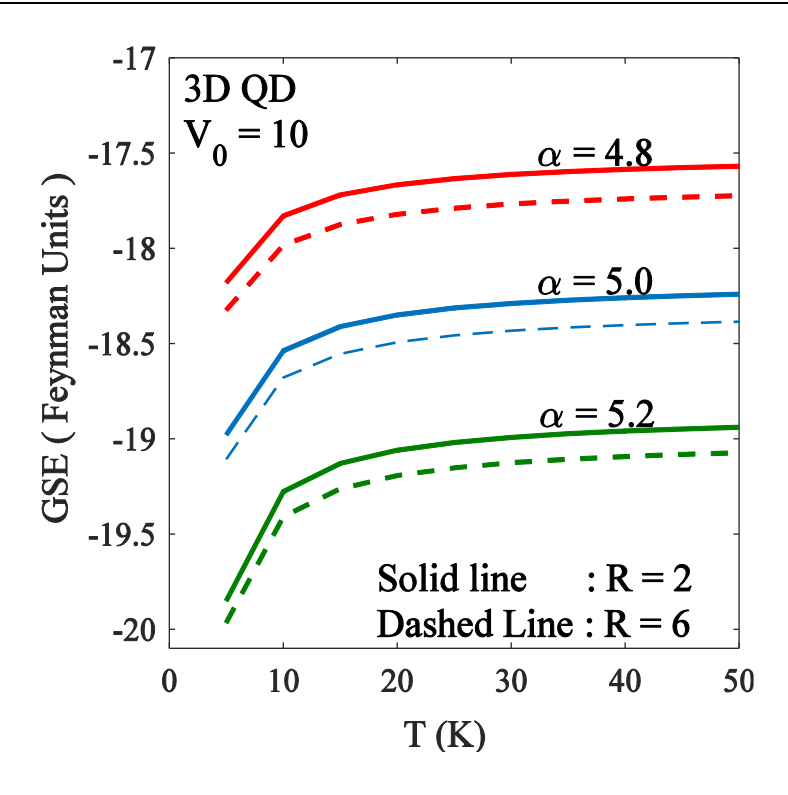


**Fig. 3.1**: Polaron GS energy (*GSE*) vs temperature T for  $V_0 = 10$ , and R = 2 and 6 in the strong-coupling regime.

is clearly evident from the figure that Polaron GSE increases with the increase in T. This implies that temperature weakens the polaronic effect. The explanation is simple. An increase in T leads to excitation of larger number of real phonons which suppresses the formation of the polaron. As expected, polaron GSE decreases with increasing  $\alpha$  and R.

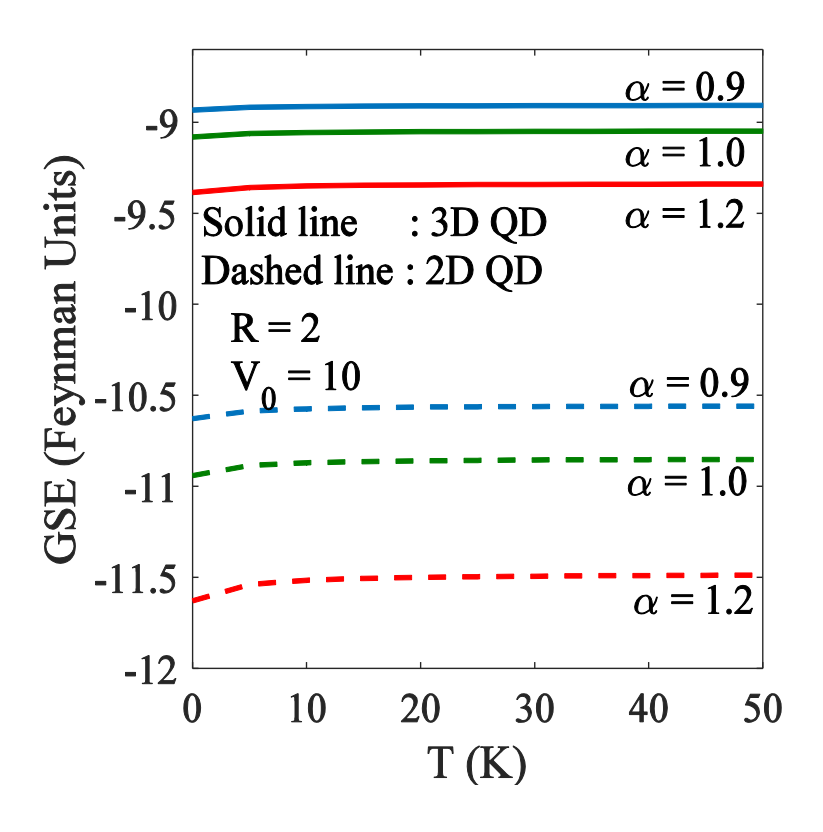


**Fig. 3.2**: Polaron GSE vs *T* for 2D and 3D GQDs in the intermediate-coupling region.

In Fig. 3.2, GSE is plotted for an intermediate-coupling polaron for both N=2 and 3. It is clearly visible that even at  $T\neq 0$ , the impact of ep interaction is stronger in 2D than in 3D. This is of course understandable from the point of view of quantum mechanics. It is interesting to note that in a 3D QD, GSE hardly shows any temperature dependence whereas for the 2D system, we find that GSE shows a marginal increase with T at low T, and then becomes essentially constant as T is increased further. The temperature variation of GSE in the weak-

coupling regime looks qualitatively similar to that in the intermediatecoupling regime (not shown here).

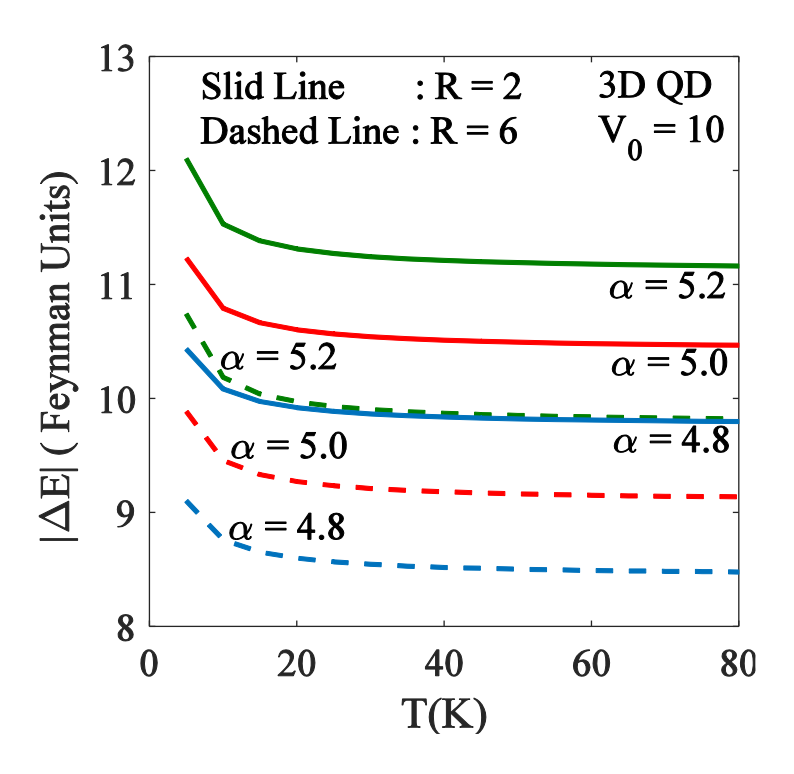


**FIG. 3.3**: GS polaron binding energy (BE) vs T in the strong-coupling regime for two values of R.

To determine the role of e-p coupling, we calculate the GS polaronic correction  $\Delta E$ , which is the energy by which the GS electron energy is modified because of the e-p interaction. This is also called the GS polaron self-energy which is defined as:  $\Delta E = E(\alpha) - E(\alpha = 0)$ . The condition of polaron formation is given by:  $\Delta E < 0$ . The negative of  $\Delta E$  or  $|\Delta E|$  gives the polaron binding energy (BE) which is the energy

required to strip off the phonons from the electron. In Figs. 3.3 and 3.4, we have shown the nature of  $|\Delta E|$  vs. T - curve in GQD. From Fig. 3.3, one can conclude that in a 3D strongly-coupled GQD, as T increases,  $|\Delta E|$  initially decreases, and then gradually reaches a saturation value. This is in conformity with Fig. 3.1. Fig. 3.4 describes the behaviour of  $|\Delta E|$  for intermediate values of  $\alpha$ . We immediately see that in 2D QDs, at low T, as T

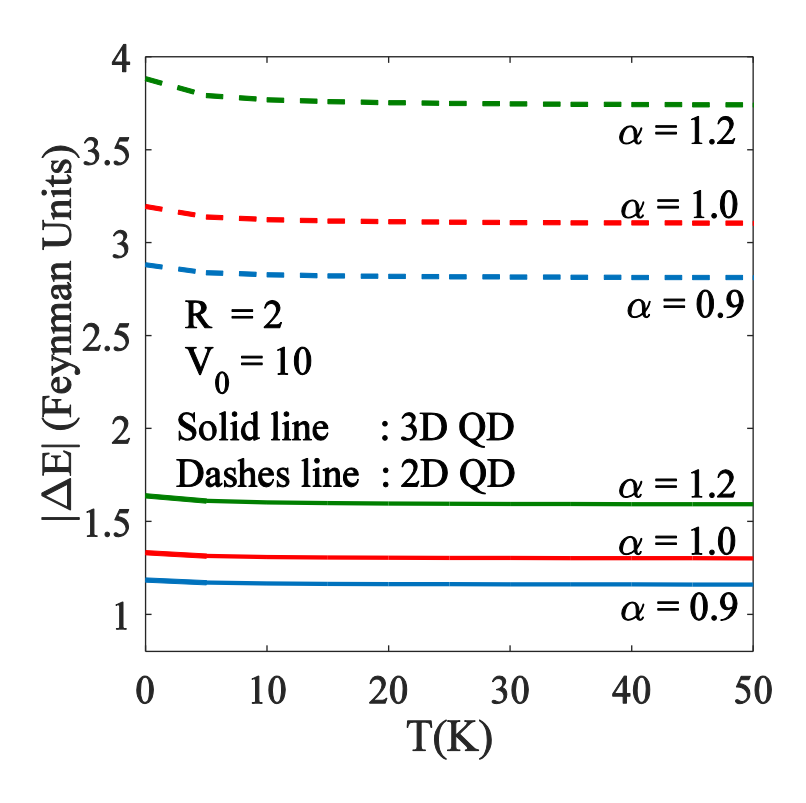


**FIG. 3.4**:  $|\Delta E|$  vs T for intermediate values of  $\alpha$  for 2D and 3D GQDs.

increases,  $|\Delta E|$  shows a small decreasing behaviour. But as T increases a little more,  $|\Delta E|$  quickly reaches a saturation value. We have already

explained this behaviour. For a 3D QD,  $|\Delta E|$  is more or less T- independent which is consistent with Fig. 3.2. From Fig. 3.4, we conclude again that even at T>0, the polaronic binding is weaker in 3D QDs than in 3D ones.

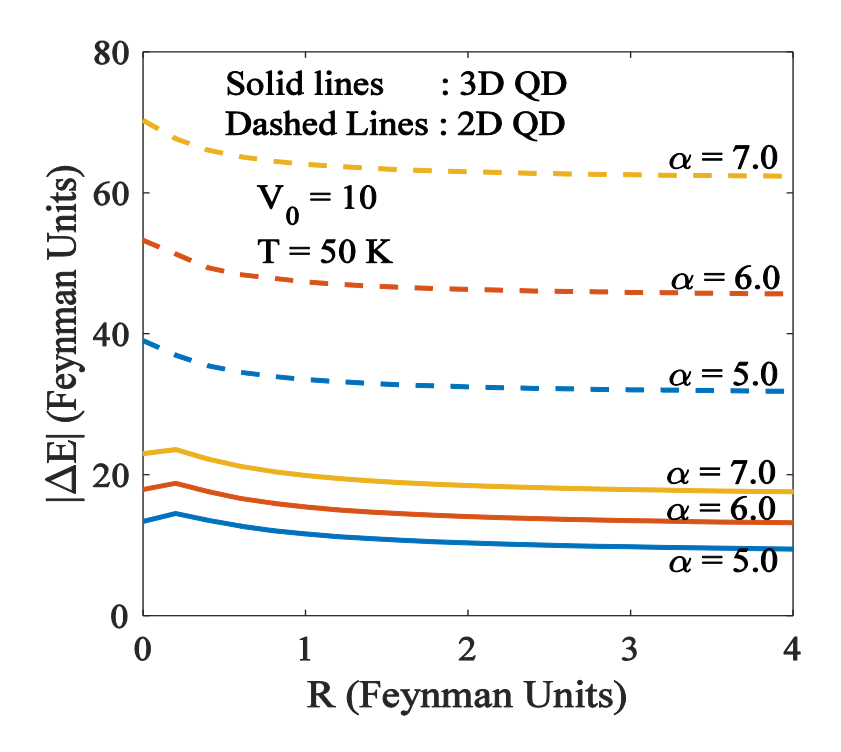


**Fig. 3.5**  $|\Delta E|$  vs R for a polaron in 2D and 3D QDs in strong-coupling regime.

In Figs. 3.5, 3.6 and 3.7, we have studied the behaviour of  $|\Delta E|$  with respect to R for large, intermediate and small values of  $\alpha$  respectively at a particular temperature namely, T = 50K. Fig. 3.5 reveals that in a strongly-coupled GQD,  $|\Delta E|$  has a weaker dependence on R in 3D than

in 2D. As R decreases in a 3D QD,  $|\Delta E|$  is found to increase, though slowly, but below a certain R, it appears to decrease with the decrease in R. The origin of this behaviour is completely quantum in nature. With the reduction in QD size, the electron kinetic energy rises leading to the reduction in the polaron binding. Interestingly enough, 2D QDs do not show this behaviour.

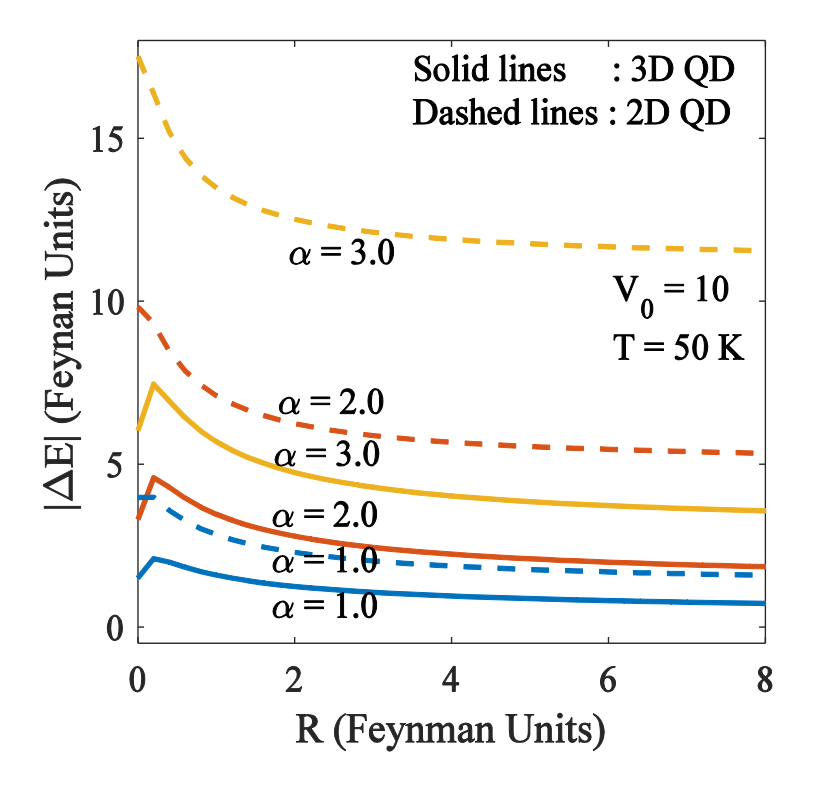


**Fig. 3.6**  $|\Delta E|$  vs R for a polaron in 2D and 3D QDs in the intermediate-coupling regime.

In Fig. 3.6, we plot  $|\Delta E|$  with respect to R in the intermediate-coupling range. The behaviour is qualitatively similar to the strong-coupling case.

However, in the case of 3D QDs now, peaks in  $|\Delta E|$ 's appear a little sharper than the corresponding strong-coupling cases.

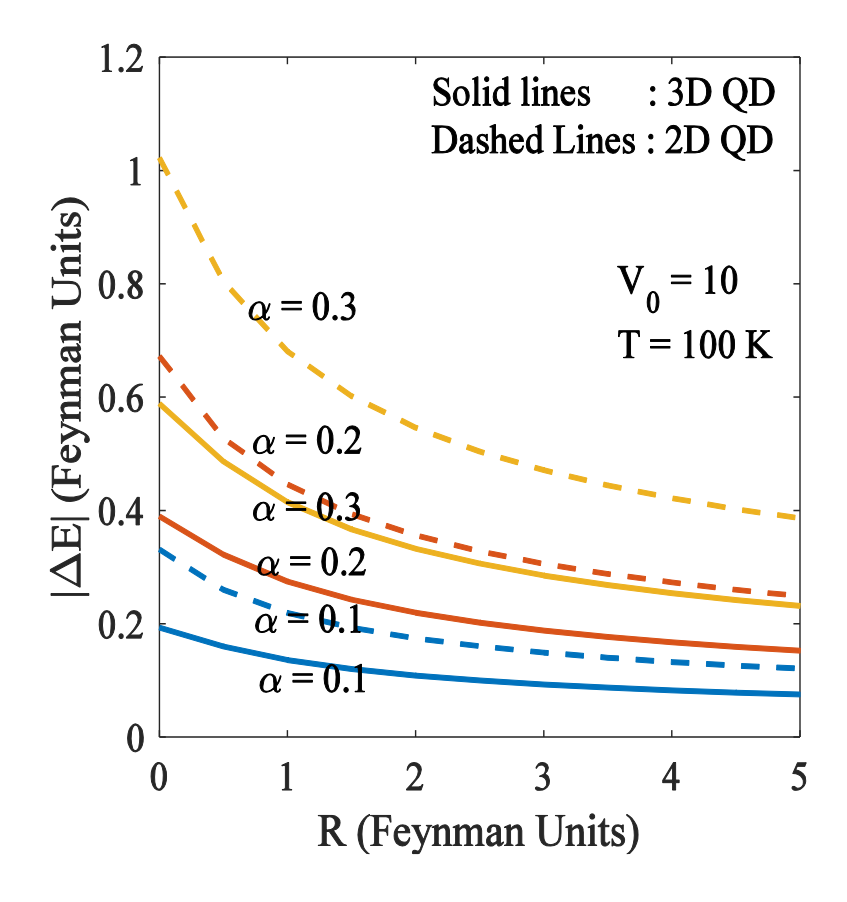


**Fig. 3.7**  $|\Delta E|$  vs R for a polaron in 2D and 3D QDs in the weak-coupling regime.

Fig. 3.7 shows the variation of  $|\Delta E|$  with R in the weak-coupling region. One can see that in this region, as R is reduced,  $|\Delta E|$  increases monotonically for 2D as well as 3D QD. However, the polaron effect in all cases, is stronger in 2D than in 3D. This is consistent with the general

result that e-p interaction effect increases with the reduction in dimensionality.

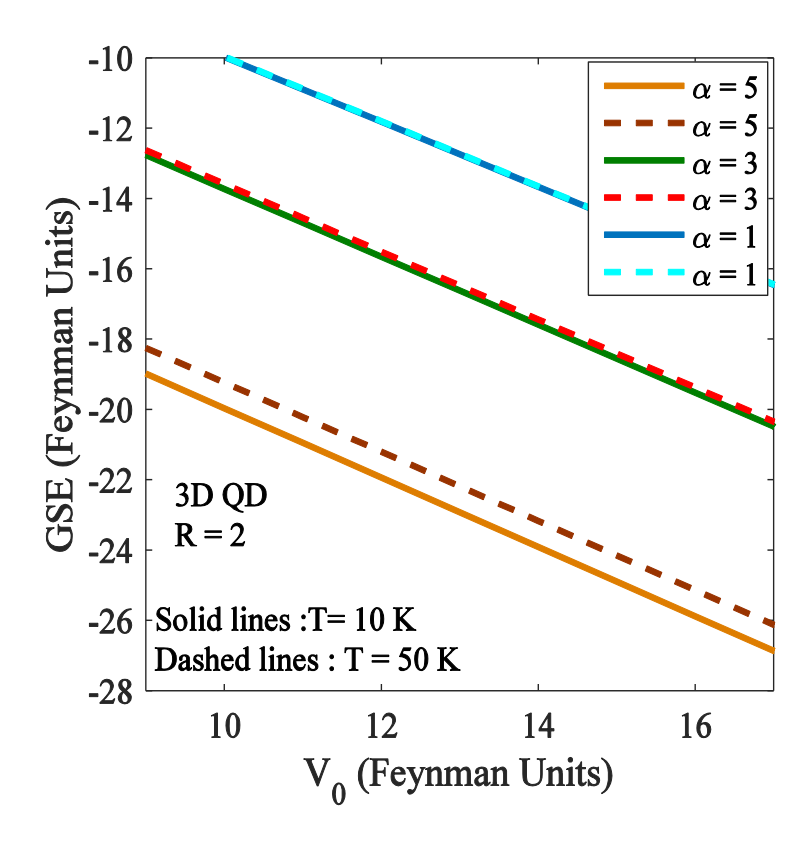


**Fig. 3.8** GSE vs  $V_0$  for a 3D QD T = 50K in T = 50K T = 50K in strong and intermediate coupling regimes.

In Fig. 3.8, we plot GSE versus  $V_0$  for R=2 at T=10K and 50K. GSE is found to decrease with increasing  $V_0$ . This indicates that the polaronic binding is strengthed as  $V_0$  is made greater. Needless to say, the polaronic effect becomes stronger with increasing  $\alpha$ . Fig. 3.9 shows

this behaviour explicitly. Again, the polaron GSE value in 2D QD lies below that in 3D QD.

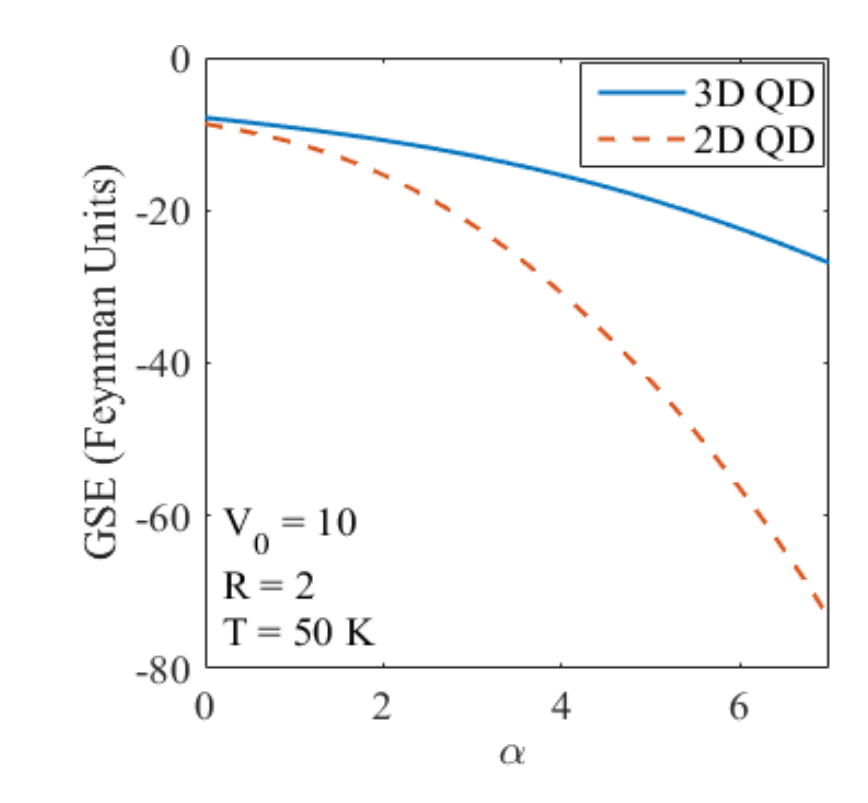


**Fig. 3.9** GSE vs  $\alpha$  in 2D and 3D QD at T = 50K.

# 3.5 CONCLUSION

In this chapter, we have presented our results on the effect of temperature on the polaronic properties in GQD. These results have been found out with the help of the variational theory of Lee, Low, Pines and Huybrechts and statistical mechanics. Our results reinforce the notion that the GS polaron binding in ND GQD becomes weaker as temperature rises and thus the polaronic effect weakens at higher temperature. The explanation for this phenomenon is as follows. With the rise in temperature, the probability of excitation of real phonons becomes certainly more. This suppresses polaron formation. Finally we observe that even at non-zero temperature, polaronic effects diminish with increasing dimensionality.

### 3.6 REFERENCES

- [1] F.M Peeters and J T Devrees, *Temperature dependence of the polaron mass in AgBr.* Phys. Rev. B, **31** 5500 (1985).
- [2] Ka-Di Zhu and S. W. Gu, *Temperature dependence of polarons in a harmonic quantum dot* Phy. Lett. A **171** 113 (1992).
- [3] S. Chen and J. Xiao, Temperature effect on impurity-bound polaronic energy levels in a GaAs parabolic quantum dot Physica B **393** 213 (2007).[4] Eerdunchaolu, and W. Xin, Temperature dependence of the properties of strong-coupling bipolaron in a quantum dot Physica B **406** 358 (2011).
- [5] J. Zhang and S. Shan, *Temperature Effect on Effective Mass of the Polaron in an Asymmetric Quantum Dot* J. Low. Temp. Phys **177** 283(2014).
- [6] N. Issofa et. al, Energy Levels of Weak Coupling Magneto-Optical Polaron and Temperature Effect in Spherical Quantum Dot Am. J. Mod. Phys 4 (2015) 158-164.
- [7] G.Whitefield and M. Engineer, *Temperature dependence of the polaron* Phys. Rev. B **12** 5472 (1975).
- [8] W. Xeaoguang, F. M. Peeters & J. T. Devreese, *Temperature dependence of the polaron mass in a GaAs*  $Al_xGa_{1-x}As$  *heterostructure*, Phys. Rev. B **36** 9765 (1987)
- [9] Eerdunchalu and Wei Xin, *The temperature dependence of the properties of the strong coupling bipolaron in a QD*, Physica B **406** 358 (2011)
- [10] Zhi-Xin Li, Temperature Dependence of Strong-Coupled Polaron in a Triangular Potential Quantum Dot, J. Low Temp Phys. 165 36 (2011)
- [11] S.P. Shan, L. Q. Cai, Y. M. Liu and J. L. Xia, Temperature and Impurity Effects of the Magnetopolaron in an Asymmetric Quantum Dot, Chin. J. Phys. 52 880 (2014)

- [12] C. Y. Cai, C. L. Zhao and J. L. Xiao, Effects of temperature on ground state binding energy of strong coupling magnetopolaron in RbCl parabolic quantum Dot. Indian J. Pure&Appl. Phys. **54** 56 (2016)
- [13] K. Zhu and S.Gu, Phys. Temperature dependence of polarons in a harmonic quantum dot, Lett. A **171** 113 (1992)
- [14] K. Zhu and S. Gu *Temperature effects on the Self-trapping energy of a polaron in a Ga As parabolic quantu dot*, J. Mater. Sci. Technol., **10** 131 (1994)
- [15] S. H. Chen, Q. Z. Yaoand Y. H. Wei, Temperature Dependence of Polaronic Correction to the Ground State Energy in a GaAs Parabolic Quantum Dot, J. Low. Temp. Phys. 168 63 (2012)
- [16] S. H. Chen and J. L. Xia, Temperature effect on impurity-bound polaronic energy levels in a GaAs parabolic quantum dot ,Physica B **393** 217 (2007)
- [17] Temperature and impurity effects of the polaron in an asymmetric quantum dot, S. P. Shan, Y. M. Liu and J. L. Xiao, J. Low Temp. Phys. **39** 607 (2013)
- [18] Temperature Effect on Effective Mass of the Polaron in an Asymmetric Quantum Dot, J. F. Zhang and S. P. Shan, J. Low. Temp. Phys. **117** 283 (2014)
- [19] Effect of temperature on vibrational frequency of strong coupling polaron in asymmetric quantum dot., X. J. Miao, Y. Sun and J. L. Xiao, Indian J Phys.88 777 (2014)
- [20] W.Xin, Wuyungimuge, C.Han, Eerdunchaolu, Magnetic field and temperature dependence of the effective mass of strong-coupling bound magnetopolaron in quantum rods with hydrogenic impurity SuperLat. Microstruct. **61** 13 (2013).

4

# Effect of confinement potential shape on the electronic, thermodynamic, magnetic and transport properties of a GaAs quantum dot at finite temperature

### Abstract

Confinement potential profile has a major role to play in influencing the quantum dot properties. Here we consider a general power-exponential potential containing a tunable parameter p. By controlling p we can create confinement potentials of different shapes. We study how different quantum dot properties are influenced by the shape of the dot. We determine the average thermodynamic energy, specific heat, persistent current and magnetic susceptibility at low temperature within the framework of the canonical ensemble approach of statistical mechanics. We show that the average energy has a strong dependence on p for small p while for large p, on the other hand, p has hardly any effect on the energy. Interestingly, it turns out that the specific heat is unaffected by the shape or depth of the confinement potential at low temperature as well as the magnetic field for the range considered. The magnetic behaviour of the system looks rather interesting. The system displays a paramagnetic-diamagnetic transition at a certain magnetic field strength. It is found that for small values of p, the system is diamagnetic in a small temperature window, then for a temperature window the system is paramagnetic and as the temperature is further increased, the system goes into a re-entrant diamagnetic phase. For large p, the system behaves in a similar way up to a certain temperature, namely till the system enters into re-entrant diamagnetic phase. Here we see that  $\chi$ exhibits well-developed minima and finally enters into the paramagnetic

phase again. We furthermore show that at magnetic fields higher than a critical value, the system is always diamagnetic for shallow confinement potentials, irrespective of their shape. Thus, for a window of p values, we expect the phenomenon of reentrant diamagnetic behaviour to show up for a range of magnetic field strength. We finally show that in a power-exponential quantum dot, the persistent current is diamagnetic at low temperature and its magnitude is larger when the potential is deeper. It is however independent of p. At high temperature, however, the persistent current can be paramagnetic for small p.

## 4.1 INTRODUCTION

In order to develop a theory of quantum dots it is absolutely necessary to have a prescription for the confinement potential. Early experimental results gave the indication that the quantum dot (QD) confinement potential has a parabolic character. This led to extensive investigations on parabolic QDs [1-29]. Some later experimental results on QDs however contended that the confinement potential is anharmonic with a depth that is finite [30,31]. Adamowsky et al. [32] have advocated the Gaussian potential as the model for confinement potential. The Gaussian potential turned out to be a more realistic model for the confinement potential in QD. Consequently, a large number of studies [33-52] have been conducted on several aspects of QDs by many researchers by making use of the attracting Gaussian potential model. Ciurla et al. [53] have introduced a general form for the QD potential namely, powerexponential (PE) potential. It contains a steepness parameter p. By tuning this parameter p one can generate potentials of different shapes. Also, some of the widely used confinement potentials can be generated from it in different limiting cases. Kwaśniowski and Adamowski [54] have considered the PE potential for the study of electron exchange interaction in coupled QDs. Xie [55] has concluded using the PE model that the photo-ionization of a donor impurity is highly influenced by the QD shape.

In this chapter, we take up the problem of a two-dimensional (2D) QD with PE potential and spin-Zeeman interaction in a magnetic field at finite temperature and examine the effect of dot shape on the average thermal energy, heat capacity and the susceptibility of the electron and

the persistent current. We shall describe QD with PE confinement as PEQD.

## 4.2 MODEL

An electron of charge e and band mass  $m^*$  moving in a 2D PEQD in a magnetic field  $\mathbf{B}$  (0,0,B) may be described by the Hamiltonian

$$H = \frac{1}{2m^*} \left( \boldsymbol{p} + \frac{e}{c} \boldsymbol{A} \right)^2 + V(\boldsymbol{\rho}), \tag{4.1}$$

where  $\rho$  (p) is the 2D electron position (momentum) operator, A is the vector potential related to B as:  $B = \nabla \times A$ , and is chosen as: A = (-By/2, Bx/2, 0) so that  $\nabla \cdot A = 0$  and  $V(\rho)$  is the PE potential [2] given by .

$$V(\boldsymbol{\rho}) = -V_0 e^{-\left(\frac{\boldsymbol{\rho}}{R}\right)^p},\tag{4.2}$$

where  $V_0$  specifies the PE potential depth and thus gives the confinement strength, R gives the effective QD size and p is the steepness parameter and determines the shape of the potential. For small values of p, the potential is soft. As p increases, the potential becomes harder. The potential becomes Gaussian for p = 2. For  $p \ge 10$ , the potential becomes very hard or steep at the QD boundary. As p increases further, we have an extremely hard potential mimicking a rectangular potential (Fig.1) [3].

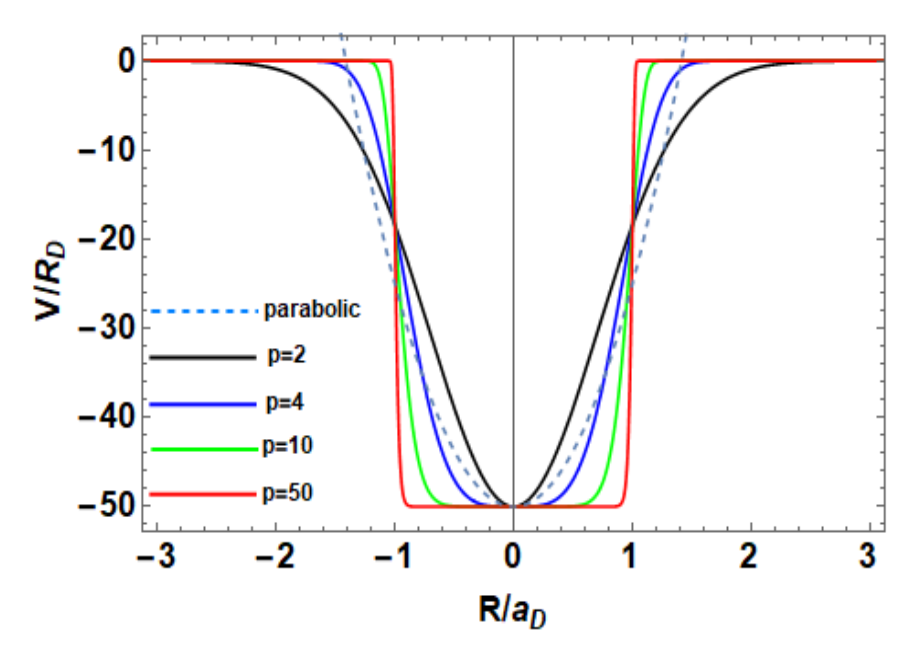


**Fig.4.1**. Shape of the Power-exponential (PE) confinement potential for p = 0, 2, 4, 10 and 50.

The Hamiltonian now reads

$$H = -\frac{\hbar^2}{2m^*} \nabla_{\rho}^2 - V_0 e^{-\left(\frac{\rho}{R}\right)^p} + \frac{m^*}{8} \omega_c^2 \rho^2 + \frac{\hbar \omega_c}{2} (\hat{L}_z + g^* \hat{S}_z), \qquad (4.3)$$

where  $L_z$  and  $S_z$  are respectively the z-components of the radial and spin angular momentum operators of the electron,  $\omega_c = eB/m^*$ 

# 4.3 FORMULATION

If the PE potential does not deviate much from the parabolic potential, then the PE potential may be approximated by a potential which contains a parabolic potential and a perturbation term. This approximation looks plausible if r takes only small values. Since in QD, the electron, in any case, is restricted to move in a nanoscale confined geometry, this approximation can be regarded as fairly reasonable. So we rewrite Hamiltonian (4.3) as

$$H = H_0 + H_1 , (4.4)$$

with

$$H_0 = -\frac{\hbar^2}{2m^*} \nabla_{\rho}^2 + \frac{1}{2} m^* \widetilde{\omega}^2 \rho^2 + \frac{1}{2} \hbar \omega_c (\hat{L}_z + g^* \hat{S}_z) - V_0, \qquad (4.5)$$

$$H_1 = -\lambda \left[ \frac{1}{2} m^* \omega_h^2 \rho^2 + V_0 \left( e^{-\left(\frac{\rho}{R}\right)^p} - 1 \right) \right], \tag{4.6}$$

where

$$\widetilde{\omega}^2 = \omega_h^2 + \frac{\omega_c^2}{4} \quad , \quad \omega_h^2 = \frac{V_0}{m^* R^2} \quad .$$
 (4.7)

One can immediately see that  $\lambda = 0$  describes a parabolic confinement while  $\lambda = 1$  implies that the PE potential is the confinement potential. We include the effect of  $H_1$  by a mean-field approach in which we assume that  $H_1$  effectively renormalizes the frequency  $\widetilde{\omega}$ . Thus we write  $H_1$  as

$$H_1 = \lambda \left[ \frac{V_0}{\langle \rho^2 \rangle} - \frac{1}{2} m^* \omega_h^2 - V_0 \frac{\langle e^{-\left(\frac{\rho}{R}\right)^p} \rangle}{\langle \rho^2 \rangle} \right] \rho^2 , \qquad (4.8)$$

where the quantum mechanical averages are carried out with respect to the ground state of the Hamiltonian:  $\mathcal{H}(\widetilde{\omega}) = [-\frac{\hbar^2}{2m^*}\nabla_{\rho}^2 + \frac{1}{2}m^*\widetilde{\omega}^2\rho^2]$ . Under this approximation, the Hamiltonian H reduces to

$$H = -\frac{\hbar^2}{2m^*} \nabla_{\rho}^2 + \frac{1}{2} m^* \omega^2 \rho^2 + \frac{1}{2} \hbar \omega_c (\hat{L}_z + g^* \hat{S}_z) - V_0, \tag{4.9}$$

where  $\omega$  given by:  $\omega = \left[\widetilde{\omega}^2 + \frac{2\lambda}{m^*} \left( (V_0/\langle \rho^2 \rangle) - \frac{1}{2} m^* \omega_h^2 - V_0 \left\{ \langle e^{-(\rho/R)^p} \rangle / \langle \rho^2 \rangle \right\} \right) \right]^{1/2}$  and  $g^*$  is the effective Lande-g factor. In the case of GaAs QD,  $g^* = -0.44$ . Thus effective Schrödinger equation is given by

$$H \Psi_{nls}(\rho, \theta, \sigma) = E_{nls} \Psi_{nls}(\rho, \theta, \sigma), \qquad (4.10)$$

where the wave function  $\Psi_{nls}(\rho, \theta, \sigma)$  is the Fock–Darwin wave function given by

$$\Psi_{nls}(\rho,\theta,\sigma) = \sqrt{\frac{\alpha^2 n!}{(n+|l|)! \pi}} (\alpha \rho)^{|l|} L_n^{|l|} (\alpha^2 \rho^2) e^{-\frac{\alpha^2}{2} \rho^2 + il\theta} \chi_s(\sigma), \quad (4.11)$$

where  $\alpha=(m^*\omega/c)^{1/2}$ ,  $n=0,1,2,3,\ldots$ ,  $l=0,\pm 1,\pm 2,\ldots$ ,  $L_n^{|l|}$  describes the associated Laguerre polynomial, and  $\chi_s(\sigma)$  satisfies the eigenvalue equation:  $S_z \chi_s(\sigma) = s \chi_s(\sigma)$  with  $s=\pm (1/2)$ . The eigenvalue  $E_{nls}$  of H is obtained as

$$E_{nls} = (2n + |l| + 1)\hbar\omega + \frac{1}{2}\hbar\omega_c(l + g^*s) - V_0.$$
 (4.12)

The partition function corresponding to (4.12) can be exactly determined and we get

$$Z(T,B) = \sum_{n=0}^{\infty} \sum_{l=0}^{\pm \infty} \sum_{s=-\frac{1}{2}}^{s=\frac{1}{2}} e^{-\beta E_{nls}}$$

$$= \frac{1}{2} cosh \left( \frac{1}{4} g^* \beta \hbar \omega_c \right) csch \left\{ \frac{1}{2} \beta \hbar \left( \omega - \frac{\omega_c}{2} \right) \right\}$$

$$\times csch \left\{ \frac{1}{2} \beta \hbar \left( \omega + \frac{\omega_c}{2} \right) \right\}, \tag{4.13}$$

where  $\beta = 1/k_BT$ . Once the partition function is calculated, one can determine the average thermodynamic energy, magnetization, susceptibility and the heat capacity or specific heat using the following relations:

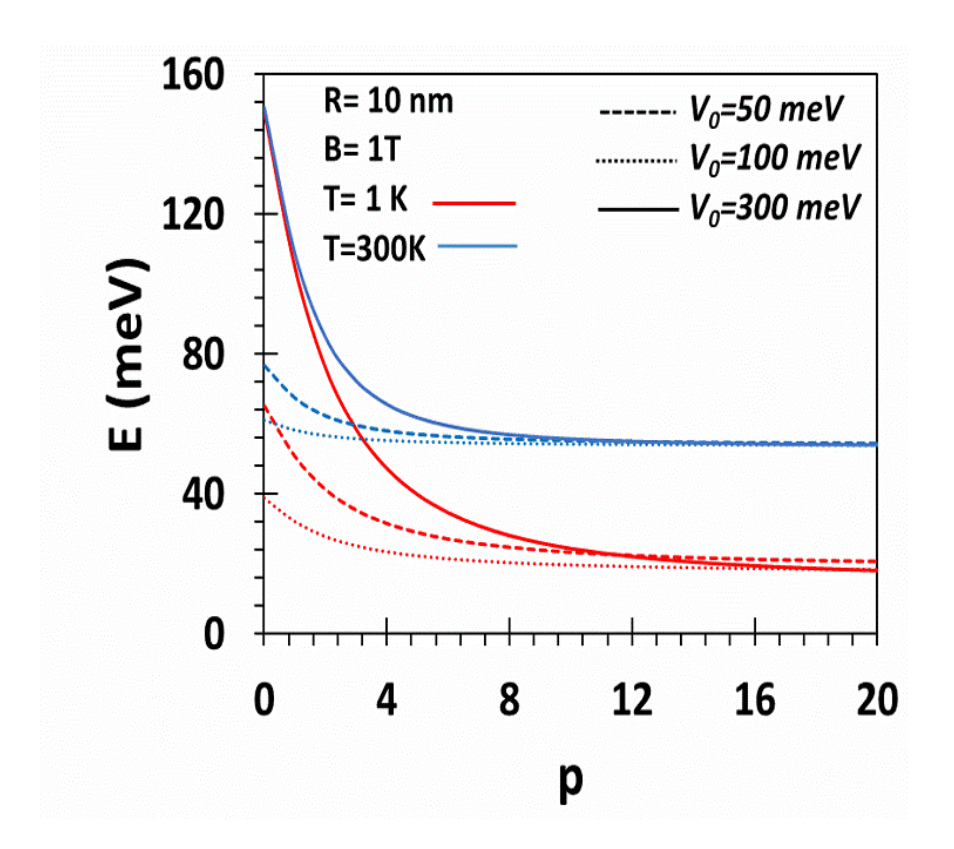
$$\langle E \rangle = -\frac{1}{Z} \left( \frac{\partial Z}{\partial \beta} \right); \langle M \rangle = \frac{1}{\beta Z} \left( \frac{\partial Z}{\partial B} \right); \chi = \frac{\partial \langle M \rangle}{\partial B}; C = \frac{\partial \langle E \rangle}{\partial T}.$$
 (4.14)

We also wish to study the effect of temperature on the persistent current. We determine the thermal average of  $J_{nl}^{spin}$  using the canonical ensemble approach [9]:

$$\langle J_{nl}^{spin} \rangle = \frac{\sum_{n,l,s} J_{nl}^{spin} e^{-\beta E_{nls}}}{\sum_{n,l,s} e^{-\beta E_{nls}}}.$$
 (4.15)

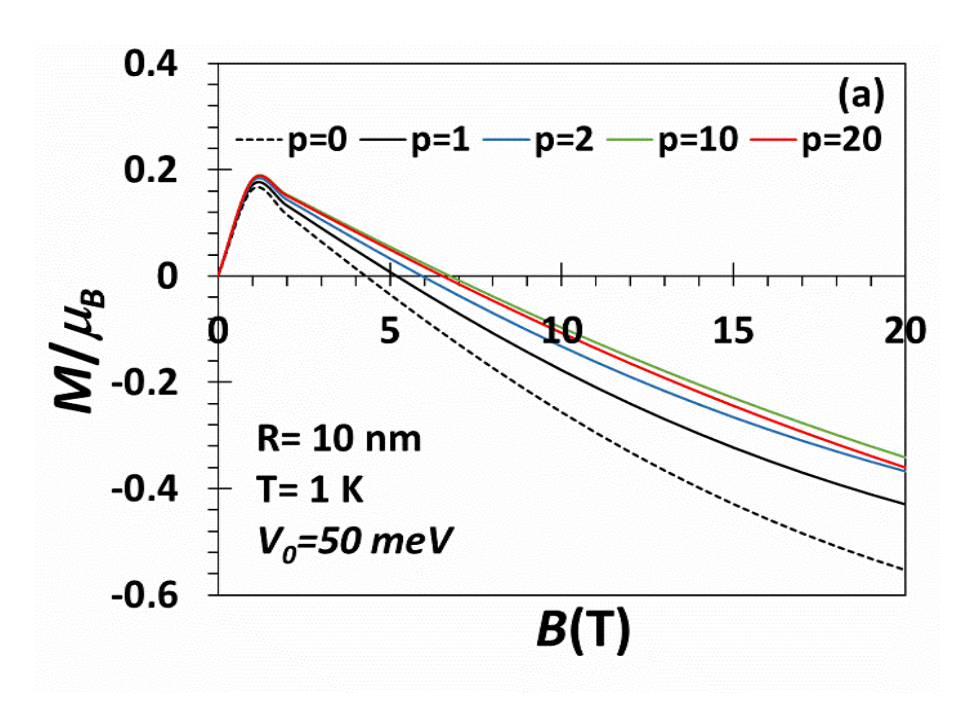
# 4.4 NUMERICAL RESULTS AND DISCUSSIONS

Fig. 4.2 presents the behaviour of the thermodynamic average of the electron energy ( $\langle E \rangle$ ) in PEQD of GaAs with respect to the steepness parameter p for R=1 nm, B=1T, T=1 and 300K, and for three values of  $V_0$  namely,  $V_0=50$ , 100, 300 meV. It is clear that as p is



**Fig. 4.2**  $\langle E \rangle$  vs p in the case of a PEQD of GaAs with  $V_0 = 50$ , 100, 300 meV, R = 10 nm, B = 1T and T = 1 and 300 K.

reduced,  $\langle E \rangle$  shows a monotonic increase and the rate of increase is higher when p is smaller and  $V_0$  is larger. The reason is simple. Softening of potential allows the sustenance of a larger number of states in the potential well in general and at the Rydberg levels in particular. This obviously leads to a higher value of  $\langle E \rangle$ .  $\langle E \rangle$  also seems to increase with increasing temperature T which is of course understandable. As p increases,  $\langle E \rangle$  approaches the same saturation value irrespective of the value of  $V_0$ . This is also an expected behavior because in the case of large p, the potential becomes very hard and then the shape of the potential remains essentially independent of p. In this limit, an increase in p does not change the number of states in the potential and consequently  $\langle E \rangle$  saturates.



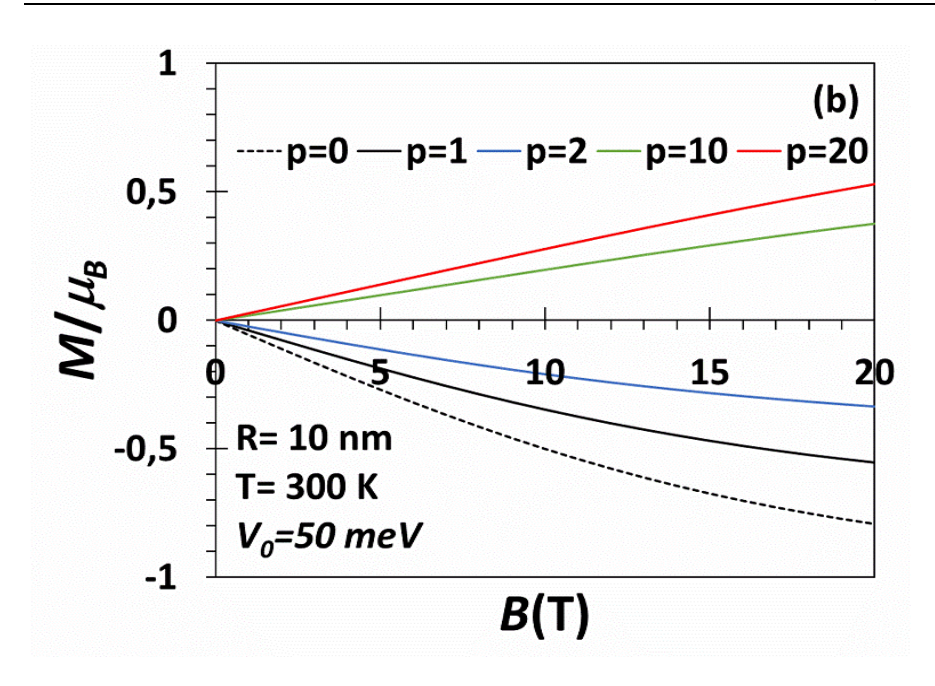


**Fig. 4.3** Magnetization  $(M/\mu_B)$  vs p of PEQD of GaAs with  $V_0 = 50$ , 100, 300 meV, R = 10 nm, B = 1T and (a) T = 1K and (b) 300 K.

Figs. 4.3 displays the behaviour of the average magnetization ( $\langle M \rangle$ ) of PEQD of GaAs against B for several p values at: (a) = 1K; (b) T=300K. At T=1K (Fig. 4.3(a)),  $\langle M \rangle$  initially grows with B, attains a peak at some critical B and then diminishes as B increases further and eventually turns negative and keeps assuming increasingly higher negative values with increase in B. A qualitatively similar behaviour is observed for different p values. At T=300K (Fig. 4.3(b)),  $\langle M \rangle$  behaves with B in a qualitatively different way. For =0,1,2,  $\langle M \rangle$  remains always negative and its magnitude keeps on increasing with B, while for p=10, and 20,  $\langle M \rangle$  remains always positive and increases with B.

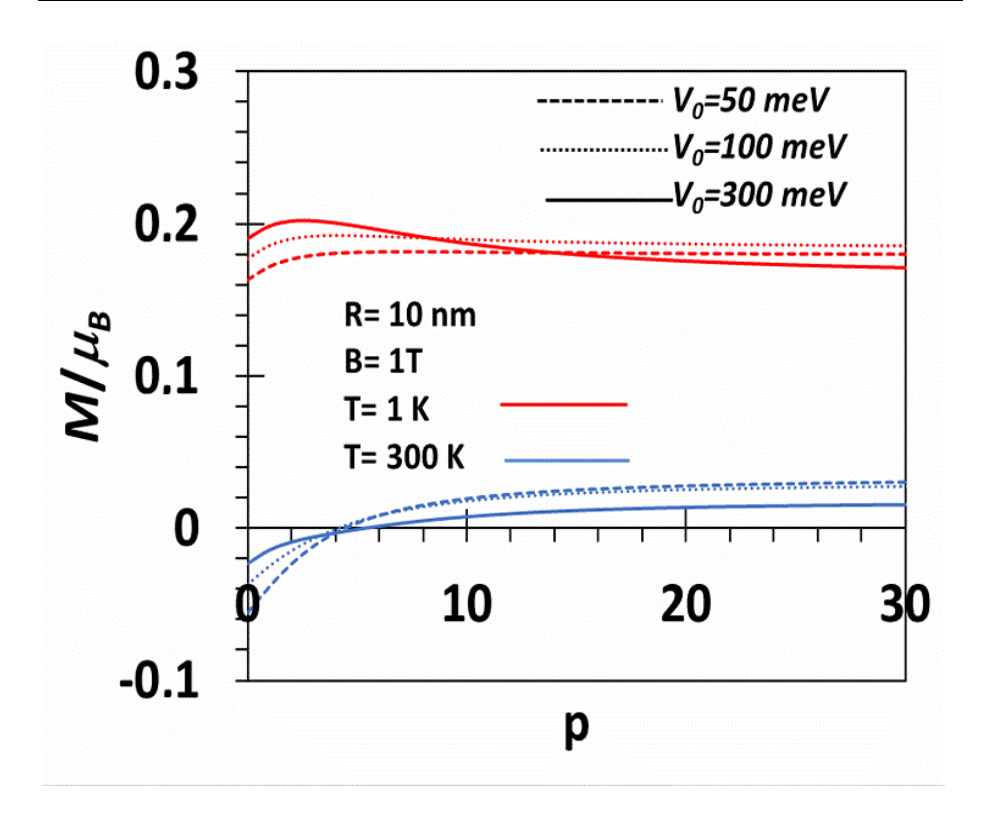


**Fig. 4.4** Magnetization  $(M/\mu_B)$  vs p of PEQD of GaAs with  $V_0 = 50$ , 100, 300 meV, R = 10 nm, B = 1T and T = 1 and 300 K.

In Fig. 4.4, we delineate the behaviour of  $\langle M \rangle$  directly with respect to p for PEQD of GaAs with R=10 nm,  $V_0=50$ , 100, 300 meV and for B=1T and T=1K and 300K. At low temperature  $(T\sim 1\ K)$ ,  $\langle M \rangle$  is found to be always positive which is an expected behavior because of low thermal disorder at low temperature. Furthermore, at small p, as p increases,  $\langle M \rangle$  grows slowly with p and reaches a small maximum and as p increases further, it falls off slowly and finally reaches saturation. At large p, the confinement potential mimics a hard rectangular potential

and then increasing p does not change the potential structure much. Under this situation, only low-energy states contribute substantially to the partition function, higher excited states (which do not change much with further increase in p) offering very little. This is the explanation for the saturation of  $\langle M \rangle$  at large p. With increasing  $V_0$ , the maximum in  $\langle M \rangle$  appears to grow at small p, while at large p,  $\langle M \rangle$  decreases with increasing  $V_0$ . This happens because when p is small, an increase in  $V_0$  gives rise to quite a few additional Rydberg-like states in the QD potential. Therefore, as a function of p,  $\langle M \rangle$  exhibits a crossing behaviour. At T=300~K,  $\langle M \rangle$  is negative if p is less than some number which is dependent on  $V_0$ . However, above a critical p,  $\langle M \rangle$  is positive and initially increases with the increase in p, but finally reaches a saturation value that is dependent on  $V_0$ .

In Figs. 4.5(a) and 4.5(b) we study the behaviour of susceptibility ( $\chi$ ) of PEQD of GaAs with T for several p values. Fig. 4.5(a) gives the results for B=1 T and Fig. 4.5(b) gives that for B=10 T. Fig. 4.5(a) shows that at very low T,  $\chi$  in PEQD of GaAs is diamagnetic and as T increases, at a certain T it acquires a paramagnetic character. Above this critical T,  $\chi$  increases with T and attains a maximum at some T ( $T_m$ ). The maximum structure is demonstrated explicitly in the inset of Fig. 4.5(a). With further increase in T beyond  $T_m$ ,  $\chi$  starts decreasing and in fact, becomes diamagnetic at another critical T. Beyond this T,  $\chi$  develops a minimum or a minimum-like structure.

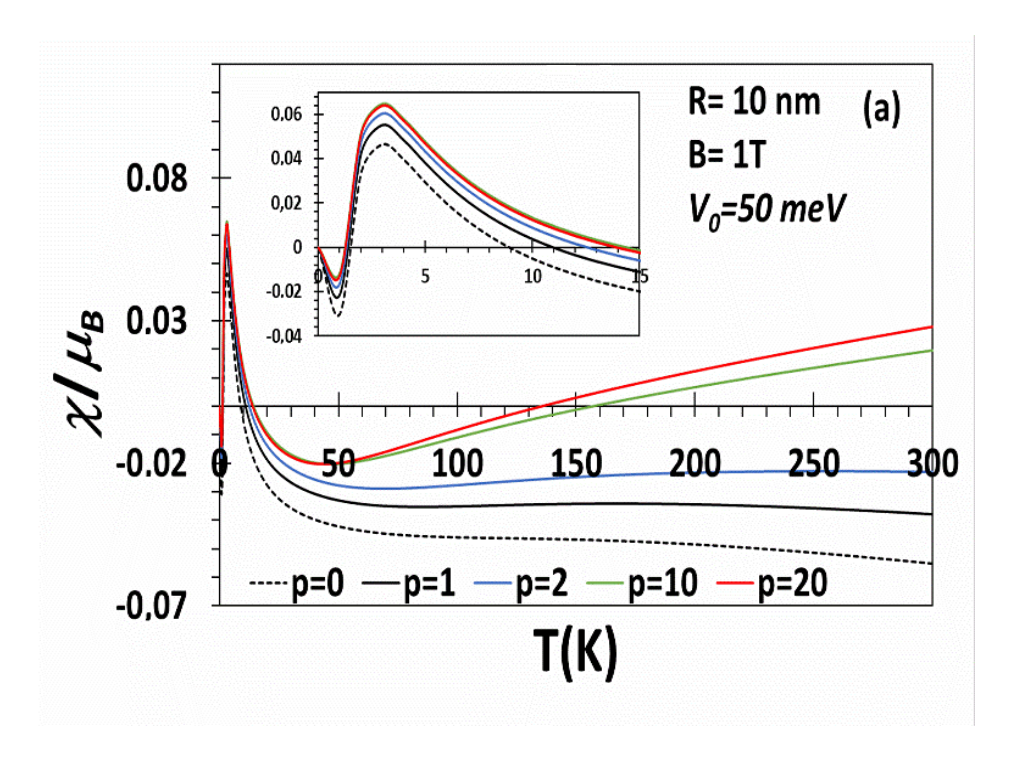


**Fig. 4.5** (a) Magnetic susceptibility  $(\chi/\mu_B)$  vs T of PEQD of GaAs at B=1T with  $V_0=50$  meV and R=10 mm.

For small values of p (p = 1, 2),  $\chi$  remains diamagnetic for all T while for large p (p = 10, 20),  $\chi$  finally becomes paramagnetic and seems to saturate at sufficiently high T value. Thus, for small values of p, there exits a small temperature window in which the system is diamagnetic, then for a temperature window the system is paramagnetic and as the temperature is further increased, the system enters into a re-entrant diamagnetic phase. For large p, the system behaves in a similar way up to a certain temperature, namely till the system enters into re-entrant diamagnetic phase. Here we see that  $\chi$  exhibits well-developed minima and it finally enters into the paramagnetic phase again. Thus it seems

there are two paramagnetic phases for large p and two diamagnetic phases for small p. Fig. 4.5(b) shows that if the magnetic field is strong enough , then for small p values, a GaAs QD is always diamagnetic whereas for large p, the system goes through a diamagnetic-paramagnetic transition at a critical T.

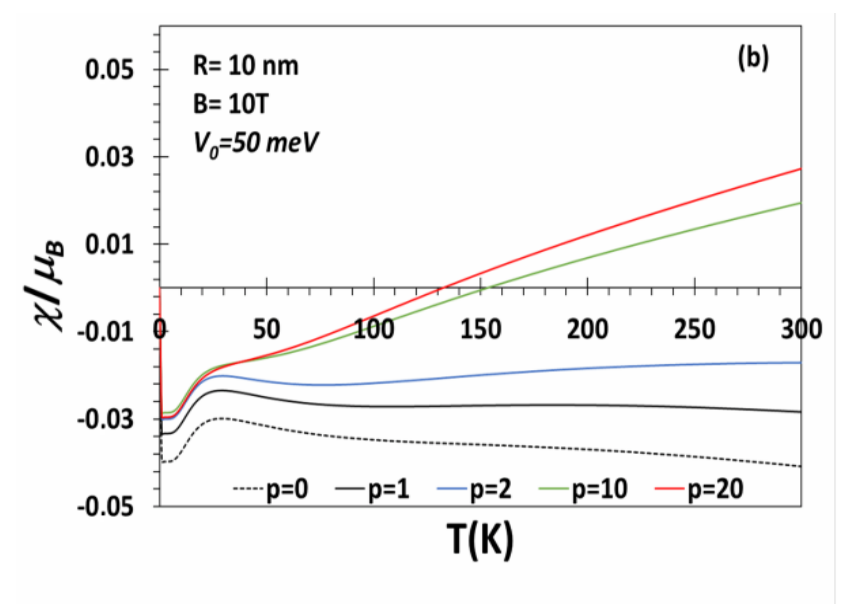


**Fig. 4.5(b)** Magnetic susceptibility  $(\chi/\mu_B)$  vs T of PEQD of GaAs at B = 1T with  $V_0 = 50$  meV, R = 10 mm.

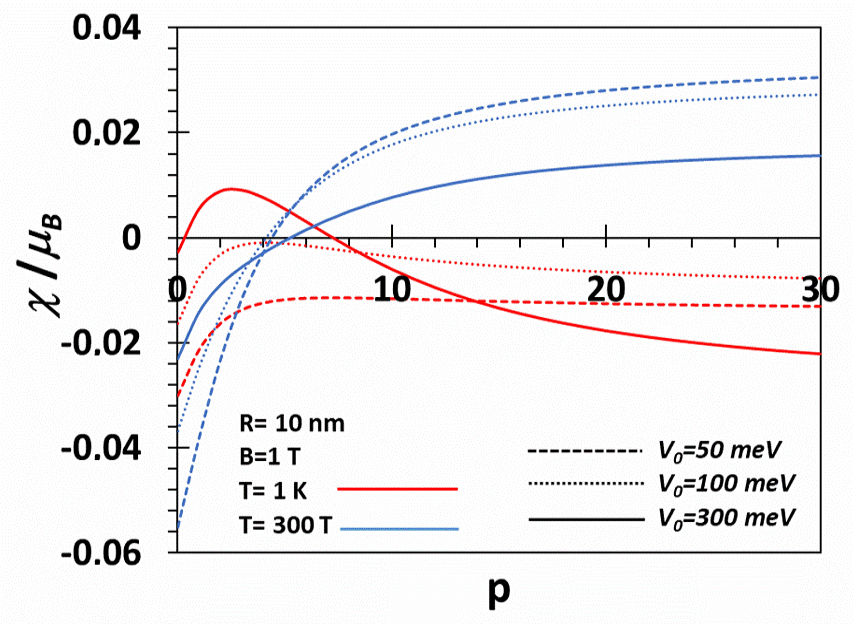


**Fig. 4.6**  $(\chi/\mu_B)$  vs *p* of PEQD of GaAs with  $V_0 = 50$ , 100, 300 meV, R = 10 nm, B = 1T and 300 K.

The behaviour of  $\chi$  with p is shown explicitly in Fig. 4.6. At high temperature (T=300~K),  $\chi$  increases monotonically with p from a diamagnetic value, undergoes a transition to the paramagnetic phase at a certain p and eventually approaches a constant paramagnetic value for all values of  $V_0$  considered here. However, at low temperature (T=1~K), the behaviour of  $\chi$  is in general more interesting. For example, at small values of p,  $\chi$  increases with the increase in p, reaches a maximum and then falls off for the values of  $V_0$  considered here. At relatively small  $V_0$  ( $V_0=50,100~meV$ ),  $\chi$  continues to be negative irrespective of the value of p. For sufficiently high  $V_0$  ( $V_0=150~meV$ ), however,  $\chi$  is negative at small p values and as p exceeds a certain

value, it becomes positive and with further increase in p, the system makes a reentrant transition into the diamagnetic phase.

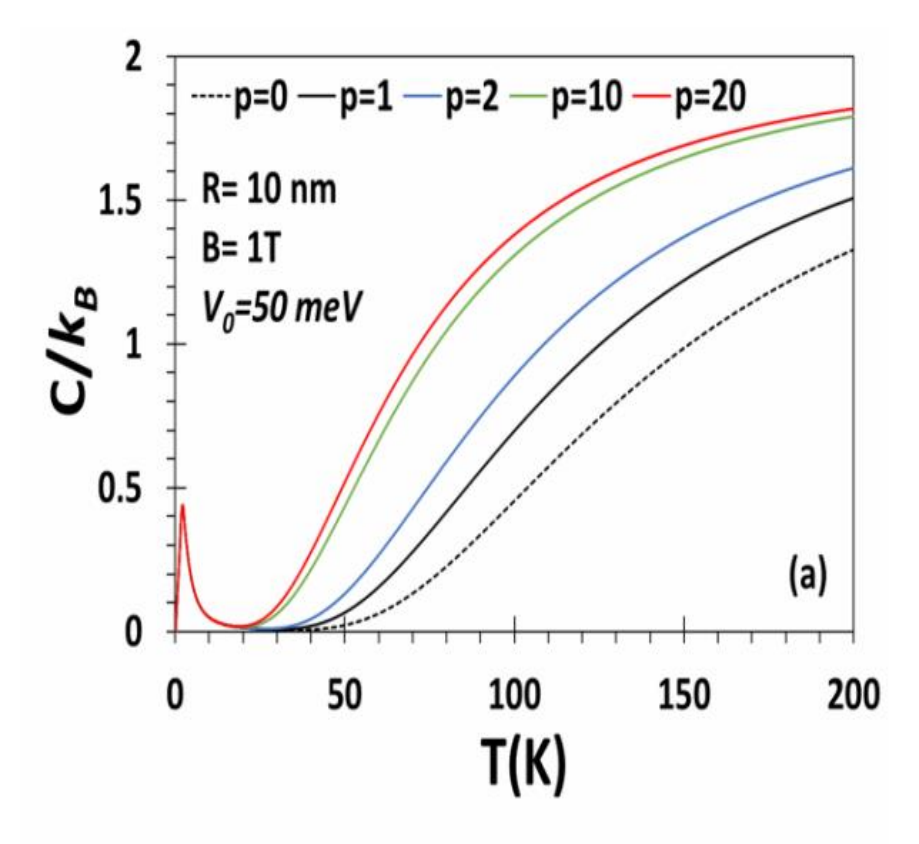


**Fig. 4.7(a)**  $C/k_B$  vs T for B=1T for PEQD of GaAs with  $V_0=50$  meV, R=10 nm, and several values of p.

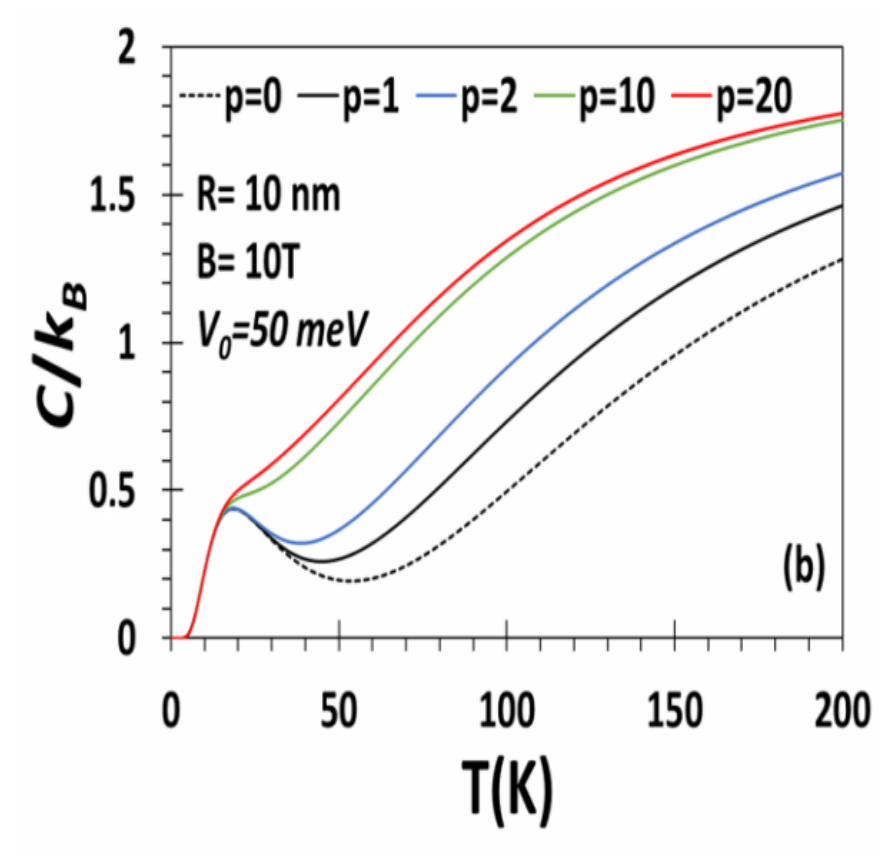


**Fig. 4.7(b)**  $C/k_B$  vs T for B=10T for PEQD of GaAs with  $V_0=50$  meV, R=10 nm, and several values of p.

In Fig. 4.7 (a) we plot the heat capacity (C) of PEQD of GaAs versus T for a few p values. At very low T, C displays a peak structure for all p and up to a certain T, the results are independent of p. Beyond this critical T, C increases with p, though for sufficiently large p, C does not depend much on p. This is understandable because for p greater than a certain value, the potential becomes almost like a square well which hardly changes with the further increase in p. With increasing T, C eventually saturates and the saturation value is about  $2k_B$ . The genesis

of the peak appearing in the C-T-graph is however not clear, though it looks similar to the Schottky anomaly one observes low T in the C-T behaviour of a two-level system. Fig. 7(b) gives the T-dependence of C for PEQD of GaAs at a large B (B=10T). Again the Schotky-like behavior is visible for low values of p, while for large p, a monotonic behavior is observed. Again at large p, the results are essentially independent of p.

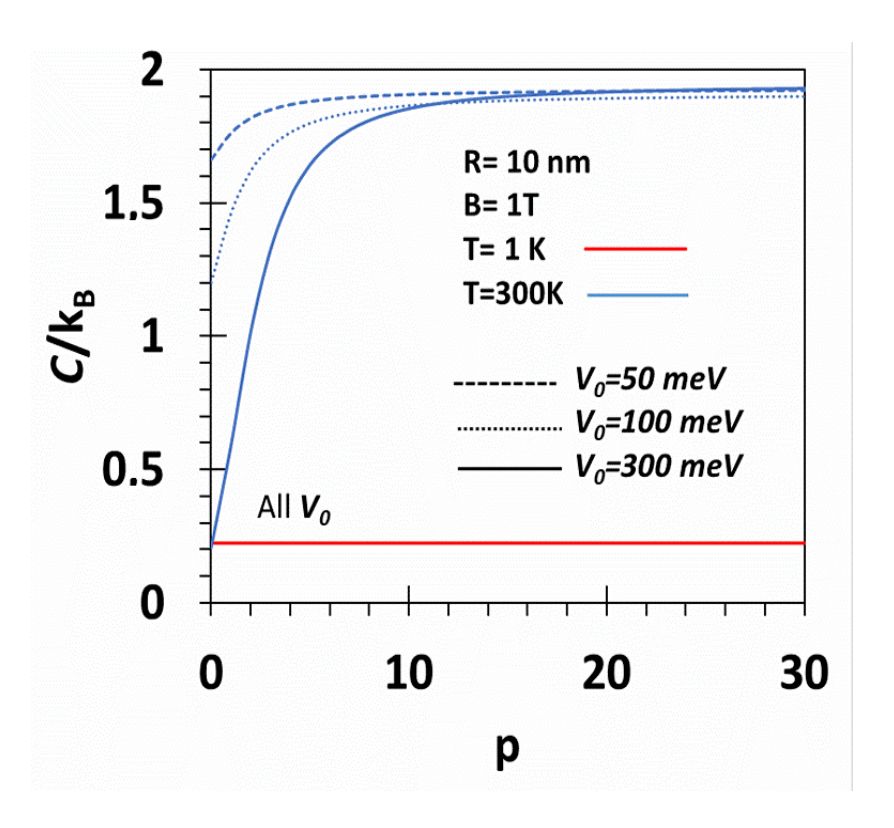


**Fig. 4. 8**  $C/k_B$  vs p for B=1T, T=1 and 300K for PEQD GaAs with R=10 nm and  $V_0=50$ , 100 and 300 meV.

C is plotted directly against p for PEQD of GaAs in Fig. 4.8. The figure shows the results for B = 1T, T = 1K and 300K at  $V_0 = 50$ , 100 and 300 meV. C turns out to be completely independent of both  $V_0$  and p at low T (T = 1K). However, at high T (T = 300 K), it increases with p and finally approaches a constant value  $2k_B$  as p gets large. The value  $2k_B$  is reminiscent of the Dulong-Petit result.

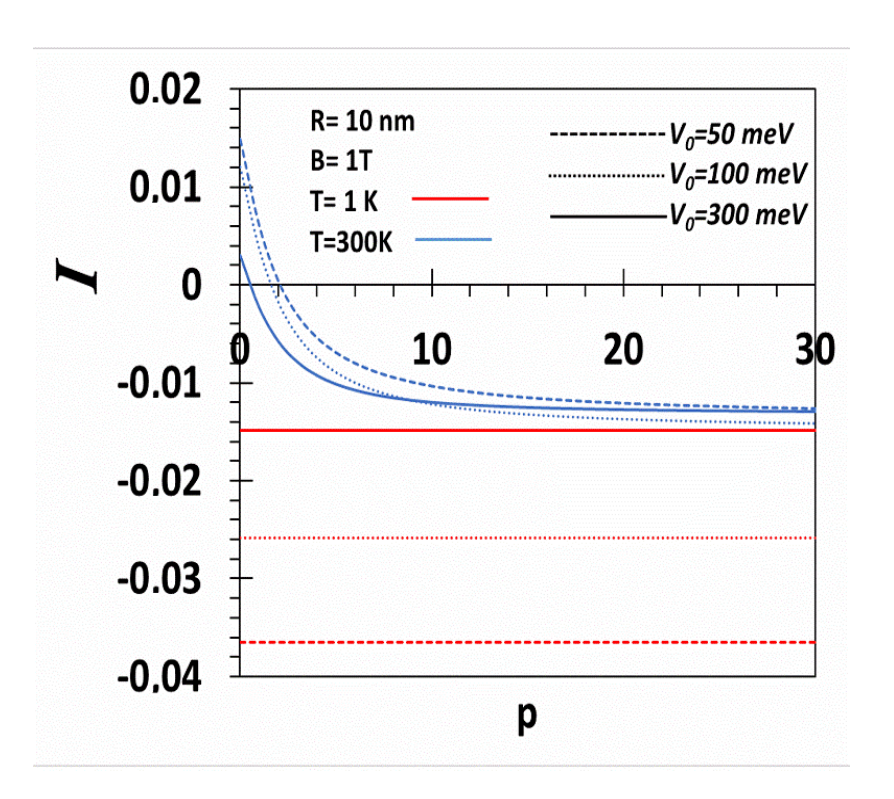


**Fig. 4.9** Persistent current (*I*) (in unit of  $e\omega_h/e\hbar$ ) vs p for B=1T, T=1 and 300K for PEQD of GaAs with  $V_0=50$ , 100 and 300 meV.

In Fig. 4.9, we study the behaviour of the average persistent current (I) with respect to p for B=1, T=1 and 300K for PEQD of GaAs with R=10 nm and  $V_0=50$ , 100 and 300 meV. One can see that I is diamagnetic at low T (T=1K) and its magnitude decreases with increasing  $V_0$ , but it is independent of p. At high T (T=300K), one can see that I is paramagnetic for small values of p. However, it sharply falls off with increasing p at small p and becomes diamagnetic at some value of p which depends on  $V_0$ . The diamagnetic persistent current rises further with increasing p and finally reaches a saturation value.

## 4.5 CONCLUSIONS

In the present chapter, the role of the confinement potential profile on the average thermal energy of the electron, specific heat of the electron, magnetization and susceptibility of the electron and the persistent current has been examined in PEQD of GaAs at non-zero temperature using the PE confinement potential model. The average energy is found to increase with T and  $V_0$ . At small p, the average energy falls off sharply with the increase in p, but as p increases, the energy approaches a T-independent saturation value.

Our calculation reveals that at low T, the shape and depth of the confinement potential have no effect on the heat capacity C of PEQD of GaAs. However, at high T (T=300~K), C increases with p and eventually reaches the saturation value  $2k_B$  at large p.

We have shown that the susceptibility  $\chi$  of PEQD of GaAs increases monotonically with p at high T ( $T=300\,K$ ). At low p,  $\chi$  is

diamagnetic and as p exceeds a critical value,  $\chi$  becomes paramagnetic. At low  $T(T=1\ K)$ , initially  $\chi$  grows with p, attains a maximum and then begins to fall off. Below a certain value of  $V_0$ ,  $\chi$  is always diamagnetic. However, if  $V_0$  is large enough ( $V_0=300\ {\rm meV}$ ), the system is diamagnetic at very small p and turns paramagnetic at some higher value of p and if p is increased further, the system goes once again into the diamagnetic phase. If  $V_0$  is made substantially large, then even at small p,  $\chi$  may be paramagnetic and the system would go into a diamagnetic phase at a larger value of p. Thus the system can exhibit a reentrant behaviour if the value of p falls in a certain window. However, at very low T and large p, the system never shows paramagnetism.

The persistent current (I) in PEQD of GaAs is found to be diamagnetic at low T (T = 1 K), and its magnitude increases with the increase in  $V_0$ . At high T (T = 300 K), I has a paramagnetic character for small values of p, but it sharply falls with increasing p and becomes diamagnetic at some value of p which depends on  $V_0$ . The diamagnetic persistent current increases as p is further increased and finally tends to a saturate.

### 4.6 REFERENCES

- [1] P.A. Maxym, T. Chakraborty, Quantum dots in a magnetic field: Role of electron-electron interactions. Phys. Rev. Lett. **65**, 108 (1990)
- [2] N.F. Johnson, M.c. Payne, *Exactly solvable model of interacting particles in a quantum dot*. Phys. Rev. Lett. **67**, 1157 (1991)
- [3] N.F. Johnson, F.C. Payne, *Many-body effects in resonant tunneling through quantum dots.* Phys. Rev. B **45**, 3819 (1992)
- [4] S.W. Gu, K.X. Guo, Nonlinear optical rectification in the electric-field-biased parabolic quantum dots Solid State Commun. 89, 1023 (1993)
- [5] R. Egger, W. Hausler, C.H. Mak, H. Grabert, *Crossover from Fermi Liquid to Wigner Molecule Behavior in Quantum Dots.* Phys. Rev. Lett. **82**, 3320 (1999)
- [6] K.D. Zhu, S.W. Gu, Cyclotron resonance of magnetopolarons in a parabolic quantum dot in strong magnetic fields Phys. Rev. B 47, 12941 (1993)
- [8] S. Mukhopadhyay, A. Chatterjee, Rayleigh-Schrödinger perturbation theory for electron-phonon interaction effects in polar semiconductor quantum dots with parabolic confinement Phys. Lett. A **204**, 411 (1995)
- [9] K.D. Zhu, T. Kobayashi, Temperature dependence of magnetopolaron masses in a GaAs/AlGaAs quantum dot in external magnetic fields Solid State Commun. 95, 805 (1995)
- [10] S. Mukhopadhyay, A. Chatterjee, *Path integral approach for electron-phonon interaction effects in harmonic quantum dots.* Int. J. Mod. Phys. **10**, 2781 (1996)
- [11] S. Mukhopadhyay, A. Chatterjee, *Polaronic enhancement in the ground-state energy of an electron bound to a Coulomb impurity in a parabolic quantum dot.* Phys. Rev. B **55**,9297 (1997)

- [12] C.Y. Chen, P.W. Jin, W.S. Li, D.L. Lin, *Thickness effect on impurity-bound polaronic energy levels in a parabolic quantum dot in magnetic fields.* Phys. Rev. **56**, 14913 (1997)
- [13] S. Mukhopadhyay, A. Chatterjee, *Relaxed and effective-mass excited states of a quantum-dot Polaron* Phys. Rev. B **58**, 2088 (1998)
- [14] S. Mukhopadhyay, A. Chatterjee, *Polaronic correction to the first excited electronic energy level in semiconductor quantum dots with parabolic confinement* Phys. Lett. A **240**, 100 (1998)
- [15] S. Mukhopadhyay, A. Chatterjee, *Polaronic correction to the first excited electronic energy level in semiconductor quantum dots with parabolic confinement* Phys. Lett. A **242**, 355 (1998)
- [16] S. Mukhopadhyay, A. Chatterjee, Suppression of Zeeman splitting in a GaAs quantum dot Phys. Rev. B **59**, R7833 (1999)
- [17] S. Mukhopadhyay, A. Chatterjee, The ground and the first excited states of an electron in a multidimensional polar semiconductor quantum dot: an all-coupling variational approach. J. Phys.: Condens. Matter 11, 2071 (1999)
- [18] S. Mukhopadhyay, A. Chatterjee, *Phonon induced suppression of the zeeman splitting in polar semiconductor quantum dots; a quantum size effect.* Int. J. Mod. Phys. B **14**, 3897 (2000)
- [19] P. M. Krishna, S. Mukhopadhyay, A. Chatterjee, *Optical absorption in Quantum dots*. Int. J. Mod. Phys. B **16**, 1489 (2002)
- [20] N. Kervan, T. Altanhan, A. Chatterjee, A variational approach with squeezed-states for the polaronic effects in quantum dots Phys. Lett. A **315**, 280 (2003)
- [21] P.M. Krishna, A. Chatterjee, Effect of electron–phonon interaction on the electronic properties of an axially symmetric polar semiconductor quantum wire with transverse parabolic confinement Physica B **358**, 191 (2005)

- [22] P.M. Krishna, A. Chatterjee, *Polaronic effects in a polar semiconductor quantum strip with transverse parabolic confinement* Physica E **30**, 64 (2005)
- [23] P.M. Krishna, S. Mukhopadhyay, A. Chatterjee, *Polaronic effects in asymmetric quantum wire: An all-coupling variational approach* Solid State Commun. **138**, 285 (2006)
- [24] P.M. Krishna, S. Mukhopadhyay, A. Chatterjee, *Bipolaronic phase in polar semiconductor quantum dots: An all-coupling approach* Phys. Lett. A **360**, 655 (2007)
- [25] S. Mukhopadhyay, B. Boyacioglu, M. Saglam, and A. Chatterjee, *Quantum size effect on the phonon-induced Zeeman splitting in a GaAs quantum dot with Gaussian and parabolic confining potentials.* Physica E **40**, 2776 (2008)
- [26] D.S. Kumar, S. Mukhopadhyay, A. Chatterjee, *Effect of Rashba interaction and Coulomb correlation on the ground state energy of a GaAs quantum dot with parabolic confinement* Physica E **47**, 270 (2013)
- [27] D. S. Kumar, S. Mukhopadhyay, A. Chatterjee, Magnetization and susceptibility of a parabolic InAs quantum dot with electron–electron and spin–orbit interactions in the presence of a magnetic field at finite temperature J. Mag. Mag. Mat. 418, 169 (2016)
- [29] A. Boda, D. S. Kumar, I. V. Sankar and A. Chatterjee, *Effect of electron–electron interaction on the magnetic moment and susceptibility of a parabolic GaAs quantum dot* J. Mag. and Mag. Mat., **418**, 242 (2016).
- [30] D. Heitmann, K.K. Bollweg, V. Gudmundsson, T. Kurth, S.P. Riege, Far-infrared spectroscopy of quantum wires and dots, breaking Kohn's theorem. Physica E 1, 204 (1997)
- [31] B.T. Miller, W. Hansen, S. Manus, R.J. Luyken, A. Lorke, J.P. Kotthaus, S. Huant, G. Mediros-Ribeiro, P.M. Petroff, Fewelectron ground states of charge-tunable self- assembled quantum dots Phys. Rev. B **56**, 6764 (1997)

- [32] J. Adamowsky, M. Sobkowicz, B. Szafran, S. Bednarek, *Electron pair in a Gaussian confining potential* Phys. Rev. B **62**, 4234 (2000)
- [33] J. Gu and J. Q. Liang, Energy spectra of D-centres quantum dots in a Gaussian Potential Phys. Lett. A **335**, 451 (2005)
- [34] B. Boyacioglu, M. Saglam, A. Chatterjee, *Two-electron singlet states in semiconductorquantum dots with Gaussian confinement: a single-parameter variational calculation* J. Phys. Condens. Matter **19**, 456217 (2007)
- [35] W. F. Xie, Binding energy of an off-center hydrogenic donor in a spherical Gaussian quantum dot Physica B **403**, 2828 (2008)
- [36] Y. P. Bao and W. F. Xie, *Binding Energy of D*<sup>-</sup> and *D*<sup>0</sup> Centers Confined by Spherical Quantum Dots Commun. Theor. Phys. **50**, 1449 (2008)
- [37] S.S. Gomez, R.H. Romero, *Binding energy of an off-center shallow donor D- in a spherical quantum dot* Physica E **42**, 1563 (2010)
- [38] A. Gharaati, R. Khordad, A new confinement potential in spherical quantum dots: Modified Gaussian potential Superlattices Microstruct. 48, 276 (2010)
- [39] B. Boyacioglu, A. Chatterjee, *Heat capacity and entropy of a GaAs quantum dot with Gaussian confinement* J. Appl. Phys. **112**, 083514 (2012)
- [40] B. Boyacioglu, A. Chatterjee, Magnetic properties of semiconductor quantum dots with Gaussian confinement Int. J. Mod. Phys. B **26**, 1250018 (2012)
- [41] B. Boyacioglu, A. Chatterjee, *Persistent current through a semiconductor quantum dot with Gaussian confinement* Physica B **407**, 3535 (2012)
- [42] B. Boyacioglu and A. Chatterjee, *Dia- and paramagnetism and total susceptibility of GaAs quantum dots with Gaussian confinement* Physica E **44**, 1826 (2012)

- [43] A. Boda, A. Chatterjee, Ground state and binding energies of  $(D^0)$ ,  $(D^-)$  centres and resultant dipole moment of a  $(D^-)$  centre in a GaAs quantum dot with Gaussian confinement Physica E **45**, 36 (2012)
- [44] A. Boda, B. Boyacioglu, and A. Chatterjee, *Ground state* properties of a two-electron system in a three-dimensional GaAs quantum dot with Gaussian confinement in a magnetic field J. Appl. Phys. **114**, 044311 (2013)
- [45] A. Boda, A. Chatterjee, Effect of an external magnetic field on the binding energy, magnetic moment and susceptibility of an off-centre donor complex in a Gaussian quantum dot Physica B 448, 244 (2014)
- [46] A. Boda, G. Madhusudhan, A. Chatterjee, *Effect of external magnetic field on the ground state properties of D*<sup>-</sup> *centres in a Gaussian quantum dot* Superlattices Microstruct. **71**, 261 (2014)
- [47] A. Boda, A. Chatterjee, The Binding Energy and Magnetic Susceptibility of an Off-Centre D<sub>0</sub> Donor in the Presence of a Magnetic Field in a GaAs Quantum Dot with Gaussian Confinement: An Improved Treatment J. Nanosci. Nanotechol. **15,** 6472 (2015)
- [48] D. Sanjeev Kumar, A. Boda, S. Mukhopadhyay, A. Chatterjee, Effect of Rashba spin-orbit interaction on the ground state energy of a D<sup>0</sup> centre in a GaAs quantum dot with Gaussian confinement Superlattices Microstruct. **88**, 174 (2015)
- [49] A. Boda, B. Boyacioglu, U. Erkaslan3 and A. Chatterjee, Effect of Rashba spin-orbit coupling on the electronic, thermodynamic, magnetic and transport properties of GaAs, InAs and InSb quantum dots with Gaussian confinement Physica B 498, 43 (2016)
- [50] A. Boda and A. Chatterjee, *Transition energies and magnetic properties of a neutral donor complex in a Gaussian GaAs quantum dot* Superlattices and Microstructures **97**, 268 (2016)

- [51] H. K. Sharma, A. Boda, B Boyacioglub, A. Chatterjee, Electronic and magnetic properties of a two-electron Gaussian GaAs quantum dot with spin-Zeeman term: A study by numerical diagonalization J. Mag.Mag. Mat. **469**, 171 (2018)
- [52] K. L. Jahan, A. Boda, I. V. Shankar, Ch. N. Raju, A. Chatterjee, Magnetic field effect on the energy levels of an exciton in a GaAs quantum dot: Application for excitonic lasers Scientific Reports 8, 5073 (2018)
- [53] M. Ciurla, J. Adamowski, B. Szafran, and S. Bednarek, *Modelling of confinement potentials in quantum dots* Physica E: Low-dimensional Systems and Nanostructures **15**, 261 (2002).
- [54] A. Kwaśniowski and J. Adamowski, *Effect of confinement potential shape on exchange interaction in coupled quantum dots* J. Phys: Condens. Matter **20**, 215208 (2008).
- [55] W. Xie, Potential-shape effect on photoionization cross section of a donor in quantum dots Superlattice Microst **65**, 271 (2014).

### **SUMMARY**

In this thesis we have examined the effect of excitonic, polaronic and electronic effects in a QD with Gaussian confinement. In the introductory chapter, i. e., Chapter 1, we have started with the definitions and properties of nanomaterials or low dimensional systems and then presented a detailed introduction to QDs and their properties. Specifically, we have discussed different types of confinement potential in QDs and the motivation behind choosing the Gaussian potential for our studies. Next, we have introduced briefly the idea of excitons (electron – hole pair) and polarons (electron – phonon interaction) and presented an overview of the experimental and theoretical investigations carried out on excitonic and polaronic effects in QDs.

In Chapter 2, we have considered an exciton in a GQD of GaAs placed in a magnetic field and calculated the exciton GS energy, binding energy and the exciton size with the help the conventional variational approach,  $\frac{1}{N}$  — expansion technique and the shifted  $\frac{1}{N}$  — expansion scheme. It is well known that the conventional variational approach provides an upper limit to the energy while the  $\frac{1}{N}$  — expansion scheme provides a lower limit. We have shown that results from the shifted  $\frac{1}{N}$  — expansion scheme fare excellently the exact numerical results. Our results have revealed that the exciton binding is strengthened as QD size is reduced

and that the binding is stronger in GQD than in a Parabolic QD. We have also demonstrated that the exciton dimension becomes smaller as QD reduces in size or the confinement strength increases or the strength of the magnetic field is enhanced. It has been observed that exciton oscillator strength reduces as QD is made smaller or the magnetic field is enhanced. Also the number of QD exciton levels can be controlled by manipulating the system parameters. This tunability of the excitonic states in a QD can be effectively used to realize a QD laser.

In Chapter 3, we have examined the role of temperature on the polaronic effects in GQD using a variant of the Lee-Low-Pines transformation method as modified by Huybrechts and the quantum statistical theory. We have been able to show that as temperature is raised, the polaron GS energy goes up. This implies lessening of polaronic effect with the rise in temperature. Our results do reveal that the self-energy of a polaron in a general N-dimensional GQD becomes smaller as the temperature rises. We understand this phenomenon in the following way. As the temperature rises, the probability of excitation of real phonons also rises. This naturally impeds the formation of polarons. We have also shown that polaronic phenomena become more strikingly visible in a 2D QD than in a 3D QD. In GQD, in general, the polaronic binding shows an increase with the reduction in R, particularly at small R. It has been observed that if R is made smaller than a critical value in 3D QD, the polaron binding starts weakening with the decrease in R. Furthermore, the GS energy of a Gaussian QD has been shown to decrease with increasing potential depth. This implies that the polaronic binding strengthens with the increae in the potential depth.

In Chapter 4, we have studied the role of the potential profile on several properties of a GaAs QD at finite temperature. For this purpose we have considered the power-exponential potential model with a steepness parameter p. For a small value of p, the potential is soft and as p increases, the potential becoms harder. In the case of p=2, the power-low potential transforms into a Gaussian potential. The thermodynamic energy, specific heat, susceptibility and persistent current have been determined at low temperature with the help of the canonical ensemble approach. It has been demonstrated that the canonical average of the thermodynamic energy increases with temperature T and the potential depth  $V_0$ . At small p, the average energy falls off sharply with the increase in p, but as p increases, the energy approaches a T – independent saturation value.

It has also been established that if the temperature is low, the specific heat of a GaAs QD is unaffected by the nature of the potential profile. However, at high temperature ( $T = 300 \, K$ ), the specific heat initially shows a rapid increase with p and then appears to a saturation value  $2k_B$  as p exceeds a certain critical value.

We have shown that the susceptibility  $\chi$  of a GaAs QD increases monotonically with p at high temperature (T=300~K). At low p,  $\chi$  is diamagnetic and as p exceeds a critical value,  $\chi$  becomes paramagnetic. Furthermore,  $\chi$  seems to decrease with increasing  $V_0$ . At low temperature (T=1~K),  $\chi$  initially increases with p, reaches a maximum and then begins to fall off. For small  $V_0$ ,  $\chi$  displays a diamagnetic character. However, in the case of large  $V_0$  ( $V_0=300$ 

meV), as p increases, the system initially exhibits a diamagnetic behaviour and as p exceeds a critical value, it displays a paramagnetic behaviour. Here too,  $\chi$  reaches a maximum at some value of p and then falls off in a monotonic way and turns negative beyond a critical p. However, if  $V_0$  is further strengthened,  $\chi$  may attain the paramagnetic character even at a smaller p value and the diamagnetic character at a larger p. Thus for a range of p values, a re-entrant phenomenon may occur. But, if the temperature happens to be very low and p large,  $\chi$  never shows any paramagnetic behaviour.

At low temperature (T = 1 K), a GaAs QD can have a diamagnetic persistent current which increases in magnitude as  $V_0$  decreases. At high temperature (T = 300 K), the persistent current is paramagnetic for small values of p, but it sharply falls off with increasing p and becomes diamagnetic at a certain p depending on  $V_0$ . The diamagnetic persistent current assumes higher values as p is increased further and finally reaches a saturation value.

### LIST OF PUBLICATIONS BASED ON WHICH THE PRESENT THESIS HAS BEEN WRITTEN

 K. Luhluh Jahan, A. Boda, I. V. Sankar, Ch. Narasimha Raju & Ashok Chatterjee. "Magnetic field effect on the energy levels of an exciton in a GaAs quantum dot: application for excitonic lasers". Scientific Reports 8 5073 (2018).

doi:10.1038/s41598-018-23348-9

### 2. **K. Luhluh Jahan** & Ashok Chatterjee.

"Effect of Temperature on the Single-Particle Ground-State and Self Energy of a Polar Quantum Dot with Gaussian Confinement"

Physica B, 579 411892 (2020).

https://doi.org/10.1016/j.physb.2019.411892

3. **K. Luhluh Jahan**, B. Boyacioglu & Ashok Chatterjee.

"Effect of confinement potential shape on the electronic, thermodynamic, magnetic and transport properties of a GaAs quantum dot at finite temperature"

Scientific Reports 9 15824 (2019).

https://doi.org/10.1038/s41598-019-52190-w

### PUBLICATIONS IN CONFERENCE PROCEEDINGS

### 1. **K. Luhluh Jahan**, Alu Boda & Ashok Chatterjee.

"Ground state energy of an exciton in a spherical quantum dot in the presence of an external magnetic field".

*AIP Conference Proceedings* **1661** 080008 (2015).

doi: 10.1063/1.4915399

### 2. **K. Luhluh Jahan** & AshokChatterjee.

"Effect of temperature on the single-particle ground-state energy of a polar quantum dot with Gaussian confinement" AIP Conference Proceedings 1731, 050088 (2016).

doi: 10.1063/1.4947742

### 3. **K. Luhluh Jahan** & AshokChatterjee.

"Ground state properties of an exciton in a GaAs quantum dot in the presence of an external magnetic field using 1/N expansion method"

AIP Conference Proceedings 1942, 050005 (2018).

doi: 10.1063/1.5028636

## PAPER PRESENTATIONS IN NATIONAL AND INTERNATIONAL CONFERENCES

- 1. **K. Luhluh Jahan**, Alu Boda & Ashok Chatterjee. "Ground state energy of an exciton in a spherical quantum dot in the presence of an external magnetic field".
  - Frontiers in Physics-2014 at School of Physics, University of Hyderabad, Telangana, India.
- 2. **K. Luhluh Jahan**, Alu Boda & Ashok Chatterjee. "Ground state energy of an exciton in a spherical quantum dot in the presence of an external magnetic field".
  - ICCMP 2014 at Department of Physics, University of Himachal Pradesh, Shimla, India.
- 3. **K. Luhluh Jahan** & AshokChatterjee. "Effect of temperature on the single-particle ground-state energy of a polar quantum dot with Gaussian confinement"
  - DAE-SSPS 2015 at Amity University, Noida, Uttar Pradesh, India. (Best Poster Presentation Award)
- 4. **K. Luhluh Jahan**, Alu Boda & Ashok Chatterjee. *Effect of external magnetic field on the binding energy and size of an exciton in a GaAs quantum dot with Gaussian confinement*. ICMAGMA -2015 at VIT, Vellore, Tamilnadu, India.

- 5. K. Luhluh Jahan & AshokChatterjee. "Effect of temperature on the single-particle ground-state energy of a polar quantum dot with Gaussian confinement" Frontiers in Physics-2016, at School of Physics, University of
  - Frontiers in Physics-2016, at School of Physics, University of Hyderabad, Telangana, India
- 6. K. Luhluh Jahan & AshokChatterjee. "Ground state properties of an exciton in a GaAs quantum dot in the presence of an external magnetic field using 1/N expansion method" DAE-SSPS-2017 at Bhabha Atomic Research Centre, Mumbai,

India

# Some Aspects of the Electronic, Excitonic and Polaronic Properties of a Quantum Dot

by Luhluh Jahan K

Submission date: 25-Mar-2021 03:34PM (UTC+0530)

**Submission ID: 1541934919** 

File name: Thesis\_Luhluh\_Jahan\_12PHPH06.pdf (2.62M)

Word count: 18992 Character count: 88379

## Some Aspects of the Electronic, Excitonic and Polaronic Properties of a Quantum Dot

### **ORIGINALITY REPORT**

6%

3%

6%

0%

SIMILARITY INDEX

INTERNET SOURCES

**PUBLICATIONS** 

STUDENT PAPERS

### **PRIMARY SOURCES**

1

### www.nature.com

Internet Source

3%

Mohammad K. Elsaid, Amal Abu Alia, Ayham Shaer. "Rashba spin-orbit interaction effects on thermal and magnetic properties of parabolic GaAs quantum dot in the presence of donor impurity under external electric and magnetic fields", Chinese Journal of Physics, 2020

Publication

3

K. Luhluh Jahan, Bahadir Boyacioglu, Ashok Chatterjee. "Effect of confinement potential shape on the electronic, thermodynamic, magnetic and transport properties of a GaAs quantum dot at finite temperature", Scientific Reports, 2019

<1%

Publication



K. Luhluh Jahan, A. Boda, I. V. Shankar, Ch. Narasimha Raju, Ashok Chatterjee. "Magnetic field effect on the energy levels of an exciton in a GaAs quantum dot: Application for

<1%

5	Soma Mukhopadhyay, Ashok Chatterjee. "Formation and stability of a singlet optical bipolaron in a parabolic quantum dot", Journal of Physics: Condensed Matter, 1996 Publication	<1%
6	K. Luhluh Jahan, Ashok Chatterjee. "Effect of temperature on the single-particle groundstate and self energy of a polar quantum dot with Gaussian confinement", Physica B: Condensed Matter, 2020 Publication	<1%
7	Springer Series in Materials Science, 2007.  Publication	<1%
8	The Physics of the Two-Dimensional Electron Gas, 1987.  Publication	<1%
9	Oliver Gywat, Hubert J. Krenner, Jesse Berezovsky. "Spins in Optically Active Quantum Dots", Wiley, 2009	<1%
10	Wu Xiaoguang. "Temperature dependence of the polaron mass in a GaAs-Al_{x}Ga_{1-x}As heterostructure", Physical Review B, 12/1987	<1%
11	M. M. Panja, R. Dutt. " Shifted large- expansion for the energy levels of relativistic	<1%

expansion for the energy levels of relativistic

Publication

- Je, Koo-Chul, Sang Youp Yim, Jaehoon Lee, <1% 12 Eun-Hee Jeang, Seung-Han Park, and Pallab K. Bhattacharya. "", Quantum Dots Nanoparticles and Nanoclusters II, 2005. Publication <1% B. Boyacioglu, A. Chatterjee. "Heat capacity 13 and entropy of a GaAs quantum dot with Gaussian confinement", Journal of Applied Physics, 2012 Publication G. Einevoll. "Confinement of excitons in <1% quantum dots", Physical Review B, 02/1992 Publication N Tokuda. "A variational approach to the <1% 15 polaron problem", Journal of Physics C: Solid State Physics, 1980 Publication Aalu Boda, B. Boyacioglu, Ashok Chatterjee. <1% 16 "Ground state properties of a two-electron system in a three-dimensional GaAs quantum dot with Gaussian confinement in a magnetic field", Journal of Applied Physics, 2013 Publication
  - Chacko, Z.. "A minimally fine-tuned supersymmetric standard model", Nuclear Physics, Section B, 20051003

<1%

Publication

18	Gilliland, G.D "Photoluminescence spectroscopy of crystalline semiconductors", Materials Science & Engineering R, 199703 Publication	<1%
19	Chatterjee, A "Multidimensional bound optical polaron revisited", Annals of Physics, 199009 Publication	<1%
20	I.M. Tsidilkovski, G.I. Harus, N.G. Shelushinina. "Impurity states and electron transport in gapless semiconductors", Advances in Physics, 2006 Publication	<1%
21	Matsumoto, Yoshiyasu, and Kazuya Watanabe. "Coherent Vibrations of Adsorbates Induced by Femtosecond Laser Excitation", Chemical Reviews, 2006.	<1%
22	mural.maynoothuniversity.ie Internet Source	<1%
23	Konstantin Kikoin, Mikhail Kiselev, Yshai Avishai. "Dynamical Symmetries for Nanostructures", Springer Science and Business Media LLC, 2012 Publication	<1%

Exclude quotes On Exclude matches < 14 words